

COMPOSITION-PROPERTY RELATIONSHIP OF PCL BASED
POLYURETHANES

A THESIS SUBMITTED TO
THE GRADUATE SCHOOL OF NATURAL AND APPLIED SCIENCES
OF
MIDDLE EAST TECHNICAL UNIVERSITY

BY

AYSUN GÜNEY

IN PARTIAL FULFILLMENT OF THE REQUIREMENTS
FOR
THE DEGREE OF MASTER OF SCIENCE
IN
POLYMER SCIENCE AND TECHNOLOGY

FEBRUARY 2012

Approval of the thesis

**COMPOSITION-PROPERTY RELATIONSHIP OF PCL BASED
POLYURETHANES**

submitted by **AYSUN GÜNEY** in partial fulfillment of the requirements for the degree of **Master of Science in Polymer Science and Technology, Middle East Technical University** by,

Prof. Dr. Canan Özgen _____
Dean, Graduate School of **Natural and Applied Sciences**

Prof. Dr. Necati Özkan _____
Head of Department, **Polymer Science and Technology**

Prof. Dr. Nesrin Hasırcı _____
Supervisor, **Chemistry Dept., METU**

Prof. Dr. Vasıf Hasırcı _____
Co-Supervisor, **Biological Sciences Dept., METU**

Examining Committee Members:

Prof. Dr. Erdal Bayramlı _____
Chemistry Dept., METU

Prof. Dr. Nesrin Hasırcı _____
Chemistry Dept., METU

Prof. Dr. Kezban Ulubayram _____
Faculty of Pharmacy, Hacettepe University

Prof. Dr. Necati Özkan _____
Polymer Science and Technology Dept., METU

Assoc. Prof. Dr. Ayşen Tezcaner _____
Engineering Sciences Dept., METU

Date: 23.02.2012

I hereby declare that all information in this document has been obtained and presented in accordance with academic rules and ethical conduct. I also declare that, as required by these rules and conduct, I have fully cited and referenced all material and results that are not original to this work.

Name, Last name: Aysun Güney

Signature :

ABSTRACT

COMPOSITION-PROPERTY RELATIONSHIP OF PCL BASED POLYURETHANES

Güney, Aysun

M.Sc., Department of Polymer Science and Technology

Supervisor: Prof. Dr. Nesrin Hasırcı

Co-advisor: Prof. Dr. Vasıf Hasırcı

February 2012, 125 pages

The desirable properties of polyurethanes (PUs) such as mechanical flexibility associated with chemical versatility make these polymers attractive in the development of biomedical devices. In this study, various segmented polyurethanes were synthesized through polymerization reactions between polycaprolactone (PCL) diol or triol and excess hexamethylene diisocyanate (HDI) with varying NCO/OH ratios and the effect of composition on the properties of the resultant polyurethane films were examined. Initially, isocyanate terminated prepolymers were synthesized through one-shot polymerization, and then these prepolymers were cured by introducing crosslinkages into the structure and thus PUs were obtained. In order to enhance biocompatibility and hydrophilicity of the resulting polymers, heparin was added into the prepolymer

before the curing process. The influence of excess HDI as a crosslinker on the degree of H-bond formation between hard-hard segments or hard-soft segments was examined by using Fourier transform infrared-Attenuated total reflectance spectroscopy (FTIR-ATR). Also the effects of HDI content on the chemical, physical and mechanical properties of the polyurethanes were examined with differential scanning calorimetry (DSC), X-Ray diffraction spectroscopy (XRD), dynamic mechanical analyzer (DMA), mechanical tester and goniometer. FTIR-ATR, DSC and DMA analyses showed that use of triol resulted in better network formation and homogenous distribution of hard segments within soft segment matrix. Incorporation of heparin into the polymer matrix produced more hydrophilic films (water contact angle reduced from 80° to 60°). Polyurethanes from PCL and HDI in the absence of any solvent, initiator, catalyst or chain extender were successfully synthesized and this kind of synthesis enhanced biocompatibility and increased the potential of polymers for use in biomedical applications.

Keywords: Polyurethane, Polycaprolactone diol, Hexamethylene diisocyanate, Heparin.

ÖZ

PCL ESASLI POLİÜRETANLARIN KOMPOZİSYON-ÖZELLİK İLİŞKİSİ

Güney, Aysun

Yüksek Lisans, Polimer Bilimi ve Teknolojisi Bölümü

Tez Yöneticisi: Prof. Dr. Nesrin Hasırcı

Ortak Tez Yöneticisi: Prof. Dr. Vasıf Hasırcı

Şubat 2012, 125 sayfa

Poliüretanların (PU) kimyasal çeşitliliğine bağlı olarak mekanik esnekliği gibi arzu edilen özellikleri, bu polimerleri biyomedikal cihazların geliştirilmesinde cazip hale getirmiştir. Bu çalışmada, çeşitli segmentli poliüretanlar polikaprolakton (PCL) diol veya triol, hekzametilen diizosiyanatın (HDI) fazlası ile polimerizasyon reaksiyonuna sokularak farklı NCO/OH oranlarında sentezlenmiş ve bileşenlerin poliüretan filmlerin özellikleri üstündeki etkisi incelenmiştir. İlk olarak, izosiyanatla sonlanan önpolimerler tek adım polimerizasyonu ile sentezlenmiş ve sonra önpolimerler kür edilerek çapraz bağlı PU'lar elde edilmiştir. Elde edilen polimerlerin biyoyumluluğunu ve hidrofiliğini arttırmak amacıyla önpolimere kür edilmeden önce heparin eklenmiştir. HDI fazlasının çapraz bağlayıcı olarak, sert-sert segmentler veya sert-yumuşak segmentler arası H-bağ oluşum derecesine etkisi Fourier dönüştürme

hafifletilmiş toplam yansıtma kızılötesi spektroskopisi (FTIR-ATR) ile incelenmiştir. Ayrıca HDI miktarının poliüretanların kimyasal, fiziksel ve mekanik özellikleri üzerine etkisi, diferansiyel taramalı kalorimetre (DSC), X-ışını kırınımı spektroskopisi (XRD), dinamik mekanik analiz cihazı (DMA), mekanik test cihazı ve goniometre kullanılarak incelenmiştir. FTIR-ATR, DSC ve DMA analizleri, triol kullanımının daha iyi bir ağ oluşmasına ve sert segmentlerin yumuşak segment yapısı içerisinde homojen dağılmasına neden olduğunu göstermiştir. Polimer yapısına heparin eklenmesiyle daha hidrofilik filmler oluşmuştur (su temas açısı 80°'den 60°'a düşmüştür). Poliüretanlar çözücü, başlatıcı, katalizör veya zincir uzatıcı olmadan PCL ve HDI kullanılarak, başarılı bir şekilde sentezlenmiştir ve bu tür sentez, polimerlerin biyoyumluluğunu ve biyomedikal uygulamalarda kullanım potansiyelini arttırmıştır.

Anahtar kelimeler: Poliüretan, Polikaprolakton diol, Hekzametilen diizosiyanat, Heparin.

To my family...

ACKNOWLEDGEMENTS

I would like to express my special thanks to my supervisor Prof. Dr. Nesrin Hasırcı for her continuous guidance, encouragement, motivation and support during all the stages of my thesis. I sincerely appreciate the time and effort she has spent to improve my experience during my graduate years.

I am also deeply thankful to Prof. Dr. Vasıf Hasırcı for his support, leadership and guidance in METU-BIOMAT Biomaterials and Tissue Engineering Research Group.

I deeply thank to special lab mates Aysel Kızıltay, Tuğba Endođan, Özge Özgen, Filiz Kara, Şeniz Uçar, Gülçin Çiçek, and Ümran Aydemir and other lab members of D-148 for the good memories, continuous help and support during my experiments.

I am thankful to Engin Özkol who taught me deconvolution method. I would like to thank to METU Central Laboratory for characterization analyses.

This study was supported by METU-BAP-07-02-2010-00-01 and METU-BAP-07-02-2011-00-01. These grants are gratefully acknowledged.

TABLE OF CONTENTS

ABSTRACT	iv
ÖZ	vi
ACKNOWLEDGEMENTS	ix
TABLE OF CONTENTS.....	x
LIST OF TABLES	xiii
LIST OF FIGURES	xv
ABBREVIATIONS	xviii
CHAPTERS	
1. INTRODUCTION	1
1.1 History and Development of Polyurethanes	2
1.2 Biomedical Applications of Polyurethanes.....	3
1.3 Raw Materials	4
1.1.1 Isocyanates	5
1.1.2 Reactions of Isocyanates.....	8
1.1.3 Polyols.....	14
1.1.4 Chain Extenders	15
1.1.5 Synthesis of Polyurethanes	17
1.4 Polyurethane Structure	19
1.4.1 Crystallinity.....	19
1.4.2 Structure Property Relationship of Polyurethanes	20
1.5 Mechanisms of Polyurethane Degradation	27
1.5.1 Biological Degradation of Polyurethanes	28

1.5.2	Hydrolysis	29
1.5.3	Oxidation.....	32
1.6	Polyurethane-Heparin Blends	33
1.7	Aim of This Study.....	34
2.	EXPERIMENTAL.....	36
2.1	Materials.....	36
2.2	Polymer Synthesis and Film Casting	36
2.3	Preparation of Polyurethane Blends.....	41
2.4	Characterization Methods	42
2.4.1	FTIR-ATR Spectroscopy	43
2.4.2	Differential Scanning Calorimetry.....	43
2.4.3	Dynamic Mechanical Analysis	43
2.4.4	X-Ray Diffraction Measurements.....	44
2.4.5	Mechanical Tests	44
2.4.6	Contact Angle Measurements	45
3.	RESULTS	46
3.1	Polymer Synthesis and Characterization.....	46
3.1.1	FTIR-ATR.....	47
3.1.2	Differential Scanning Calorimetry.....	70
3.1.3	Dynamical Mechanical Analysis Measurements	76
3.1.4	X-Ray Diffraction Measurements.....	82
3.2	Tensile Test Results	84
3.3	Hydrophilicity Results	87
3.4	Effect of Heparin Blending on Mechanical and Hydrophilicity	
Properties	88

4. CONCLUSION.....	90
REFERENCES	93
APPENDICES.....	115
A. POLYMER SYNTHESIS SETUP	113
B. IMAGES OF PREPARED FILMS	114
C. DMA RESULTS AT 2 Hz	115
D. DMA RESULTS AT 4 Hz	116
E. DMA RESULTS AT 10 Hz.....	117
F. DMA RESULTS AT 20 Hz.....	118
G. DMA RESULTS: TAN δ VALUES AT DIFFERENT	
FREQUENCIES.....	119
H. FORMATION AND CHARACTERIZATION OF	
POLYURETHANE BLENDS	121

LIST OF TABLES

TABLES

Table 1-1 : List of aromatic diisocyanates	6
Table 1-2 : List of aliphatic diisocyanates	7
Table 1-3 : Chemical structure of commercial polyether polyols.....	14
Table 1-4 : Chemical structure of typical commercial polyester	
polyols.....	15
Table 1-5 : The chemical structures of aliphatic and aromatic diol.....	
chain extenders.	16
Table 1-6 : The chemical structures of aliphatic and aromatic.....	
diamine chain extenders.....	16
Table 1-7 : Classification of crystalline polymers	20
Table 2-1 : Composition and the experimental conditions used.....	
in the preparation of polyurethanes.....	41
Table 3-2 : Peak assignments in the IR spectra of PU2.5-1250.....	52
Table 3-3 : Infrared stretching band assignments of the N–H group.....	
in the PUs as seen from the deconvoluted IR spectra.....	57
Table 3-4 : Deconvolution results of the N–H region with peak.....	
position for all PUs	59
Table 3-5 : Deconvolution results of the N–H region with peak.....	
area for all PUs	61
Table 3-6 : Infrared stretching band assignments of the C=O	
group in the PUs	64

Table 3-7 : Deconvolution results of the C=O region with
peak position for all PUs.....	66
Table 3-8 : Deconvolution results of the C=O region with peak area
for all PUs	67
Table 3-9 : Results of the DSC analysis of PU.....	74
Table 3-10 : Transitions Obtained from Storage Modulus at 1 Hz.....	80
Table 3-11 : Storage Modulus and Loss Modulus of PUs
at 1 Hz at 25°C and 37°C.....	81
Table 3-12 : Tensile properties of PU films.....	85
Table 3-13 : Static water contact angle measurement of PUs
with different hard segments	88
Table 3-14 : Mechanical properties and static water contact
angle results of PUU5-2000 and PUU5-2000-HP	89

LIST OF FIGURES

FIGURES

Figure 1-1 : Urethane linkages in polyurethanes	4
Figure 1-2 : Addition polymerization of diisocyanate and polyol.....	4
Figure 1-3 : Electronic structure of isocyanate group.....	5
Figure 1-4 : Reaction of isocyanate with alcohol	8
Figure 1-5 : Reaction of isocyanate with water	9
Figure 1-6 : Reaction of isocyanates with carboxylic acid.....	10
Figure 1-7 : Reaction of isocyanate with urethane	11
Figure 1-8 : Reaction of isocyanate with urea groups	11
Figure 1-9 : Formation of uretidinedione	12
Figure 1-10 : Trimerization of isocyanates.....	13
Figure 1-11 : Formation of uretoneimine	13
Figure 1-12 : One-shot and prepolymer method of polymerization	17
Figure 1-13 : The ideal structure of segmented linear polyurethane	18
Figure 1-14 : Scheme of prepolymer route for the formation of	
polyurethane elastomers	19
Figure 1-15 : Illustration of microphase separation of hard and soft.....	
segment into domains in segmented polyurethanes.....	22
Figure 1-16 : Hydrogen bonding in polyurethanes between hard-hard	
segments and between hard-soft segments	27
Figure 1-17 : Polyurethane degradation mechanisms.....	28
Figure 1-18 : Hydrolytic degradation mechanism of polyurethane bonds	30

Figure 1-19 : The illustration of ester bond	31
Figure 2-1 : Chemical route for synthesis of PUs.....	37
Figure 2-2 : Synthesis of PUU	39
Figure 3-1 : Schematic representation of vibrational modes of	
amide I, amide II and amide III	48
Figure 3-2 : IR spectra of PU2.5-1250.....	50
Figure 3-3 : Representative IR spectra of different PU films	51
Figure 3-4 : IR spectra for different segmented PU films;	
(a) N–H region, (b) C=O region	54
Figure 3-5 : The deconvoluted N–H region of IR spectra for all PUs.....	56
Figure 3-6 : The dual-cis bond.....	58
Figure 3-7 : The deconvoluted C=O region of IR spectra for all PUs.....	65
Figure 3-8 : The hard segments in PUU5-2000 constitute	
hydrogen bonding between the chains via urea bonds	69
Figure 3-9 : DSC thermograms of PU's: (a) PCL diol 1250,	
(b) PU1.5-1250, (c) PU2.5-1250, (d) PU5-1250	72
Figure 3-10 : DSC thermograms of PU's: (a) PCL diol 2000,	
(b) PU5-2000, (c) PUU5-2000.....	73
Figure 3-11 : DSC thermograms of PU's: (a) PCL triol 900,.....	
(b) PU5-900T	75
Figure 3-12 : DMA curves of all PUs : (a) PU1.5-1250;.....	
(b) PU2.5-1250; (c) PU5-1250; (d) PU5-2000;.....	
(e) PUU5-2000; (f) PU5-900T.....	78
Figure 3-13 : The XRD curves of different PU films in the range	
between 5 and 80°	82

Figure 3-14 : The XRD curves of different PU films in the range	
between 5 and 40°	83
Figure 3-15 : Stress-strain graphs of PUs	84
Figure B-1 : DMA Results; (a) PU1.5-1250; (b) PU2.5-1250;.....	
(c) PU5-1250; (d) PU5-2000; (e) PUU5-2000;	
(f) PU5-900T at 2 Hz	115
Figure C-1 : DMA Results; (a) PU1.5-1250; (b) PU2.5-1250;.....	
(c) PU5-1250; (d) PU5-2000; (e) PUU5-2000;	
(f) PU5-900T. at 4 Hz	116
Figure D-1 : DMA Results; (a) PU1.5-1250; (b) PU2.5-1250;	
(c) PU5-1250; (d) PU5-2000; (e) PUU5-2000;	
(f) PU5-900T. at 10 Hz	117
Figure E-1 : DMA Results; (a) PU1.5-1250; (b) PU2.5-1250;.....	
(c) PU5-1250; (d) PU5-2000; (e) PUU5-2000;	
(f) PU5-900T at 20 Hz	118
Figure F-1 : Tan δ Values; (a) PU1.5-1250; (b) PU2.5-1250;.....	
(c) PU5-1250; (d) PU5-2000; (e) PUU5-2000; (f) PU5-900T.....	120

ABBREVIATIONS

BSA	Bovine serum albumin
DMA	Dynamic mechanical analysis
DMAC	<i>N,N</i> -dimethylacetamide
DMF	Dimethylformamide
DMSO	Dimethylsulfoxide
DSC	Differential scanning calorimetry
E	Young's modulus
E'	Storage modulus
E''	Loss modulus
EAB	Elongation at break
FTIR-ATR	Fourier transform infrared spectroscopy-Attenuated total reflectance
HDI	1,6-Hexamethylene diisocyanate
HP	Heparin
HS	Hard segment
IAB	Intra-aortic balloon pump
MPa	Mega Pascal
MW	Molecular weight
PCL	Poly(ϵ -caprolactone)
PU	Polyurethane
PUU	Polyurethane urea
SS	Soft segment
T _g	Glass transition temperature
THF	Tetrahydrofuran
T _m	Melting temperature
XRD	X-Ray diffraction

CHAPTER 1

INTRODUCTION

A material that is to be used for the treatment of injuries and diseases requires a broad range of biological and physical properties including biocompatibility, biodegradability, strength, and elasticity [1]. Polymers encompass a large class of compounds of both natural and synthetic materials that can be used in the biomedical field. Synthetic polymers are adaptable and can be modified for use in a variety of applications due to the versatility of their composition and structure [2].

Although biocompatible polymers are well tolerated by the body, the mechanical properties of these polymers may not match those of the natural tissue. For example, brittle polymers cannot be expected to be appropriate for applications of soft tissues including skin, heart, blood vessels, skeletal muscle, tendon, etc. all of which are very elastic. Thus, several biomimetic approaches have been developed to optimize the material properties in an effort to mimic the structure and function of natural tissues. In this context, developing new classes of synthetic polymers is an interesting research area in materials science for medical applications [3].

Among the various synthetic polymers intended for biomedical applications, polyurethanes (PUs) showed that they possessed the desired features because the versatility in their chemistries used in their synthesis allows the development of polymers with diverse physical, chemical, mechanical, and degradation properties [1,4-8]. A priori knowledge of the particular properties needed for site specific applications enables researchers a control over the PU properties and performance to meet these requirements. Furthermore, their capacity to undergo bulk and

surface modifications confers unique biological functionality to these synthetic materials and the flexibility of their processing conditions allow them to be produced in various forms such as foam, fiber, film, sheet and tube [6].

1.1 History and Development of Polyurethanes

Polyurethanes were discovered by Professor Otto Bayer and coworkers via polyaddition reaction between aliphatic diisocyanates and aliphatic diols in 1937 [9-11]. In 1958, Pangman introduced the first biomedical application of polyurethanes as polyester-urethane foam-covered breast prostheses [12,13]. In the same year, Mandrino and Salvatore also applied rigid a polyester-urethane foam called Ostamer for the treatment of fractured and diseased bones in six patients [14-16].

In the years 1959 and 1960, the application of polyester-urethane, Polyurethane Estane® VC, was proposed by Dreyer et al. to be used as components for heart valves and chambers, and aortic grafts [17,18]. In the mid-1960s, Cordis Corporation started to commercialize polyester-urethane diagnostic catheters [19]. In 1954, textile chemists at DuPont developed Lycra® spandex as a high performance alternative to natural rubber in elastic thread. It was first introduced as a biomaterial in 1967 by Boretos and Pierce who obtained the polymer in solution directly from the DuPont spinning line that produced Lycra spandex yarn. This material was first used as the elastomeric components of a cardiac assist pump and its arterial cannulae [20-22]. The year 1971 marked the arrival of the earliest polyurethane specifically designed for medical use; Avcothane-51™, a polyurethane/silicone hybrid, was invented by AVCO-Everett Research Laboratory. In 1972, Biomer™, a version of Lycra® T-126 produced by Ethicon Corporation under a license from Dupont, was made available. Avcothane and Biomer were regarded as the first 'real' biomedical polyurethanes and were studied intensively. Avcothane was used clinically in the first intra-aortic balloon pump (IAB), starting in about 1971, and is still in clinical use today in IABs.

Biomer™ components were used in the ‘Jarvik Heart’ in 1982, the first artificial heart used for implantation. From the 1990s, biodegradable PUs have been widely investigated for soft and hard tissue regeneration [23].

1.2 Biomedical Applications of Polyurethanes

Polyurethane materials utilized in medical applications can be degradable or nondegradable to meet the desired specifications of applications. Nondegradable polyurethanes have been applied in a number of biomedical areas such as pacemaker lead insulators, heart valves, breast implants, and gastric bubbles [24-33]. Degradable polyurethane has drawn considerable interest in the development of tissue constructs since after the completion of the function; the material should degrade and be absorbed by the biological medium. In 1980s biodegradable polyurethanes are used to replace defective tissues by using tissue constructs [34-47]. Biodegradable polyurethanes can be used in tissue engineering scaffolds; in terms of its application area they should have appropriate requirements such as for soft tissue engineering requiring elasticity and cartilage and bone regeneration requiring rigidity [48]. In terms of their chemical and physical properties, such biodegradable polyurethanes can be manipulated for cardiovascular implants, drug delivery devices, cancellous bone graft substitutes, injectable materials, and tissue-organ regeneration scaffolds [49]. Elastic, degradable PUs have found widespread use in most soft tissue regeneration studies, such as vascular smooth muscle [50], cardiac muscle [51], blood vessel [52], skeletal muscle, tendon, ligament, and skin repair. In addition, elastic, degradable PUs are also investigated for use in hard tissue regeneration, such as cartilage [53,54] and bone [37,55]. Moreover, degradable polyurethanes can be used in blood contact devices as long or short term medical implants [56-58].

1.3 Raw Materials

Polyurethanes are a heterogeneous family of polymers consisting of carbamate groups (-NHCO₂-) in their backbone. These groups, called urethane linkages, form the basis of the urethane backbone and are illustrated in Figure 1-1 . Variations in the R group produce different urethanes with diverse properties.

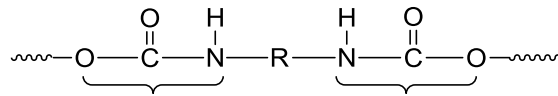


Figure 1-1 : Urethane linkages in polyurethanes.

Urethane bond, formed through the addition reaction between an isocyanate and a hydroxyl group, is shown in Figure 1-2 [59].

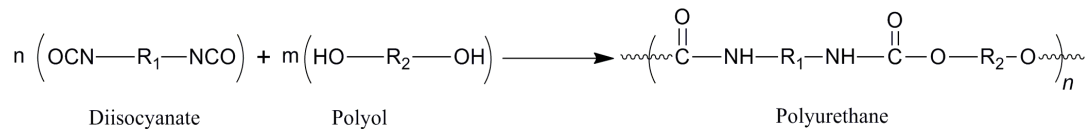


Figure 1-2 : Addition polymerization of diisocyanate and polyol.

Although polyurethanes contain many different functional groups in their backbones consisting of esters, ethers or urea groups, these materials are typically comprised of three basic components: (a) an aromatic or aliphatic diisocyanate, (b) a polyether or polyester diols, and (c) a low molecular weight chain extender (either a diol or a diamine) [60,61].

1.1.1 Isocyanates

The polyurethane chemistry is focused on the isocyanate reactions. The high reactivity of isocyanate groups toward compounds containing active hydrogen can be explained by the following resonance structures illustrated in Figure 1-3 [9,61-67]. The pronounced electropositive charge on the C-atom holding the lowest electron density is caused by the delocalization of electrons onto oxygen atom, nitrogen atom and on the R group. Moreover, the substituents on the aromatic ring can alter the delocalization of negative charge. While an electron withdrawing group in the para or ortho position increases functionality of isocyanate group, an electron donating group diminishes it. Consequently, the electron density exhibit following order: C < N < O in the isocyanate group.

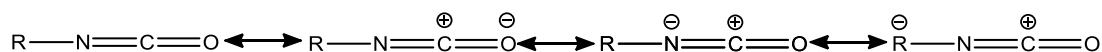


Figure 1-3 : Electronic structure of isocyanate group.

Some of aromatic and aliphatic diisocyanates commonly used in the preparation of polyurethanes are catalogued in Table 1-2 and Table 1-2, respectively.

Table 1-1 : List of aromatic diisocyanates.

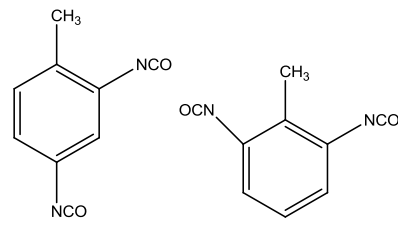
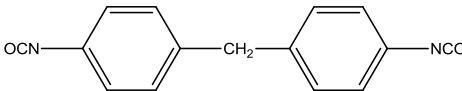
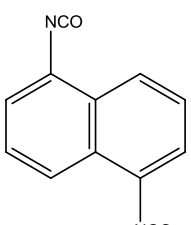
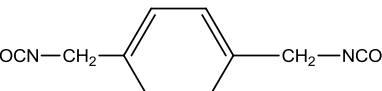
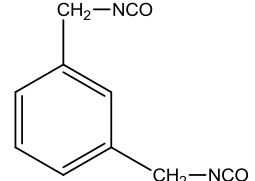
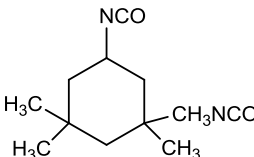
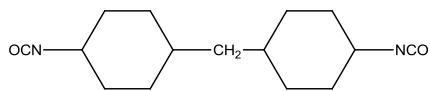
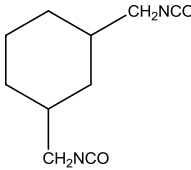
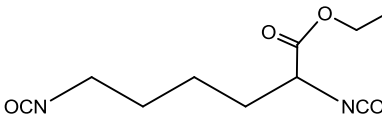
Chemical Name	Structure
<p>2,4,6-Toluene diisocyanate (TDI)</p>	
<p>4,4'-Methylene diphenyl diisocyanate (MDI)</p>	
<p>Naphthalene-1,5-diisocyanate (NDI)</p>	
<p>p-Phenylene diisocyanate (PPDI)</p>	
<p>p-Xylene diisocyanate (XDI)</p>	
<p>m-Xylene diisocyanate (XDI)</p>	

Table 1-2 : List of aliphatic diisocyanates.

Chemical Name	Structure
1,6-Hexamethylene diisocyanate (HDI)	
Isophorone diisocyanate (IPDI)	
4,4'-Dicyclohexylmethane diisocyanate (H ₁₂ MDI)	
1,4-Cyclohexane diisocyanate (CHDI)	
1,3-Bis(isocyanatomethyl)cyclohexane (H ₆ XDI)	
Lysine diisocyanate (LDI)	

1.1.2 Reactions of Isocyanates

In addition to the chemical components, temperature is another determining factor of the progress of isocyanate reactions. At ordinary temperatures (up to 50°C), reactions of isocyanates with hydroxyl groups produces urethanes, while with amine and with water they produce urea. At higher temperatures (up to 150°C), further reactions that yield allophanates, biurets, and isocyanurates occur at a significant rate [66,67].

The reactions of isocyanates can be classified into three main groups: Primary reactions are the ones taking place between the initial components. Secondary reactions are the reactions of isocyanates with reactive hydrogens to give addition products, and the third group is the self-polymerization of isocyanates [61,62,68]. The second and third group reactions form crosslinks among the polyurethane chains without using another crosslinker as an additive.

1.1.2.1 Primary Reactions of Isocyanates

Diisocyanates can react with alcohols, water, amines, and other compounds containing active hydrogen atom. The addition reaction of isocyanate with polyol produces urethane bonds as shown in Figure 1-4. The process is an exothermic equilibrium reaction and influenced by the structure of both reactants. [9,66,67,69].

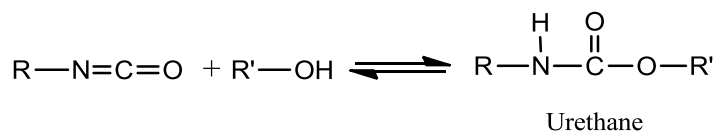


Figure 1-4 : Reaction of isocyanate with alcohol.

The reaction between isocyanates and water produces a substituted urea and gaseous carbon dioxide. In this reaction, the primary product of the reaction is the unstable carbamic acid, which decomposes immediately into an amine, liberating carbon dioxide. Carbon dioxide acting as a blowing agent is the source for polyurethane foam formation. The amine reacts immediately with other isocyanate molecules and produces a symmetrical disubstituted urea as illustrated in Figure 1-5 [70-72]. In the presence of isocyanate, amines can also form urea bonds single-handedly. The reactivity of primary amines is about 100 to 1000 times faster than primary alcohols (conditions; at room temperature in the absence of catalyst) [70]. In any case, the reaction between isocyanate and water creates storage problems.

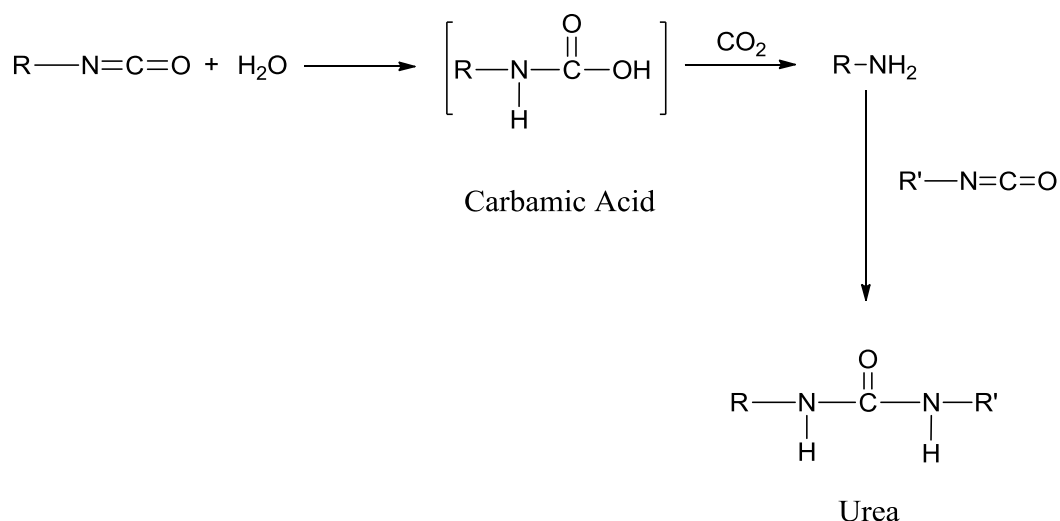


Figure 1-5 : Reaction of isocyanate with water.

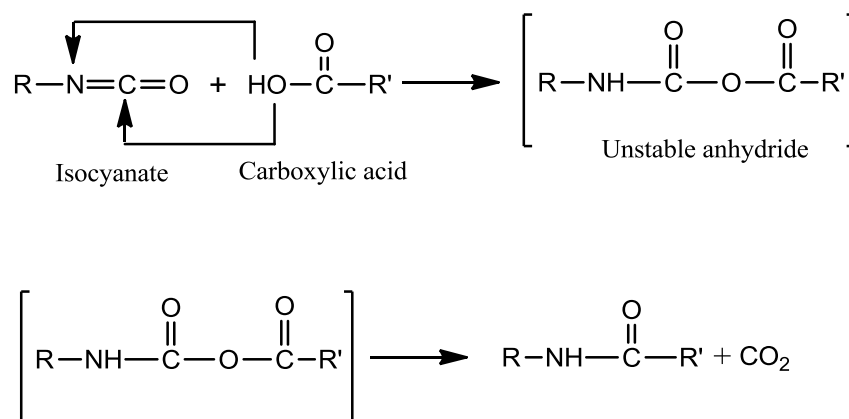


Figure 1-6 : Reaction of isocyanates with carboxylic acid.

1.1.2.2 Secondary Reactions of Isocyanates

Previously formed urethane and urea linkages still include active hydrogen atoms. Under certain conditions, excess isocyanates may react with the active hydrogen atoms of the urethane and urea groups to promote covalent crosslinking. The allophanate formation occurs when another isocyanate molecule reacts with the urethane linkage through the hydrogen on the nitrogen atom as shown in Figure 1-7. Similar to the allophanate formation, biuret linkages are produced when one of the active hydrogens on the disubstituted urea reacts with an isocyanate as shown in Figure 1-8. Both processes result in covalent crosslinks and as a consequence lead to the formation of a polymer network. Allophanate and biuret form over the temperature intervals 100-150°C and 120-150°C, respectively.

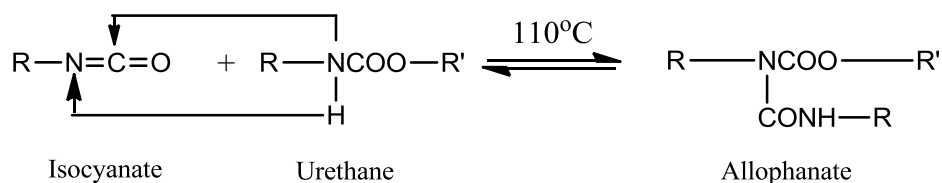


Figure 1-7 : Reaction of isocyanate with urethane.

The reaction between isocyanates and urea groups is substantially faster than that with urethane groups. This is principally due to electron withdrawing effect of the urethane or urea carbonyl groups, which makes the nitrogen less electron dense to active hydrogen. Because of their low thermal stability, allophanates and biurets will decompose into their initial reagents at higher temperatures [67,73,74].

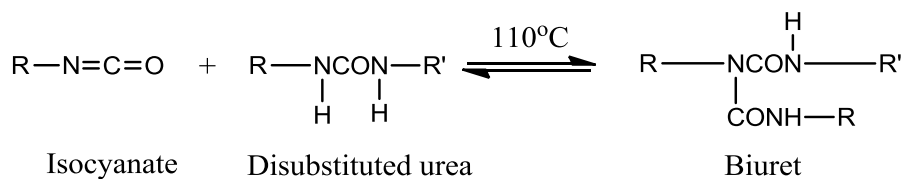


Figure 1-8 : Reaction of isocyanate with urea groups.

Reaction of urea with an isocyanate group can result in the formation of trifunctional biuret leading to gelation [75].

1.1.2.3 Self Reactions of Isocyanates

An isocyanate can also undergo chemical reaction with itself, specifically in the existence of basic catalysts to form uretidinediones (dimers), isocyanurates (trimers), carbodiimides and uretoneimines [76-78]. The formation of uretidinediones takes place at low temperatures, as given in Figure 1-9 and it arises only from reactive aromatic isocyanates. Moreover, dimerization is also an easily reversible reaction above 150°C.

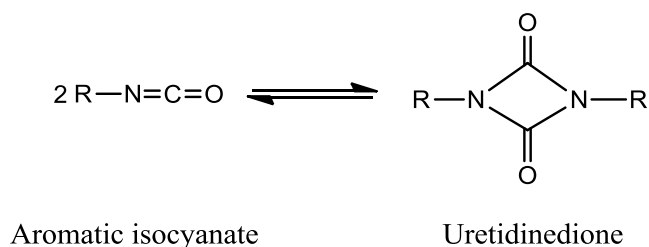


Figure 1-9 : Formation of uretidinedione.

In the presence of basic catalysts, heterocyclic isocyanuric rings resulting from trimerization of isocyanates oligomers can be formed by heating both aromatic and aliphatic isocyanates. The formation of isocyanurates is very stable and the reaction is not readily reversible, as illustrated in Figure 1-10 [79,80]. Polymers consisting of few isocyanuric rings do not have the desired properties and those consisting of too many isocyanurates are brittle and friable [81].

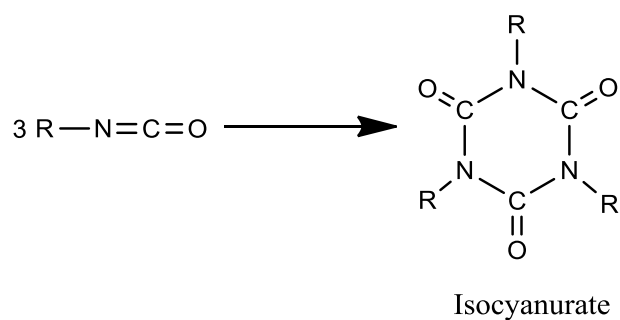


Figure 1-10 : Trimerization of isocyanates.

Another significant self reaction of an isocyanate is the generation of carbodiimides with the elimination of carbon dioxide, [82-85], which exists at high temperature without catalyst [86-90]. The carbodiimides formed in the dimerization reaction can further react reversibly with excess isocyanate to produce an uretoneimine as shown in Figure 1-11 [91].

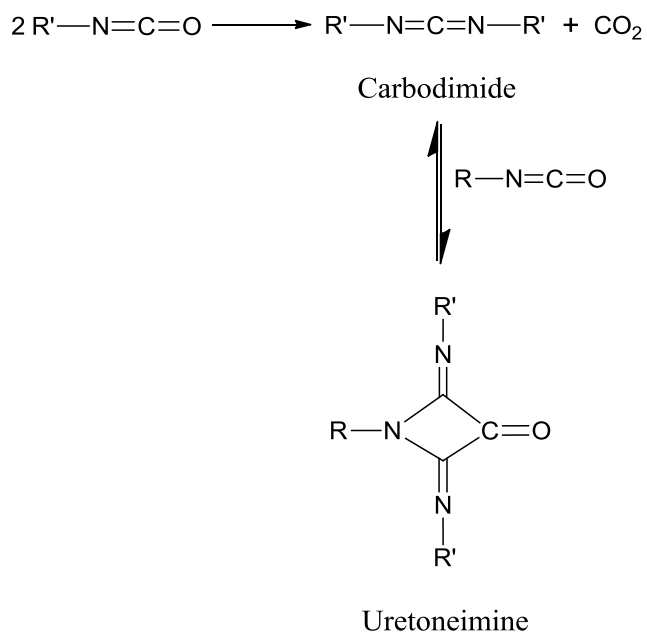


Figure 1-11 : Formation of uretoneimine.

1.1.3 Polyols

Polyols used for polyurethane synthesis are hydroxyl terminated long chain macroglycols with various molecular weights [68]. The structure of polyol is an crucial factor in determining the polyurethane characteristic. They can be classified into two main classes: hydroxyl terminated polyethers and polyesters. In addition, polydienes or polyolefins and polydimethylsiloxanes are also employed in the polyurethane production. The functionality of macroglycols has a great importance in the extent of synthesis. The chemical structures of common polyether polyols and polyester polyols are listed in Table 1-3 and Table 1-4. Compared with ether-based polyols, ester-based polyols possess lower hydrolytic stability; however, they exhibit better thermal and oxidative stabilities.

Table 1-3 : Chemical structure of commercial polyether polyols.

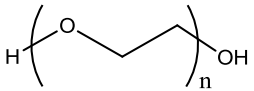
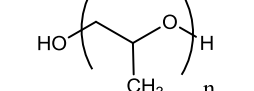
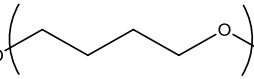
Types of Polyols	Structure
Polyethylene glycol (PEG)	
Polypropylene glycol (PPG)	
Polytetramethylene oxide (PTMO)	

Table 1-4 : Chemical structure of typical commercial polyester polyols.

Chemical Name	Structure
Poly(ϵ -caprolactone) diol (PCL diol)	
Poly (D,L-lactide) (PLA)	
Poly(glycolide) (PGA)	
Polyethylene adipate (PEA)	

1.1.4 Chain Extenders

Chain extenders raise the molecular weight of polymers by chain extension or they contribute degradable linkages into the structure if degradable groups exist. They are generally low molecular weight molecules, which can be classified into two groups: aliphatic diol or diamine, and aromatic diol or diamine. In addition, unsatisfactory chain extension efficacy and failure of mechanical properties of the polyurethane can be observed as a result of unbalanced use of chain extenders in the polyurethane synthesis [92]. Table 1-5 and 1-6 list some common chain extenders.

Table 1-5 : The chemical structures of aliphatic and aromatic diol chain extenders.

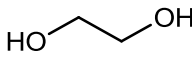
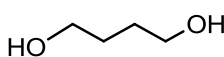
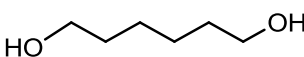
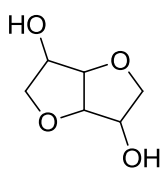
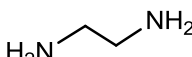
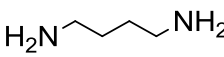
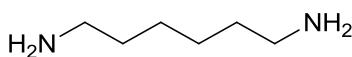
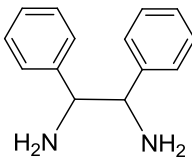
Chemical Name	Structure
Ethylene glycol	
1,4-Butanediol	
1,6-Hexanediol	
Isosorbide diol	

Table 1-6 : The chemical structures of aliphatic and aromatic diamine chain extenders.

Chemical Name	Chemical structure
Ethylenediamine	
Butanediamine	
Hexamethylenediamine	
Diphenylethylenediamine	

1.1.5 Synthesis of Polyurethanes

In general, segmented polyurethane polymerizes with step-growth polymerization in two principle routes: the one-shot method and the prepolymer method. A schematic illustration of the synthesis types is displayed in Figure 1-12 [93-96].

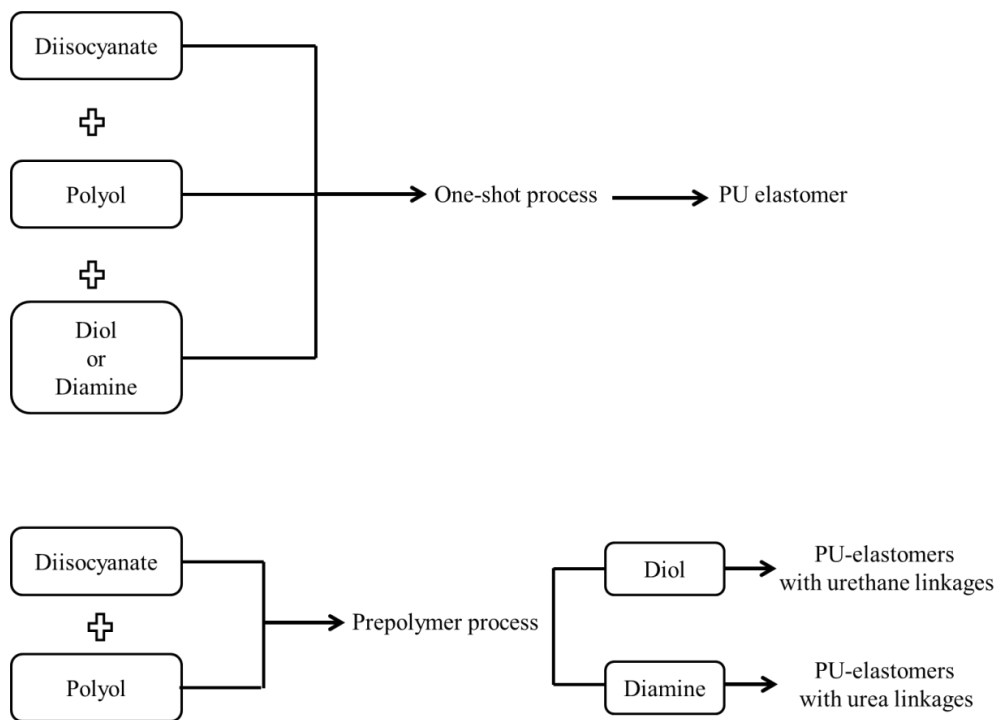


Figure 1-12 : One-shot and prepolymer method of polymerization.

In the one-shot method, all of the reactants, namely isocyanate, polyol and chain extender are combined simultaneously with or without catalyst, and allowed to polymerize. This procedure, however, results in polyurethanes with high molecular weight polydispersity. The reaction is carried out below 80°C to inhibit the formation of side reactions; allophanate and biuret [97].

On the other hand, the prepolymer method is a two-step polymerization; firstly macroglycol is prereacted with excess diisocyanate to form isocyanate terminated prepolymer and it is then mixed with a low molecular weight chain extender during synthesis in order to bond prepolymer chains yielding a high molecular weight polymer [97]. There are several factors that affect polymerization including the use of solvent, the choice of chain extender and the amount of the reactants. Both reactions mentioned above are often carried out in the presence of polar aprotic solvents such as *N,N*-dimethylacetamide (DMAC), dimethylformamide (DMF), tetrahydrofuran (THF), and dimethylsulfoxide (DMSO). In order to obtain high molecular weight polyurethane with linear structure (as shown in Figure 1-13), polymerization in solution is preferred [98].

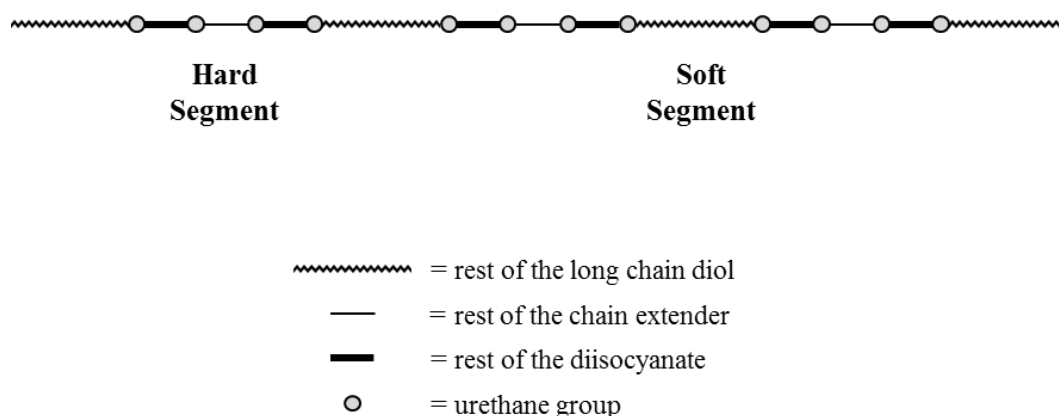


Figure 1-13 : The ideal structure of segmented linear polyurethane.

Curing of the cast mixture yields an elastomeric product. In order to obtain rubber elasticity, the reactants should be chosen such that they produce a lightly crosslinked network structure [99]. The choice of chain extender determines the urethane or urea formation, which is illustrated in Figure 1-14. If a diol based chain extender reacts with the isocyanate terminated prepolymers, urethane linkages are produced.

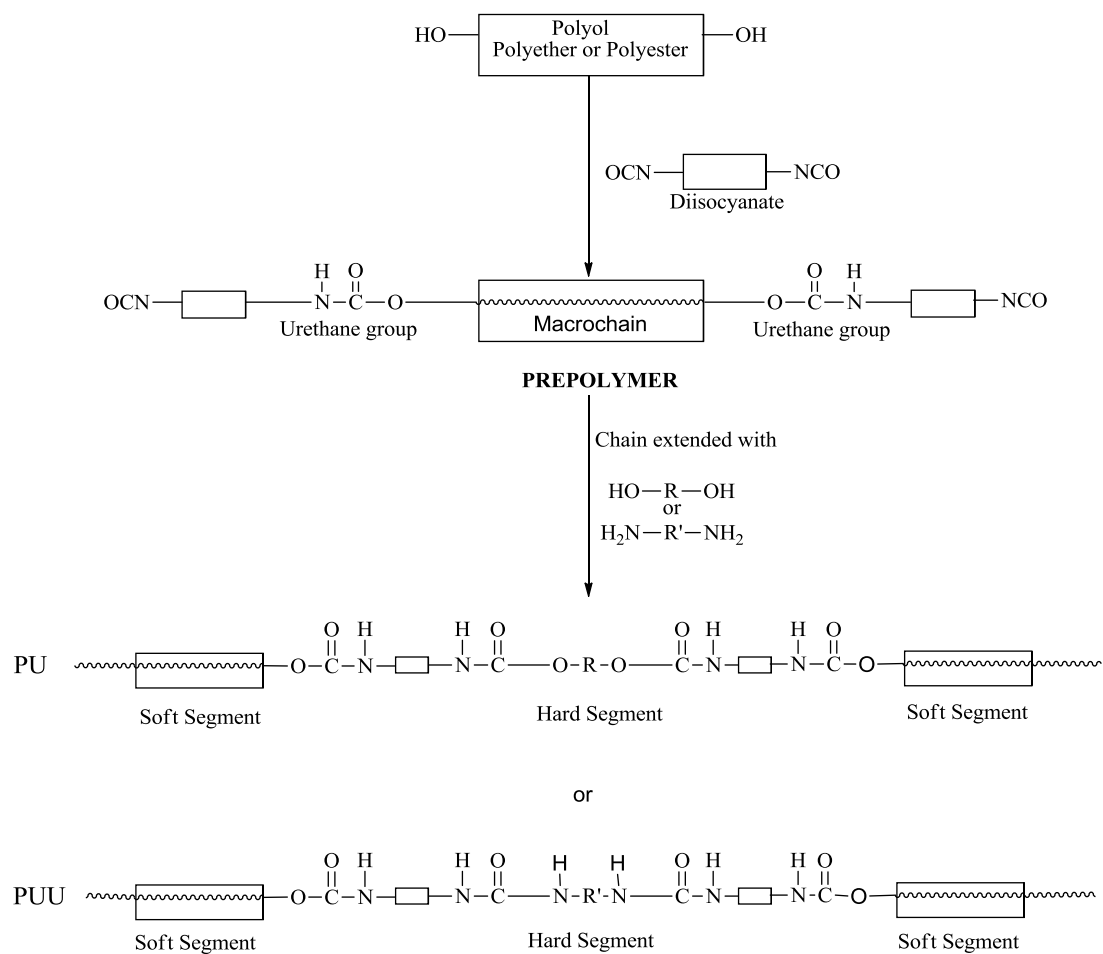


Figure 1-14 : Scheme of prepolymer route for the formation of polyurethane elastomers.

1.4 Polyurethane Structure

Segmented polyurethane (PU) and its analog polyurethane-urea (PUU), containing randomly alternating hard and soft blocks, constitute an industrially important class of block copolymers.

1.4.1 Crystallinity

Crystallization is the process whereby phases are aligned into an ordered structure. One of the determining factors for the physical and mechanical properties of the polymer is the extent of crystallinity, their size and arrangement

of the crystallites particularly with respect to tensile properties [100]. The physical descriptions of crystalline polymers are listed in Table 1-7. Van der Waals or hydrogen bonding interactions hold the polymer segments in their crystal structure. Polymers are never completely crystalline due to amorphous region in the structure [101]. Factors affecting the crystal structure of the polymers contain the linearity of the polymer chains and the degree of copolymerization [100].

Table 1-7 : Classification of crystalline polymers [Adapted from Billmeyer (1984)].

Temperature Range	Degree of Crystallinity		
	Low	Intermediate	High
Above T _g	Rubbery	Leathery, tough	Stiff, hard, brittle
Below T _g	Glassy, brittle	Hornlike, tough	Stiff, hard, brittle

1.4.2 Structure Property Relationship of Polyurethanes

In general, PU usually exhibits a two-phase structure in which hard segment-enriched domains are distributed in a matrix of soft segments, where the segments alternate along the whole length of the chain and appear as isolated or interconnected hard segments in a continuous soft segment matrix [102]. The hard segment-enriched domains are formed mainly by reaction between the diisocyanate and the chain extender, while the soft segments contain a sequence of macroglycol moieties. For this reason, polyurethanes are generally mentioned as segmented block copolymers [103]. This particular molecular architecture, as well as the intrinsic properties of each ingredient used for the synthesis of polyurethanes, explain the unique characteristics of this class of materials when compared to other polymers [6]. The ultimate properties of segmented polyurethanes are strongly governed by microphase separation, which is a consequence of the relative thermodynamic incompatibility between the polar hard segment and less polar soft segments.

The structure of phase separated morphology, which can be seen in Figure 1-15 induces at least two phase microphases; ordered domains of hard segment, and amorphous domains predominantly consisting of soft segment. As in the case of crystalline soft segment, another phase is also present in the polyurethane structure [104]. The segregated morphology is also contingent on two structures of polyurethanes. The primary structure of polyurethane is controlled substantially by the nature (chemical structure, polarity, type and molecular weight) of compositional variables and relative amounts of the reactants, distribution of hard and soft segments, the corresponding dimensions of these segments, crosslinking, and degree of branching. Depending on these parameters, the secondary structure, three-dimensional chain orientations and crystallinity (hard segment domain organization), are formed. Therefore; the morphology, with contributions from both primary and secondary structure as well as processing conditions, is determined [103,105-107].

The phase separation of hard and soft segment domains has been examined by: differential scanning calorimetry (DSC) [108-111], infrared (IR) spectroscopy [112], microscopy, and dynamic mechanical analysis (DMA) [113].

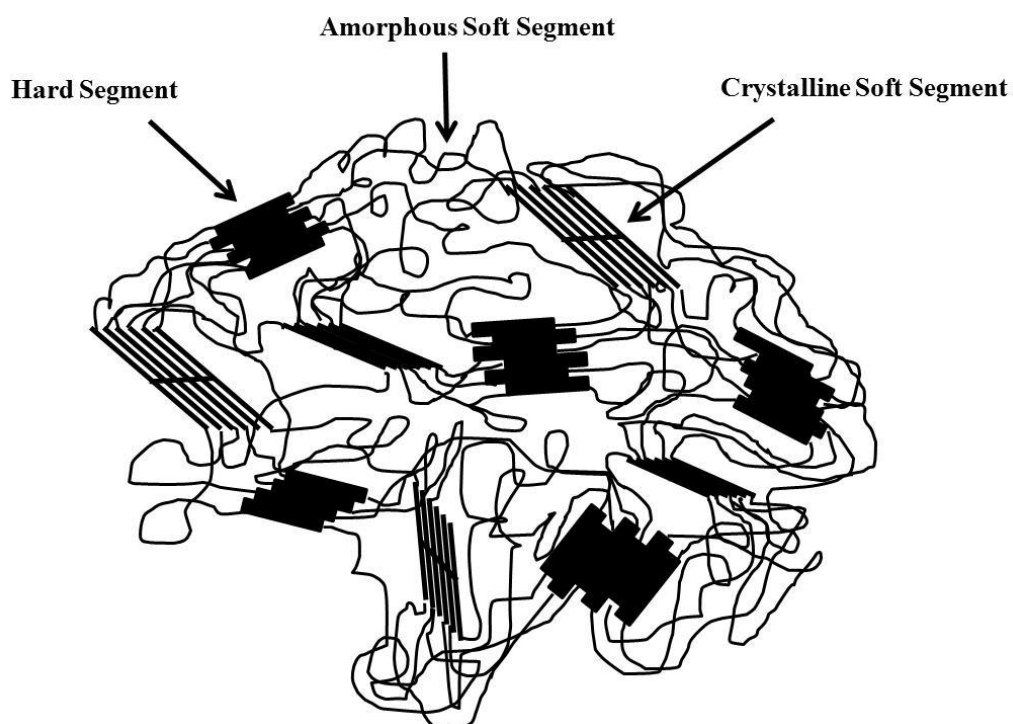


Figure 1-15 : Illustration of microphase separation of hard and soft segment into domains in segmented polyurethanes.

Increased phase separation generally results in improved mechanical properties due to hard segments acting as physical crosslink sites and soft segments adding some flexibility to the polymer [114]. However, it may also impact the degradation rate of the polymer. Increased phase separation, for example, has been shown to protect susceptible functional groups present in hard blocks from hydrolytic agents [115,116]. Similarly, increased phase separation promotes uninterrupted packing of polymer molecules leading to semicrystalline domain formation. Water and other hydrolytic agents are restricted from reaching labile bonds within the semicrystalline domains and reduce the rate of degradation compared to amorphous domains [117]. As a result, high phase separation may lead to increased PU stability and relatively slow degradation rates. Biodegradable elastomeric PUs designed e.g. for tissue engineering applications, should, therefore, promote phase separation for achieving elastic mechanical

properties while still allowing access to labile bonds for degradation to occur at the appropriate rate. Ultimately, the reactant chemistries must be chosen to obtain the properties for specific applications.

Chemical composition, the selection of chain extender and diisocyanate, their relative amounts and processing conditions are known to affect the degree of phase separation, hard segment domain organization, and subsequent polyurethane properties [118]. Generally, polyurethanes chain extended with an aliphatic diol or diamine produce a softer material than do their aromatic chain extended counterparts [119].

A number of parameters can influence the elastomeric properties of PU. The most significant ones are the types of raw materials, the molecular weight of soft segment, and the content of hard segment in polymer. In the previous pages of this thesis, it was shown that polyurethanes are not homogeneous materials at the nanometer scale. A microphase separation process leads to form at least two-microphase structure such as hard and soft segments. In the case of crystalline soft segment, there is another phase. This separation is thermodynamically driven by unfavorable interactions between polar urethane and relatively nonpolar macroglycol segments. The heterogeneous morphology of polyurethanes is perturbed at an interphase where the chemical composition and morphology ultimately attained is a balance between bulk and interfacial interactions.

1.4.2.1 Hard Segment (HS)

Hard segment microdomains are formed when bifunctional isocyanate and polyol react to give urethane linkages and bifunctional isocyanate and chain extender molecules react to give urea bond. Hard segment sequences are imbedded in a matrix of soft segment in polyurethanes. The elastomeric properties of polyurethane segmented block copolymers result from the phase separation between soft segment and hard segments which are respectively above and below

their T_g at ambient conditions. Hard segment organization, rigidity, inter- and intra-segment interactions and existence of bulky side groups determine the hard segment interconnectivity, orientation and consequently, and the phase separation of polyurethane [120]. The hard domains in this two phase microstructure act as strong physical sites, besides reinforcing filler particles to the soft segment phase [121]. Both microphase segregation and ability to form hydrogen bonding between hard segment chains markedly enhance the highly ordered structures among this segment [60]. Therefore; hard and rigid segments segregate into crystalline, semicrystalline or glassy domains [122-124]. Urea containing polyurethanes exhibit better phase separation, resulting from more organized structures since an urea linkage consist of two hydrogen atoms to form hydrogen bonding between the hard segment; however, a urethane bond composed of one hydrogen atom [103,125]. It is demonstrated that a higher degree of crystallinity in the hard segment and better phase segregation is achieved by enhanced domain purity and orientation on condition that the length of hard and soft segment distribution will be uniform [11,126]. The crystallization in hard segment improve the strength of polyurethane acting as powerful and reversible sites maintaining the chains from slipping away from each other under applied force [127]. Furthermore, the selection of a diisocyanate and a chain extender having a more symmetrical structure leading to highly ordered crystallization exhibited improved mechanical properties despite less hard segment content in the polymer [128]. It was demonstrated that shorter hard segments have a lower driving force for phase segregation [111]. Moreover, typical hard segments have a molecular length of only about 25-100 Å [103]. Hydrogen bonds between the urethane or urea moieties yield physical crosslinks between the hard segment domains. These crosslinks fixate the soft segments in a three dimensional network structure and give the material elasticity and excellent tear strength [129]. Due to the physical crosslinks in hard segments by hydrogen bonds, the material exhibits characteristics of a crosslinked elastomer. The physical crosslinks between polymer chains can be reversible in contrast to chemical croslinks. When the temperature increased above the melting point of the hard crystalline part, the

chains of hard segments become mobile. This makes the polyurethane readily processed by extrusion, solvent casting, or freeze drying. By cooling down the material, the crosslinked network will restore and the properties are restored beside [130].

1.4.2.2 Soft Segment (SS)

The soft segments, which are long-chain polyols, strongly control the flexibility and the low temperature behavior of polyurethanes, resulting from amorphous or its low crystallization (semicrystalline) feature. Generally, soft segment sequences soften the material and facilitate flexible and elastic behavior to the polyurethane as well as susceptibility to degradation [121]. Soft segments facilitate them to perform excellent elastomeric behavior even in cold temperatures [127]. The use of more hydrophobic macroglycols in the synthesis improves the phase separation on account of more polar groups in the hard segment [131]. Since the glass transition temperature of the hard segments is substantially higher than that of the soft segments, the soft segments keep rubber elasticity between glass transition temperatures [118].

The polyester based PUUs exhibit better phase mixing than polyether based counterparts synthesized from the same molecular weight soft segment. Moreover, the extent of phase separation in polyether based polymer enhanced with increased molecular weight of soft segment [132]. Silver and colleagues found that phase separation, crystallinity, and the hard segment content at the surface increased with polyol molecular weight [133].

Since PCL and its degradation products are nontoxic to cells confirmed by the Food and Drug Administration (FDA), they are overviewed for many tissue repair and drug delivery applications [134-137]. Due to its low hydrophilicity and semi-crystalline structure lead to very slow degradation [134]. In those studies,

polyurethanes synthesized from PCL exhibited enhanced elasticity and tensile strength compared to PCL because of the existence of physical crosslinks.

1.4.2.3 Hydrogen Bonding

The hard segments are formed from the strong inter- or intra-molecular hydrogen bonds between the hard-hard segments of urethane or urea bonds which leads to phase separation in hard segment domain and phase mixing between hard and soft segments [97]. Hydrogen bonding results from the attraction of hydrogen atoms in one molecule with an oxygen or nitrogen atom in another molecule. The hydrogen bond is the strongest secondary chemical bond with a strength calculated to about 20-50 $\text{kJ}\cdot\text{mol}^{-1}$ [138]. N-H group in urethane group is the proton donor whereas the carbonyl and the etheric oxygen are the proton acceptors. Hydrogen bonding in urethane and urea chains was illustrated in Figure 1-16 [108,139,140]. Considerable efforts have been made to elucidate the nature of hydrogen bonding in polyurethanes. Hydrogen bonding along with microphase composition is an important parameter when designing biostable or biodegradable materials. Tang et al. [141] suggested that the range of the susceptibility to hydrolytic degradation of the various carbonyls in polycarbonate-based polyurethane was as following order: nonhydrogen bonded carbonate > nonhydrogen bonded urethane > hydrogen bonded carbonate > hydrogen bonded urethane. Thus, knowledge of hydrogen bonding distribution in the polyurethane materials becomes essential when designing biodegradable materials and degradation rate has to be fixed.

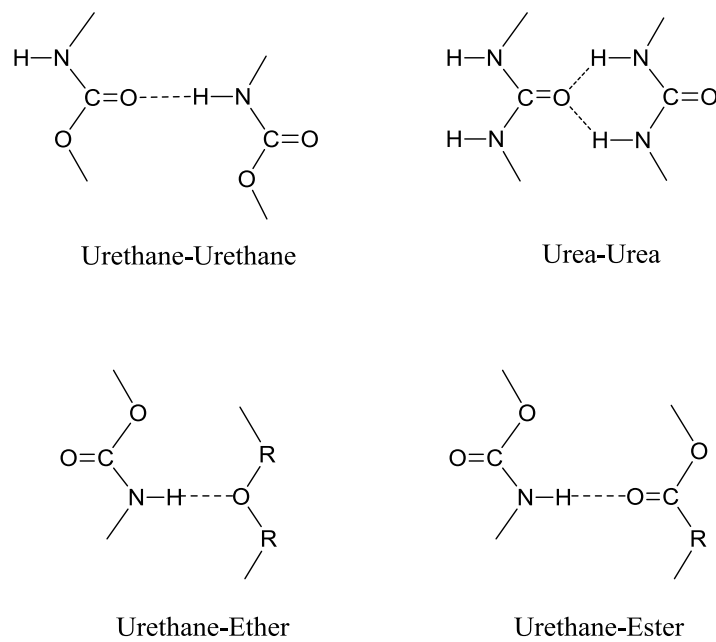


Figure 1-16 : Hydrogen bonding in polyurethanes between hard-hard segments and between hard-soft segments.

1.5 Mechanisms of Polyurethane Degradation

Polyurethanes have been reported to undergo chemical, physical, and biologically induced mechanisms of degradation as described in Figure 1-17. All of these mechanisms affect polyurethane properties, for example during production, processing, and sterilization, however mechanical and chemical degradation will have the most significant effects on PU degradation in living organisms.

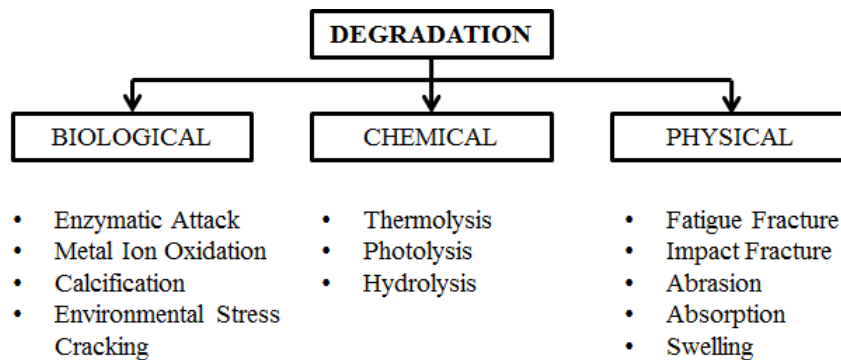


Figure 1-17 : Polyurethane degradation mechanisms [Adapted from Scyher (1991)].

1.5.1 Biological Degradation of Polyurethanes

The diverse properties that may be achieved by segmented polyurethanes make them attractive candidates for use in several biomedical applications. In general, these handmade polymers can be used as long-term implants in pacemaker lead insulation, cardiac assist devices, breast implants, and others [97]. In these uses, polymer stability is vital to the success of the device. The clinical relevance of polyurethane biodegradation is highlighted with the failure of pacemaker lead composed of polyether urethane due to cracking. Furthermore, polyurethanes can be applied as biodegradable constructs in short-term implants when the tissue weakened by disease, injury or surgery and healing wound, broken bone, damaged blood vessel in the form of sutures, bone fixation devices, or vascular grafts. Santerre et al. defined multifaceted mechanical and chemical mechanisms that work synergistically in degrading PUs in the body as environmental degradation, which leads to changes in physical properties. Environmental biodegradation encloses environmental stress cracking, the aqueous tissue environment, hydrolytic enzymes, oxidative agents, calcification, mechanical stresses, metallic ions, salts, acids, etc. [58]. For example, the cyclic mechanical stresses experienced during the cardiac cycle can physically cleave bonds within biodegradable polyurethane chains, resulting in polyurethane fatigue.

Chemical degradation of polyurethanes is mediated by oxidation and hydrolysis. Typically, when a biomaterial is implanted, it is exposed to physiological fluids and recognized as a foreign matter by the body. The human body perceives biomaterials as foreign body and then attacks, destroys or isolates the this foreign matter. In general, polyurethane degradation is achieved by being exposure to the cellular components in foreign body response [142]. After formation of hydrated layer on the surface of the biomaterial, cells adhere to the surface to recognize the matter. Adherent cells release a number of degradative agents including acid, reactive oxygen intermediates species and hydrolytic enzymes leading to polymer erosion [143].

For segmented PUs used as biomaterial scaffolds for cardiac tissue engineering, a combination of cyclic stresses, inflammatory cells, oxidative agents, inflammatory and injury-related enzymes, as well as other factors will likely contribute to the environmental biodegradation of these synthetic polyurethanes.

1.5.2 Hydrolysis

Hydrolysis is a chemical reaction during which a water molecule break down the material involving scission of susceptible functional groups. The bonds of interest that are most susceptible to hydrolytic degradation are the ester, urea, and urethane linkages. The proposed degradation mechanisms are illustrated in Figure 1-18. In hydrolysis of an ester bond, it decomposed into an acid and an alcohol, and the produced acid in the reaction catalyses further ester hydrolysis. Owing to the autocatalytic nature of this degradation, in which at least one of the reactants is also a product, polyester based polyurethanes generally degrade more rapidly than their polyether counterparts [144,145]. Ester hydrolysis occurs when the nucleophile (e.g., water or hydroxyl ion) attacks the carbon of the carbonyl group of the ester. In an aqueous base, hydroxyl ions are better nucleophiles than water molecules. In acidic environment, the carbonyl group becomes protonated, and resulted in a much easier nucleophilic attack. Thus; polyurethanes are attacked

and hydrolyzed in the presence of anions and cations acting as strong catalysts for hydrolysis, as well as salts and enzymes [97]. The urea bond can undergo hydrolysis to produce a carbamic acid and an amine, and the urethane yields a carbamic acid and an alcohol resulting from degradation. The carbamic acids are then irreversibly reduced to amines, liberating carbon dioxide. Under normal circumstances, the urethane bond remains relatively resistant to hydrolysis, but high temperature and other factors can affect this resistance [144]. Severe hydrolysis results in chain cleavage and an accompanying reduction in polymer molecular weight.

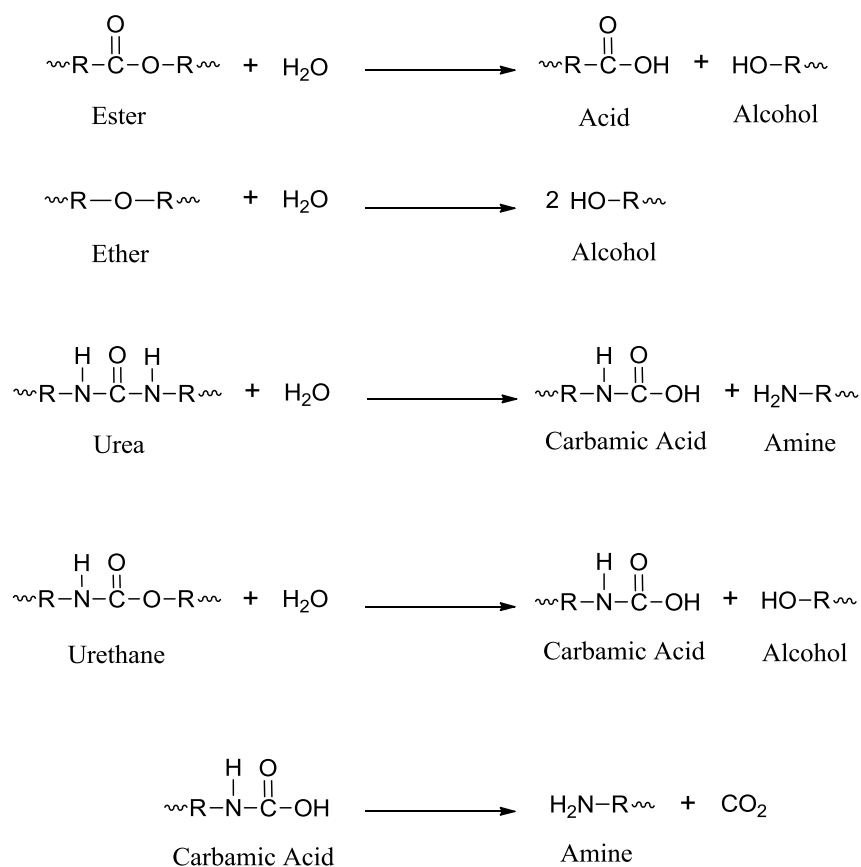


Figure 1-18: Hydrolytic degradation mechanism of polyurethane bonds [Adapted from [97]].

The aliphatic ester linkages in polyurethanes are known to be degraded by hydrolysis [146]. The bulk modification of polyurethane in terms of the degradation rate is generally achieved through changes to the soft segment. Most degradable polymers are polyesters. Ester is a covalent bond with polar nature, can be broken down by hydrolysis, oxidation and esterase enzymes. The C–O bond, as can be seen in Figure 1-19, breaks during degradation. One other thing keep in mind is that the rate of scission of ester-based polyurethanes in biological environment was about 10 times greater than for the same materials aged in a 50% relative humidity atmosphere [147].

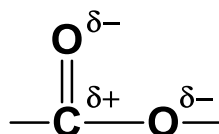


Figure 1-19 : The illustration of ester bond.

1.5.2.1 Enzyme-Catalysed Hydrolysis of Polyurethanes

Under physiological conditions, enzymes in particular have been shown to affect the kinetic of hydrolysis of polyurethanes [60]. It was reported that ester-based polyurethanes are susceptible to hydrolysis by enzymes such as esterase, papain, bromelain, ficin, chymotrypsin, trypsin, and cathepsin C [148]. With the development of biodegradable polyurethanes, the enzyme-sensitive polyurethanes have much potential to mimic biomaterials in soft tissues by incorporating amino acids and peptides into the polymer backbone [149,150].

1.5.3 Oxidation

Mechanisms of oxidation include auto-oxidation, metal-catalysed oxidation, as well as oxidation by peroxides, free radicals, and enzymes [97]. Among the cellular components oxidative agents including superoxide, hydrogen peroxide, hypochlorous acid (HOCl), and peroxynitrite anion (ONOO^-) are the most rapid and destructive ones in biodegradation of polyurethanes [151-154]. Christenson et al. studied the biostability of polycarbonate urethanes and polyether urethanes, and concluded that the degree of biodegradation of carbonate based polyurethane was limited to a thinner surface layer and was significantly less than that exhibited by ether based ones. They found also in vitro oxidative degradation was inhibited by antioxidants [154].

Sutherland and colleagues determined that phagocyte-generated oxidants are involved in polymer oxidation [155]. Cells such as neutrophils and monocytes produce hypochlorite and peroxide [156], which can attack and degrade the polyurethane surface, causing fissures and cracks. In phagocytic vacuoles, superoxide radicals are converted into hydrogen peroxide, hydroxyl radicals, and other reactive products in a process termed the oxidative burst [157]. The release of these chemical oxidants contributes to the oxidative degradation of polyurethanes in their models of polyurethane oxidation, Sutherland and colleagues suggest that there are three dominant mechanisms in the oxidative degradation of polymers: polymer scission, increment in surface oxygen content, and reaction of the aliphatic ether or ester bridges [155]. Many polymer-derived species are involved in the oxidation reactions, notably carbonyl and hydroxyl groups such as $\text{ROO}\cdot$, ROOR , $\text{RCO}\cdot$, $\text{RO}\cdot$, and $\text{R}\cdot$ [97]. Polyether soft segments are particularly susceptible to oxidation, where a hydrogen atom can be abstracted from the methylene carbon. This carbon radical is then susceptible to oxygen addition, forming peroxide radical [158]. Zhao and colleagues investigated the in vivo oxidation of Pellethane[®] 2363-80A (a commercial polyether polyurethane)

and attributed the surface cracking to the activity of oxygen free radicals, such as superoxide anions and hydrogen peroxide [159].

1.6 Polyurethane-Heparin Blends

Medical uses of polyurethanes are well known especially in the production of blood contacting devices such as heart valves and veins. Although PUs have inherent hemocompatibility, preparation of composites by using organic and inorganic substances is a novel area. Heparin is one of these chemicals used in scaffolds to enhance the compatibility of PU matrices.

Heparin is a highly-sulfated glycosaminoglycan, having the highest negative charge density of any known biological molecule. For many years, heparin has been used as an anticoagulant, other properties have recently been investigated in biological processes such as its interaction with a great number of proteins related to adhesion, proliferation [160,161] or osteogenic differentiation [162-165]. Oligomerization of FGF molecules and maintaining BMPs in extracellular space is also achieved by heparin [165,166]. Due to its special interactions with proteins and antithrombogenic properties it has been used to design scaffolds especially for bone and hepatic tissue engineering [167,168]. In tissue engineering, endothelization is a major problem which is critical for new tissue regeneration. In a bone tissue engineering approach, heparin was used to modify the underlying scaffold material in order to promote cell proliferation and differentiation by promoting the adsorption of attachment proteins like fibronectin and vitronectin [167]. Yu et al. prepared heparin containing collagen/chitosan complex membranes and investigated their potential use for hepatic tissue engineering. Their results indicates that heparin has improved blood compatability of the membranes. Normally, under in vitro conditions hepatocytes will lose their functions rapidly. Therefore, it is stated that anticoagulant or vascularization of the scaffolds is crucial for hepatocyte culture. Thus, incorporation of heparin to

the scaffolding material will increase antithrombogenicity and neovascularization [168].

1.7 Aim of This Study

Aim of this study is to synthesize biomedical grade polyurethanes, and examine the effects of preparation parameters on the properties of the resulting polymers. For that reason, biomedical grade PUs were synthesized from poly(ϵ -caprolactone) diol (PCL diol) or from poly(ϵ -caprolactone) triol (PCL triol) and 1,6-Hexamethylene diisocyanate (HDI) without adding any other ingredients (solvent, initiator, stabilizer) via one-shot polymerization. In this study, HDI, which is suggested as a non-toxic amine producer and PCL diol or triol which is suggested as a non-toxic to cells during degradation of polyurethanes has been used. One of the main advantages of using polyurethane is the ability to tailor the structural and functional properties of these materials to meet these requirements for site-specific applications. The effect of the diisocyanate on the properties of polyurethanes was investigated by Fourier transform infrared spectroscopy-Attenuated total reflectance (FTIR-ATR), differential scanning calorimetry (DSC), dynamic mechanical analysis (DMA) and X-Ray diffraction (XRD). The resulting polymer films were also examined by mechanical tests and water contact angle measurements. Hence, comprehensive knowledge of the effects of several parameters such as the stoichiometric ratio and type of polyol on the relative amounts of urethane and/or urea groups are important to obtain optimum properties. The morphology of a multiphase system, such as the one present in polyurethanes, plays an important role in determining the final properties of the product. Therefore, in order to obtain desired product properties, a control over the morphology is essential.

Further, an aqueous solution of heparin was added into the one of the various prepolymers before curing process to enhance biocompatibility and hydrophilicity of the resulting polymer. Heparin containing polymer films were characterized by

mechanical tests and contact angle measurements. The morphology of polyurethanes and its key role in mechanical and hydrophilic behavior were extensively examined in this study.

CHAPTER 2

EXPERIMENTAL

2.1 Materials

1,6-Hexamethylene diisocyanate (HDI) (molecular weight: 168.2 g.mol^{-1} ; boiling point: 261°C ; density at 25°C : 1.047 g.cm^{-3}) was purchased from Sigma (St. Louis, Missouri, USA) and was stored at 4°C . This reactant was carefully manipulated since it has a low vapor pressure and is potentially toxic by inhalation. Since these preparations involved toxic and reactive isocyanates, all the necessary precautions for their safe handling and during their reactions under anhydrous conditions were taken. Poly(ϵ -caprolactone) diol (PCL diol) ($M_n = 1250 \text{ g.mol}^{-1}$ and $M_n = 2000 \text{ g.mol}^{-1}$) and poly(ϵ -caprolactone) triol (PCL triol) ($M_n = 900 \text{ g.mol}^{-1}$) were purchased from Sigma-Aldrich (St. Louis, Missouri, USA) and were stored at room temperature. Nevparin (5000IU/mL) was purchased from Mustafa Nevzat İlaç Sanayi.

2.2 Polymer Synthesis and Film Casting

A series of polyurethanes were prepared through one-shot polymerization (as shown in APPENDIX A) by addition of 1,6-Hexamethylene diisocyanate (HDI) to poly(ϵ -caprolactone) diol (PCL diol) or poly(ϵ -caprolactone) triol (PCL triol) without adding any other ingredients such as solvent, catalyst, and stabilizer, etc., followed by curing. It is known that presence of catalysts, solvents, fillers, monomers etc. reduce biocompatibility since these molecules may leach out from the polymer and may induce toxic responses. These properties fulfill the design criteria of reactive and functional crosslinkable polyurethane films. In accordance with the above discussions and to develop high performance curable polymer films, it was decided to study the effect of NCO/OH ratio and different

types of polyols on the thermal and mechanical properties of PUs. Initially an isocyanate terminated polyurethane (PU) was synthesized through one-shot polymerization. In the next step, these prepolymers were cured in a vacuum oven to obtain the crosslinked films via formation of allophanate linkages. The synthesis route for preparation of diisocyanate terminated polyurethane is outlined in Figure 2-1. Excess diisocyanate gives the opportunity to form cross-linked structures in polymer matrix through curing via allophanate linkage formation as shown in the second step of Figure 2-1.

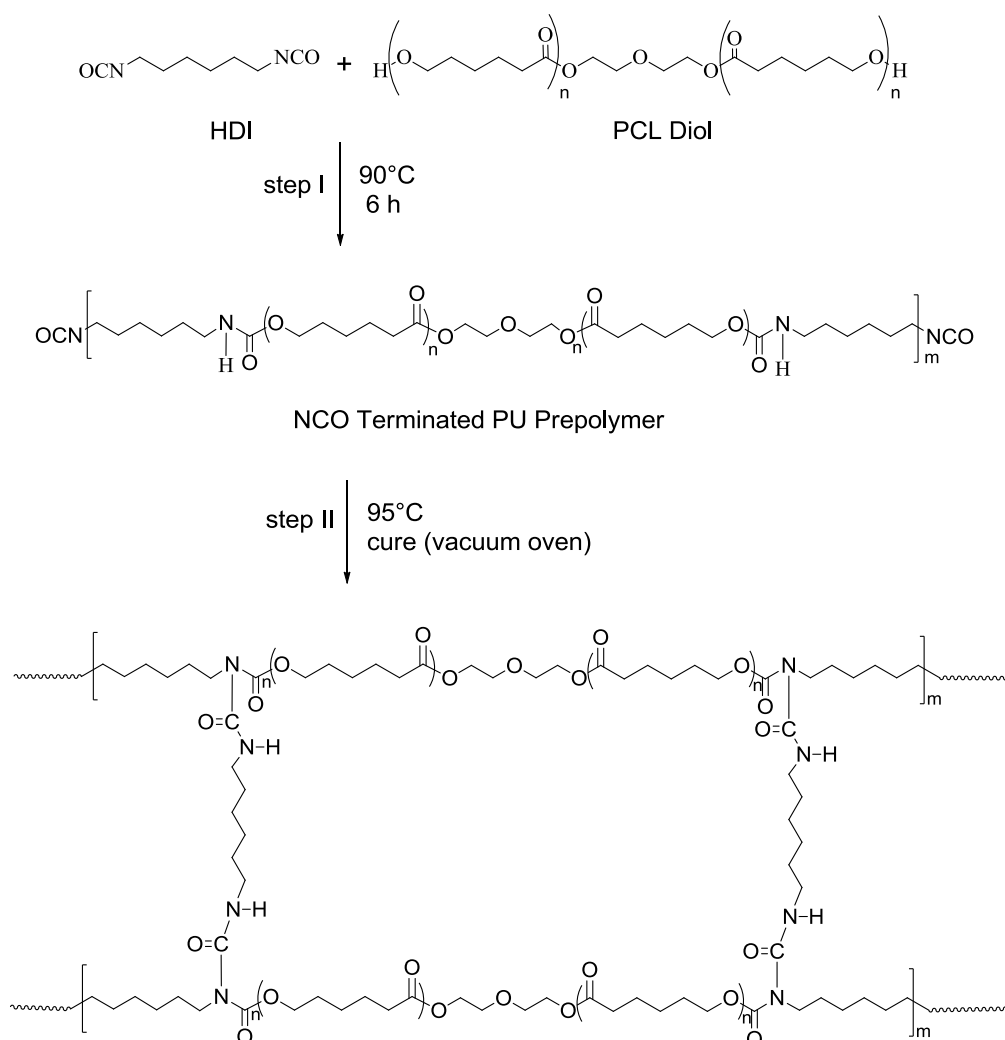


Figure 2-1 : Chemical route for synthesis of PUs.

In brief, synthesis was carried out in a 25 mL three-necked round bottom flask attached to a reflux condenser. The vessel was immersed in an oil bath, and kept under a constant nitrogen flow to avoid humidity in the reaction vessel. Firstly, polyester based soft segment component such as PCL diol with molecular weight 1250 or 2000 or PCL triol with molecular weight 900 was placed into the reaction vessel. The temperature of the oil bath was adjusted to 80°C, and PCL diol or triol was vacuumed and dried for 2 h to remove residual moisture. Then, N₂ was purged through the viscous liquid for 1 h. During this time interval, the temperature was increased to 90°C. Then, HDI was added to the solution dropwise by means of a syringe while stirred continuously at 120 rpm. The mixture was allowed to react at 90°C under nitrogen atmosphere for 6 h, time enough to form isocyanate terminated prepolymer according to kinetic studies previously reported [169]. The nitrogen purge was kept throughout the synthesis to ensure a dry atmosphere to minimize the secondary reactions. The final product was a viscous, transparent fluid, and it was poured into glass petri dishes at ambient conditions. The petri dishes were then placed in a vacuum oven at 95°C and were allowed sufficient time for curing. In the case of polyurethane urea (PUU) synthesis, the same procedure was followed, but the second step was carried out in an oven at 95°C under atmospheric conditions so that the present humidity resulting in the formation of biuret linkages as well as allophanate linkages. The schematic representation of moisture-cured polyurethane ureas is shown in Figure 2-2. The curing reaction continued until isocyanate groups peak totally disappeared in the IR spectra of the sample taken from the reaction balloon at different time intervals. The thickness of films, which ranged from 200 to 400 μm, was controlled by adjusting the amount of the polymer solution cast and macro images of films are shown in APPENDIX B. The films were maintained in a vacuum desiccator until use.

The nomenclature used for this polymer identifies two of the main constituents of the polyurethane: the first pointing molar ratio of diisocyanate to polyol followed by a second set pointing the molecular weight of the polyol. For example, nomenclature in PU5-1250 means that molar ratio of diisocyanate to polyol is 5 and PCL diol with molecular weight 1250 was used. Polyurethane ureas were named as PUU followed a number representing molecular weight of soft segment. The triol soft segment based polyurethanes were named with the diisocyanate employed followed by a number representing the weight fraction of hard segment in the polyurethane.

Theoretical values of hard segment (HS) content were calculated from the molecular masses of the reactants and their relative stoichiometric in terms of the following formula:

$$\text{HS}\% = \frac{n(M_{\text{HDI}})}{n(M_{\text{HDI}}) + n(M_{\text{PCL}})} \times 100 \quad (2-1)$$

where M is the average molecular weight of the reactant ($\text{g}\cdot\text{mol}^{-1}$) and n is the number of mole. Table 2-1 demonstrates the different reagents employed to synthesize the different PU along with their abbreviations and component ratios. The concentration of the HS in the polymer was varied between 17 and 48 wt.% by changing the length and type of the soft segment.

The extent of curing time for PU5-900T compared to PU5-2000 most probably comes from the change in the number of functional groups of polyol. Branched polymer involves more chain ends than its linear counterpart of equal molecular weight. Although the mol ratio is similar for both samples ($\text{HDI}/\text{PCL} = 5/1$), the functional group number is 3 times higher for PU5-900T than that of PU5-2000.

Table 2-1 : Composition and the experimental conditions used in the preparation of polyurethanes.

Polymer code	Molar ratio	HDI / PCL	Curing conditions		HS content
	HDI / PCL	(mL /g)	T (°C)	t (h)	(wt.%)
PU1.5-1250	1.5 / 1	2 / 10	95	>250	17
PU2.5-1250	2.5 / 1	3 / 10	95	40	25
PU5-1250	5 / 1	6 / 10	95	60	40
PU5-2000	5 / 1	4 / 10	95	150	30
PUU5-2000	5 / 1	4 / 10	95	130	30
PU5- 900T	5 / 1	9 / 10	95	230	48

(For 10 g PCL diol 2000; number of moles = $10 \text{ g} / 2000 \text{ g.mol}^{-1} = 5 \times 10^{-3}$ moles;
number of functional groups = $2 \times 5 \times 10^{-3}$ moles = 1×10^{-2} moles.

For 10 g PU5-900T; number of moles = $10 \text{ g} / 900 \text{ g.mol}^{-1} = 11 \times 10^{-3}$ moles;
number of functional groups = $3 \times 11 \times 10^{-3}$ moles = 3.3×10^{-2} moles)

Although it is not significant, the curing time decreased in the presence of humidity in the curing environment by forming allophanate and biuret linkages (which were observed in IR spectra). The experimental parameters were used to evaluate the effect of hard segment content on overall properties of the polymers.

2.3 Preparation of Polyurethane Blends

For the preparation of polyurethane blend, nevparin which was a solution of heparin was used. Previously prepared PU5-2000 was subsequently mixed with nevparin solution generating urea bonds with high yield. The polymer blend was named as PUU5-2000-HP. In brief, 200 μL solutions were added to 1 g PrePU5-2000 and it was stirred by a spatula for 5 minutes. The final product was a viscous, transparent fluid, and it was poured into glass petri dishes under ambient conditions. The petri dishes were then placed in an oven at 95°C and were allowed sufficient time for curing. The main outcome of all these studies

was to improve biocompatibility, hydrophilicity and mechanical behavior. It was intended to design the present study to assess the importance of the blend formation on material properties.

2.4 Characterization Methods

Experimental part was divided into mainly three steps. In the first step, during the synthesis of six different polyurethanes FTIR-ATR was used to characterize curing time of reaction. In the second step, after preparation of films, they were characterized by FTIR-ATR, DSC, DMA, XRD, mechanical test and water contact angle. In the last step of this study, one of the resulting polymers was blended with heparin and characterized by mechanical test and water contact angle.

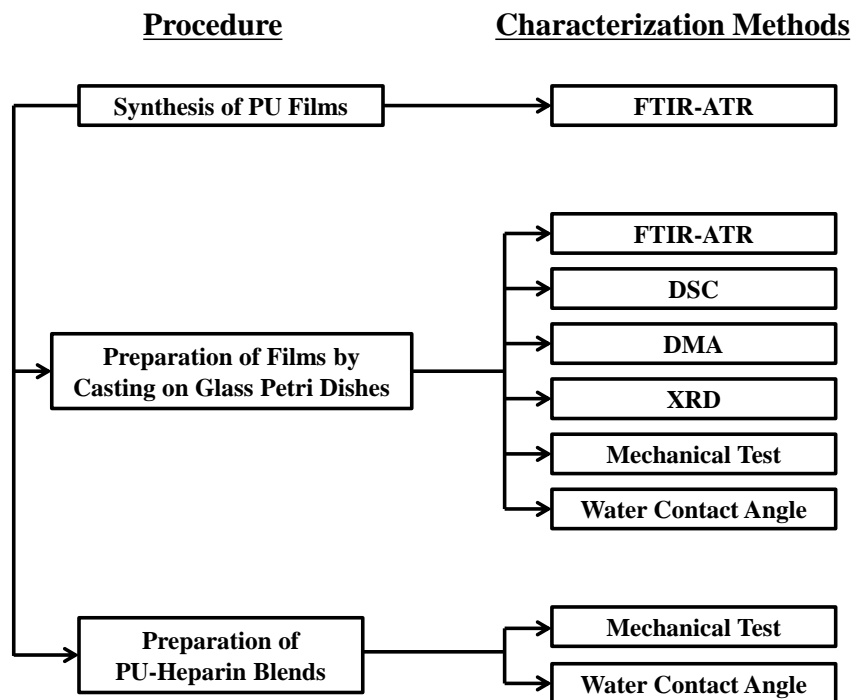


Figure 2-3 : Experimental procedures and characterization methods.

2.4.1 FTIR-ATR Spectroscopy

The polymerization reactions of PUs and characteristics of the polymers related with composition were characterized by Perkin Elmer Spectrum BX-FTIR-ATR Spectrometer. IR spectra of the viscous prepolymer solution that was taken at different times of the synthesis were obtained by applying a thin film over a dry KBr disc. Each sample was scanned for 32 times with a resolution of 4 cm^{-1} between $4000\text{-}400\text{ cm}^{-1}$. After the formation of solid PU films IR spectra were followed using ATR attachment which has a ZnSe crystal. All spectra were collected in the spectral range of $4000\text{-}600\text{ cm}^{-1}$ using 32 scans with a resolution of 4 cm^{-1} . The spectral data were acquired by using ORIGIN 8 software. The $\nu(\text{N-H})$ and $\nu(\text{C=O})$ bands were deconvoluted considering peaks as a Gaussian-Lorentzian sum function with a number of iterations to obtain the best fit peaks to estimate complex band envelopes and to identify underlying component bands by using the Peakfit Version 4.12 software. The maximum frequency (ν) and area of each band were recorded.

2.4.2 Differential Scanning Calorimetry

Differential scanning calorimetry is a common tool to determine molecular organization changes, such as phase separation, glass transition and melting. DSC thermograms were recorded to evaluate the thermal properties of the polymers. Samples of films were sealed in standard aluminium capsules and thermal analysis was carried out using Scinco DSC N-650 (Korea) Differential Scanning Calorimeter at a heating rate of $10^\circ\text{C}\cdot\text{min}^{-1}$ over the range $-100^\circ\text{C}\text{-}200^\circ\text{C}$ under nitrogen atmosphere. The glass-transition temperature (T_g) and crystalline melting temperature (T_m) were recorded.

2.4.3 Dynamic Mechanical Analysis

The viscoelastic behavior of all samples was analyzed with Perkin Elmer Pyris Diamond DMA instrument (USA). The samples were measured in an oscillatory

tensile mode at a frequency of 1, 2, 4, 10 and 20 Hz at a heating rate of $5^{\circ}\text{C}\cdot\text{min}^{-1}$ under nitrogen atmosphere from -100 to 150°C . The storage modulus (E'), loss modulus (E'') and tan delta values were recorded against temperature at different frequencies. The T_g values were obtained from the peak maxima of tan delta curves.

2.4.4 X-Ray Diffraction Measurements

X-Ray diffraction measurements were followed using a Rigaku Ultima-IV X-Ray Diffractometer (Japan) with a copper target ($\lambda = 1.54 \text{ \AA}$), 40 kV 30 mA, and equipped with a graphite monochromator. The data collection was performed in the range $2\theta = 5-80^{\circ}$ with a step of 0.02° at the rate of 2°min^{-1} .

2.4.5 Mechanical Tests

Mechanical properties of films were determined by a mechanical testing machine (Lloyd Instruments, Ltd., Fareham, UK), equipped with a 100 N load cell and a crosshead speed of $10 \text{ mm}\cdot\text{min}^{-1}$. For tensile tests; film were cut as rectangular strips (10 mm x 50 mm). In tensile tests; the gauge length was 10 ± 2 mm. The thickness of each sample was determined by a micrometer making measurements at different parts and the average values were estimated. At least 5 specimens for each type of films were tested. Ultimate tensile strength (UTS), Young's modulus (E) and percent elongation at break (EAB%) values were calculated from the load versus deformation curves which were obtained as print outs for each specimen. The overall stress deformation curves were converted to engineering stress–strain curve, where stress is the load applied per unit area (F/A) and strain is the deformation per unit length. The engineering UTS was obtained from the equation $\sigma = F/ A_0$, where σ is the tensile strength (MPa), F is the maximum load applied (N) before rupture, and A_0 is the initial area (mm^2) of the specimen. Young's modulus is defined as the slope of the straight line in the elastic deformation region (initial linear portion of the stress-strain curve).

2.4.6 Contact Angle Measurements

In order to determine the hydrophilicity of the polyurethane surfaces, water contact angles of the films were measured by using a goniometer (CAM 200, Finland). 5 μ L deionized water droplets were placed on the polymer surface using a micro-syringe and at least five angle measurements were made for each sample.

CHAPTER 3

RESULTS

3.1 Polymer Synthesis and Characterization

Various polyurethanes were synthesized by changing the molar ratio of diisocyanate to polyol and the type of polyol. As mentioned in section 1.1.1, although isocyanate containing molecules have been very reactive in the formation of polyurethanes, synthesis of very homogeneous films of PUs for practical applications without using any solvent is laborious. In this study, solvents were not used since they may cause toxic effects in biomedical applications. The presence of excess isocyanate in the formulation is one way of producing viscous prepolymer with isocyanate terminal groups. The polyaddition process takes place in the melt of the reactants and the prepolymers undergo further reactions resulting in crosslinking. Depending on the initial composition polyurethanes with varying hard segment contents were obtained. It was easier to obtain smooth PU films using compositions with high hard segment ratios. This situation is attributed to the plasticizing effect generated by low density of HDI monomers compared to that of polyol.

IR results provided a justification for the successful synthesis of the polyurethane polymer, and it is also a helpful method to extensively investigate the relationship between the monomer composition and the product structure. By using DSC, DMA and XRD the effect of reactants on thermal behaviors, dynamic properties and phase variation respectively, were studied. Furthermore, mechanical properties and surface hydrophilicity were characterized by mechanical tester and goniometer. As will be explained in detail in the following examinations, it is suggested that these techniques are complementary to each other and provide clear, quantitative and qualitative insights of hydrogen bonding in the PU films.

3.1.1 FTIR-ATR

Absorbance of electromagnetic radiation in the infrared range is related to vibrational and rotational energy levels in bonds [170]. FTIR is a convenient method for the analysis of functional groups and the investigation of the characteristics of hydrogen bonding and phase separation between the hard and soft segments using these vibrations [171]. It is known that bonds vibrate at different frequencies depending on the elements and nature of bonds. The total energy of a specific bond (determined by the wavelength) in a molecule consists of translational, rotational, vibrational, and electronic energies [172] and for any given bond there are several frequencies at which it can vibrate. Occasionally, the local vibration arises from inter or intra molecular interactions (e.g., weak London forces or hydrogen bonding) [173]. Thus, it should be noticed that any change in peak positions or peak areas changes have occurred in the environment of that particular vibration mode. In recent years, much effort has been devoted to characterize the vibration of the CO–NH group in PUs [121,130,174]. The principal vibrational frequencies are related with amide groups shown in Table 3–1.

Amide I vibration mode includes several components related with C=O groups in different environments and is sensitive to the characteristics of hydrogen bonding. Amide I mode is a highly complex vibration and has some contributions from the C=O in-plane bending, C–N stretching and C–C stretching. Amide II mode is an out-of-plane combination of largely N–H in plane bending and C–N stretching and smaller contributions from C=O in-plane bending and C–N stretching, and it is usually very weak compared to amide I.

Table 3-1 : Principal vibrational frequencies of amide modes.

Wavenumber (cm^{-1})	Assignment
3000-3600 cm^{-1}	arises from a Fermi resonance between N–H stretching and the amide I overtone
1600-1800 cm^{-1}	amide I, involves C=O stretching vibrations
1520-1570 cm^{-1}	amide II, corresponds to coupling between N–H bending and C–N stretching vibrations
1220-1330 cm^{-1}	amide III, contains a large percentage of N–H bending and C–N stretching
<800 cm^{-1}	amide IV-amide V, corresponds to out-of-plane vibrations of CO–NH group

Amide III mode is the in-phase combination of N–H in-plane bending and C–N stretching. Other amide modes (from IV to V) are less intensive in IR region, and therefore, not suitable to evaluate the role of hydrogen bonding in PUs. Amide IV and amide V at frequencies below 800 cm^{-1} correspond to out-of-plane vibrations of the CONH group and are strongly coupled to vibration of nearby groups [175]. On the other hand, amides III and IV are very complex bands and are only of limited use for the deducing structural information. Figure 3-1 serves as a model of vibrational modes of amide I, II and III.

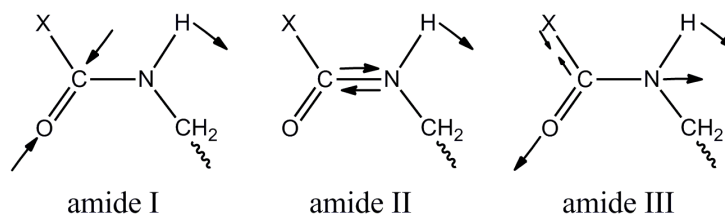


Figure 3-1 : Schematic representation of vibrational modes of amide I, amide II and amide III.

Polyurethanes can constitute different hydrogen bonds. In each case, the hydrogen atom of the N–H group in the urethane and urea fragments is the donor proton, while the acceptor group can be either oxygen atom of the urethane or urea carbonyl or ester carbonyl in soft segments. The charge transfer phenomena from the C=O to N–H results in a reduction in electron density around the carbonyl bond i.e., the C=O bond strength is weakened a bit, and hence the wavenumber of the amide I decreases. Similarly, the wavenumber of N–H group decreases upon formation of hydrogen bonds with C=O. Therefore, the shift of corresponding IR absorbance peaks to lower frequencies is an evidence for the strength of hydrogen bonding [176], which in turn depends on the different interactions associated with them [177-181].

During the synthesis of all polyurethanes, samples were taken at different times to follow the polymerization process and disappearance of the monomeric isocyanate peaks was studied. The decrease in intensity of isocyanate stretching vibration at 2270 cm^{-1} in time as the curing reaction proceeds can be clearly seen in Figure 3-2 in the synthesis of PU2.5-1250. The reactions were stopped upon the complete disappearance of this absorption band in the spectra. The times required for the completion of curing reactions are given in Table 2-1. During the disappearance of isocyanate peak, the changes in $\nu_{\text{N-H}}$, $\nu_{\text{C=O}}$ and $\nu_{\text{C-O-C}}$, urethane regions, the characteristic urethane bonds, were observed (Figure 3-2).

The typical IR spectra of all PUs are shown in the zone $4000\text{--}600\text{ cm}^{-1}$ in Figure 3-3. Furthermore; Table 3-2 provides detailed structural information for PU2.5-1250 and in order to ease identification of peaks, the peaks are numbered. The PU spectra are mainly characterized by bands at $3500\text{--}3200\text{ cm}^{-1}$ (N–H stretching vibrations), 2931 cm^{-1} and 2859 cm^{-1} (C–H stretching vibrations: anti-symmetric and symmetric modes of methylene groups, respectively), $1800\text{--}1600\text{ cm}^{-1}$ (amide I: C=O stretching vibrations). The absorption of amide II is located at $1594\text{--}1496\text{ cm}^{-1}$. Amide II vibration consists of a large percentage of

N–H in-plane bending, C–N stretching, and C–C stretching [182]. Band at 1462–1452 cm^{-1} is attributed CH_2 scissoring and CH_3 deformation.

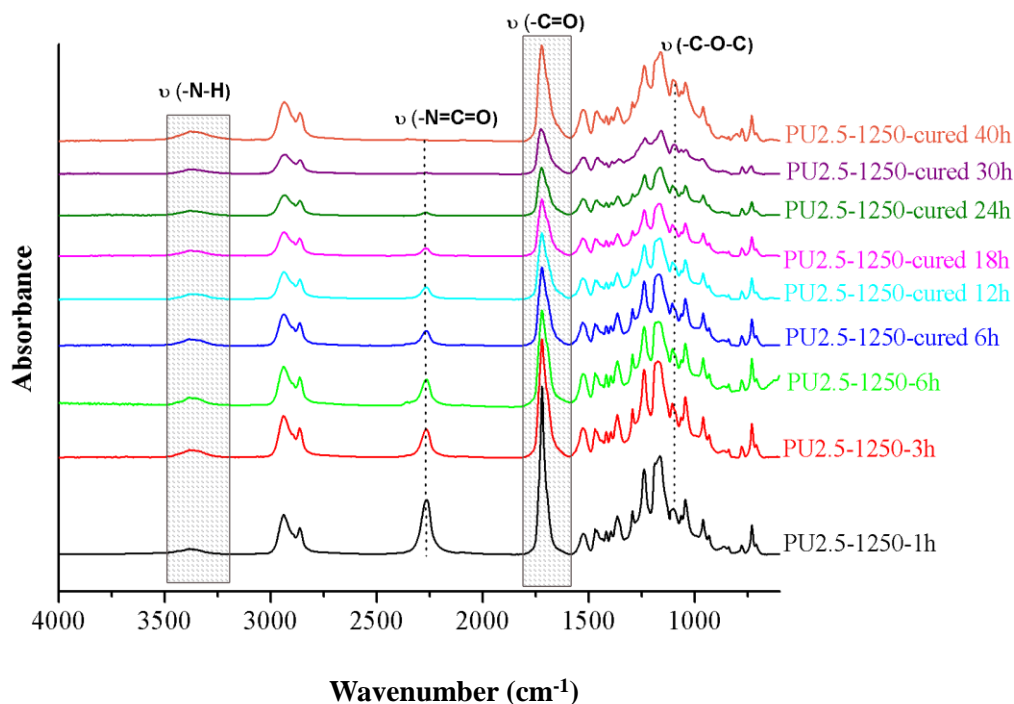


Figure 3-2 : IR spectra of PU2.5-1250.

The peak of CH_2 bending adjacent to carbonyl was located at 1391–1337 cm^{-1} . The amide III is observed in the range 1296–1212 cm^{-1} , and arises from contributions of N–H in-plane bending and C–N stretching. The band at 1209–1104 cm^{-1} is assigned to C–O–C stretching vibration of ester functions of the polyester backbone. The absorbance in the range 1100–1067 cm^{-1} was attributed to C–O–C stretching vibration of urethane linkages. Absorbance at 1051–1021 cm^{-1} is attributed to the stretching and rocking vibrations of the C–C and CH_2 groups. The band at 963 cm^{-1} is assigned to the C–O stretching and CH_2 rocking. Amide IV and V bands are produced by highly mixed modes containing

a significant contribution from the N–H out-of-plane deformation mode. Amide IV and amide V appeared at 780 and 727 cm^{-1} , respectively.

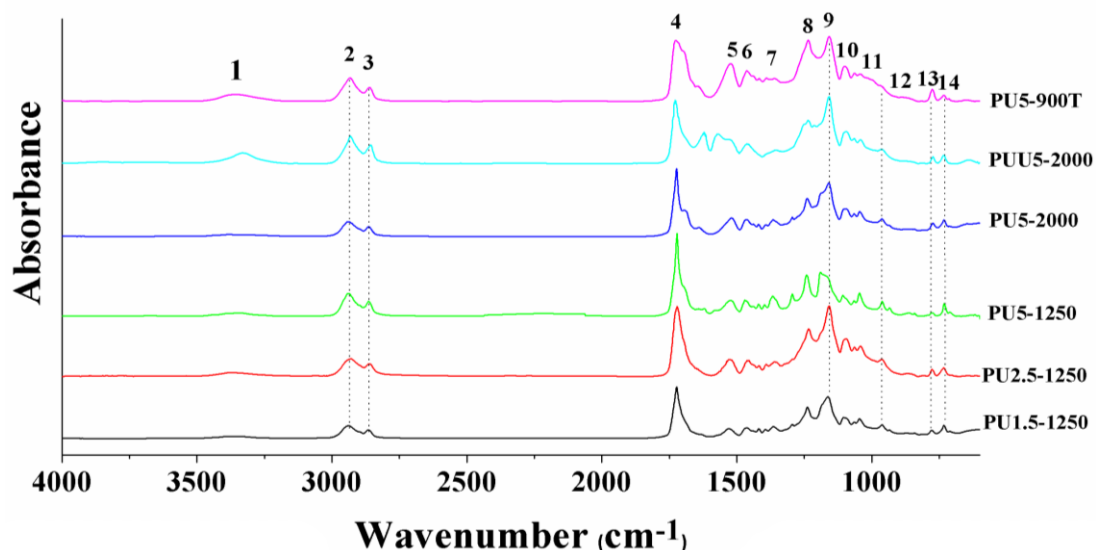


Figure 3-3 : Representative IR spectra of different PU films.

As mentioned in section 1.4.2.3, hydrogen bonding in the hard segment triggers microphase separation and if there is a strong interaction between hard and soft segments, this usually leads to phase mixing and therefore, significantly reduces the hydrogen bonding in the hard segments. Phase segregation and phase mixing are critical in determining the overall properties (mechanical, thermal and degradation) of polyurethanes. Stronger hydrogen bonding in the hard segments (where the hard segment is urethane or urea) results in improved thermal and mechanical properties. The extent of microphase separation and mixing of segmented PUs can be determined from the extent of hydrogen bonding in the hard segments [183].

Table 3-1 : Peak assignments in the IR spectra of PU2.5-1250.

Peak Index	Wavenumber (cm ⁻¹)	Assignment
1	3500–3200	ν (N–H)
2	2931	ν_{as} (–C–H)
3	2859	ν_s (C–H)
4	1800–1600	ν (C=O), amide I
5	1594–1496	δ (N–H) + ν (C–N) + ν (C–C), amide II
6	1462–1452	δ (–CH ₃) and δ_{sciss} (–CH ₂ –)
7	1391–1337	δ (–CH ₂ –), adjacent to carbonyl
8	1296–1212	δ (N–H) + ν (C–N), amide III
9	1209–1104	ν (C–O–C), ester functions from polyester backbone
10	1100–1067	ν (C–O–C), urethane
11	1051–1021	ν (C–C) + δ (–CH ₂ –)
12	963	ν (C–O) + δ (–CH ₂ –)
13	780	γ (N–H), amide IV
14	727	γ (N–H), amide V

ν ; stretching vibrations, δ ; bending or rocking vibrations, as; asymmetrical, s; symmetrical, γ ; out of plane bending.

The hydrogen bonded groups are characterized by a frequency shift to lower values. Particularly for polyester-based PUs, the fraction of the hydrogen-bonded carbonyls is controlled by the hard-hard segment hydrogen bond between urethane or urea hydrogen and urethane or urea carbonyl (N–H••••O=C bond), and this was used to assess the extent of phase separation. On the other hand, the fraction of the hydrogen-bonded carbonyl oxygens in soft segments with urethane or urea hydrogen in hard segment (N–H••••O=C bond) represents the extent of phase mixing.

Even though the chemical structures of urethane or urea groups are identical in different macromolecules, there is a significant difference in N–H and O=C

regions arising from their environmental diversity. In order to directly study the extent and strength of hydrogen bonding in both hard-hard and hard-soft segments, experiments were performed and the infrared absorption of the two spectral regions were studied by varying the hard segment content and the polyol type. In this regard, two major spectrum regions in this work are of the main interest: the N–H stretching vibration and the amide I stretching vibration. For the reasons mentioned above, IR was employed extensively to study the effect of hydrogen bonding on the phase morphology of the PUs as shifts in N–H and C=O stretching frequencies to lower frequencies.

As can be seen in Figure 3–4, the complexity and diversity of inter- and intra-molecular environments surrounding the N–H and C=O groups in polyurethanes make these ranges considerably broader. The fact that peaks are overlapping indicates that many frequencies are common to each vibrational mode, as would be expected. Deconvolution method has been used to quantify and identify characteristics of hydrogen bonding in these regions.

The effect of variation of NCO/OH ratio and the polyol type on the hydrogen bonding of PUs have been performed by the deconvolution procedure for stretching vibration modes of hard segments of all PUs in the wide region of absorptions of $\nu_{\text{N-H}}$ (between 3500 and 3200 cm^{-1}) and $\nu_{\text{C=O}}$ (between 1800 and 1600 cm^{-1}). The iteration process of deconvolution, based on a Gaussian-Lorentzian sum function, was used to resolve more specific absorption peaks corresponding to different kinds of hydrogen bonding [106,184]. In this manner, the six materials synthesized in this study (PU1.5-1250, PU2.5-1250, PU5-1250, PU5-2000, PUU5-2000 and PU5-900T) were studied by deconvolution process in both regions.

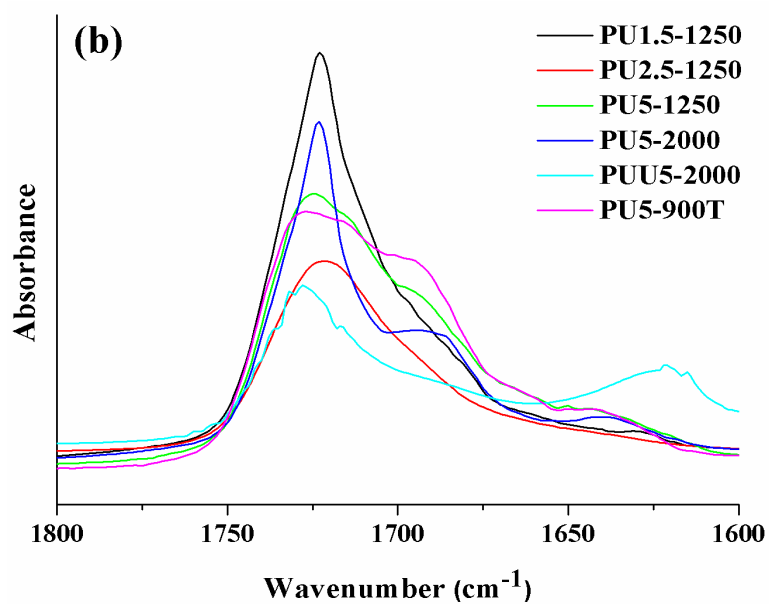
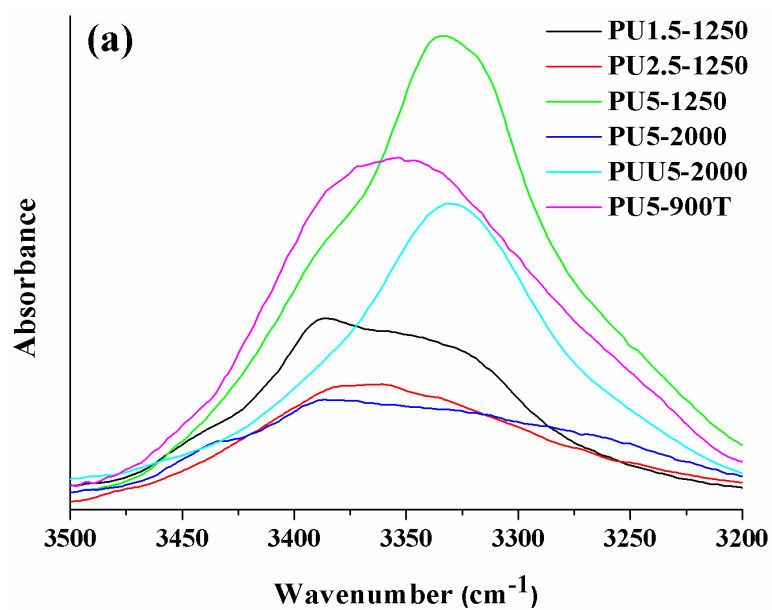


Figure 3-4 : IR spectra for different segmented PU films; (a) N-H region, (b) C=O region.

The deconvolution phenomena is based on that a number of closely associated peaks merge and each narrow band is responsible for individual characteristics of bands. Because of the hydrogen bonding between C=O group and the N–H group, the experimentally observed N–H and C=O bands contain a plenty of single bands with different frequencies. Therefore, a curve-fitting procedure can be applied to determine the exact peak positions and areas of a set of overlapping peaks arising from the relative contributions of the different groups. Thus, each resolved peak represents the extension of the self-association in these materials.

3.1.1.1 The N–H Stretching Region

The N–H stretching vibration is helpful to determine the types of hydrogen bonding and yields complementary structural information to the C=O stretching vibration. It was reported that the splitting of the bonded N–H band was related to different acceptors with which the N–H groups were hydrogen bonded [185,186]. A flat baseline correction was performed in between 3500 and 3200 cm^{-1} by subtracting the baseline. The correlation coefficients of the fitting process were more than 0.998. Figure 3-5 shows the N–H stretching region spectra of polyurethane series having different compositions (as HDI/polyol ratio and type of polyol) and different percentages (as 17, 25, 30, 40 and 48 wt. %) of hard segments.

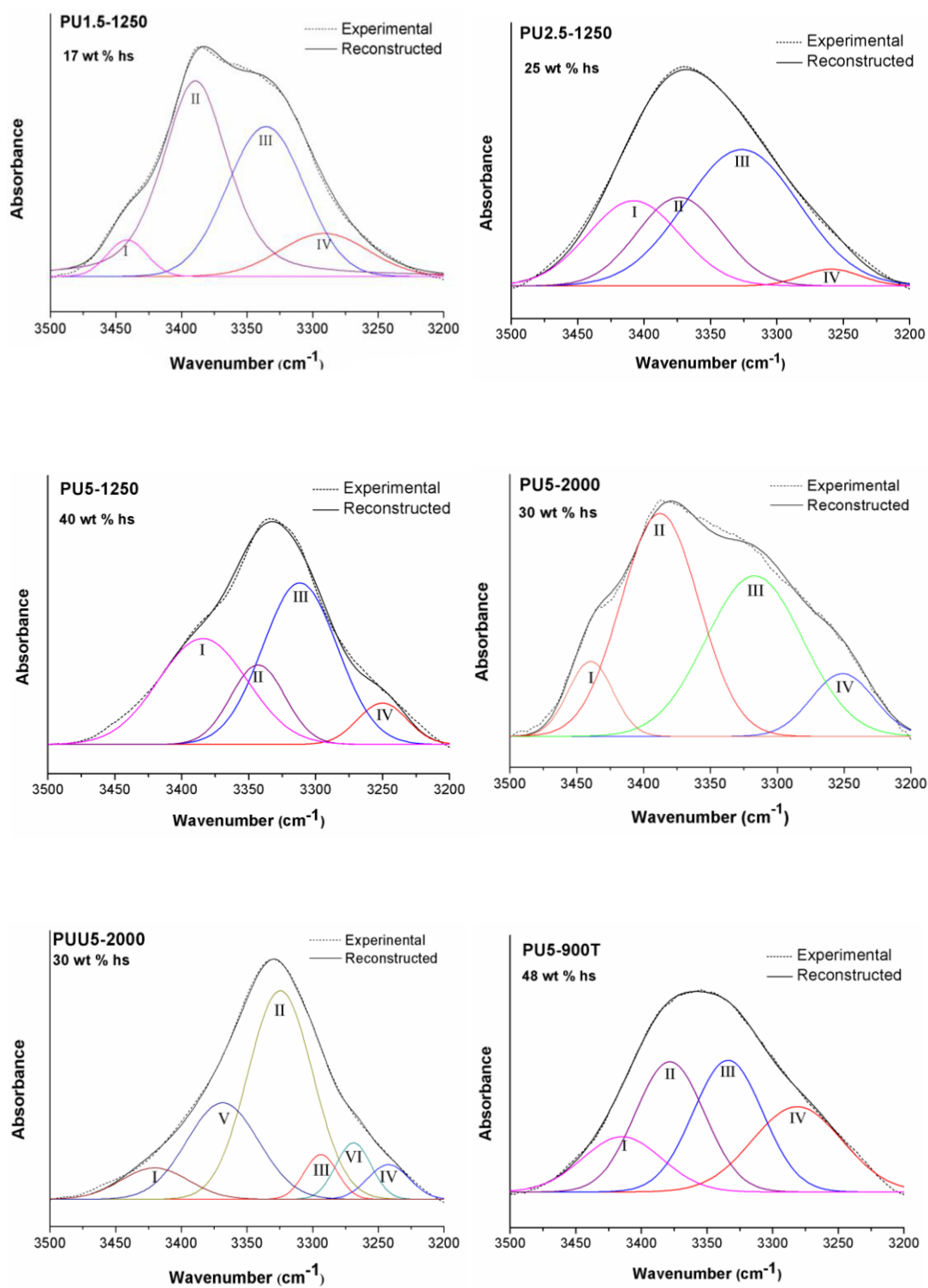


Figure 3-5 : The deconvoluted N–H region of IR spectra for all PUs

Hydrogen bonding between the N–H group in HS and C=O groups in HS systems is responsible for the phase separation behavior, whereas hydrogen bonding interaction between the N–H group in HS and ester linkages in SS favors a phase mixing features in PU structure.

As listed in Table 3-2 peak I, peak II, peak III, and peak IV were assigned to free N–H bonding in urethane groups, N–H groups in urethane linkages bonded with carbonyl in HS (H-bonding in hard-hard segments which was employed to evaluate the extent of phase separation, N–H.....O=C), N–H groups in urethane or urea linkages bonded with carbonyl in SS (H-bonding in hard-soft segments, represents the extent of phase mixing between hard and soft segments, N–H.....O=C) and a two-phonon vibration involving the intense carbonyl vibrations in Fermi resonance with the fundamental N–H stretching vibration [182,187] in the system, respectively. Urea linkages in the structure attributed two additional peaks to deconvolution of PUU5-2000 sample. These peaks are peak V and peak VI, assigned to N–H groups in free urea linkages and N–H groups in urea linkages bonded with carbonyl (H-bonding in hard-hard segments which was employed to evaluate the extent of phase separation, N–H.....O=C).

Table 3-2 : Infrared stretching band assignments of the N–H group in the PUs as seen from the deconvoluted IR spectra.

Band	Wavenumbers (cm⁻¹)	Assignment
I	3442-3384	free N–H (urethane)
II	3389-3324	H bonding in HS-HS (urethane)
III	3336-3294	H bonding in HS-SS (urethane or urea)
IV	3291-3242	overtone of C=O and N–H (Fermi resonance)
V	3368	free N–H (urea)
VI	3269	H bonding in HS-HS (urea)

Peak IV is assigned to the overtone of the amide II mode with N–H stretching. There are many definitions for this band such as a two-phonon band by Queiroz et al. [188], an overtone of deformation vibration of N–H group increased by Fermi resonance by Romanova et al. [187] and the N–H groups bonded with the carbonyl of urethane by forming a dual-cis bond by Bellamy et al. [189] and Liu and Ma [190].

There are several interpretations to define this band. Queiroz et al. [188] commented this band as a two-phonon band in their study. According to Romanova et al. [187], an overtone of deformation vibration of N–H group increased by Fermi resonance appears at 3162 cm^{-1} , whereas Bellamy et al. [189] and Liu and Ma [190] assigned the bands at 3190 cm^{-1} to the N–H groups bonded with the carbonyl of urethane by forming a dual-cis bond as shown in Figure 3-6.

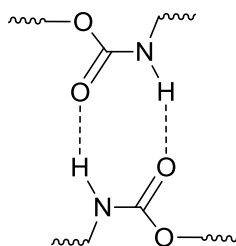


Figure 3-6 : The dual-cis bond.

Several factors contribute to the transformation of hydrogen-bonded N–H band to free N–H band. The deconvolution peak positions for all PUs are listed in Table 3-3 for this region. In each spectrum, the N–H stretching vibration exhibits peak II centered at around $3389\text{-}3324\text{ cm}^{-1}$ arising from H-bonding in hard segment domains, is a proof of phase separation, whereas the free N–H stretching (peak I) vibration appears at $3442\text{-}3384\text{ cm}^{-1}$. In addition, peak III centered at around $3336\text{-}3294\text{ cm}^{-1}$ arises from H-bonding between hard segment and soft segment domains. The deconvoluted spectrum that comprised bands at 3291, 3270, 3250,

3251, 3242 and 3281 cm^{-1} representing an overtone of deformation vibration of N–H group increased by Fermi resonance (peak IV) was observed for each material as listed in the Table 3-3. Valuable information can not be obtained from peak IV for microphase separation.

Table 3-3 : Deconvolution results of the N–H region with peak position for all PUs.

Sample	Peak Position (cm^{-1})					
	I	II	III	IV	V	VI
	(Free) Urethane	(HS-HS) Urethane	(HS-SS) Urethane or urea	Fermi resonance	(Free) Urea	(HS-HS) Urea
PU1.5-1250	3442	3389	3336	3291	-	-
PU2.5-1250	3409	3376	3331	3270	-	-
PU5-1250	3384	3343	3311	3250	-	-
PU5-2000	3440	3388	3317	3251	-	-
PUU5-2000	3420	3324	3294	3242	3368	3269
PU5-900T	3414	3378	3334	3281	-	-

As seen in the Table 3-3, the absorbance of the free N–H band (peak I) shifted to lower frequencies (from 3442 to 3384 cm^{-1}) when increasing the hard segment content in the polyurethanes synthesized from PCL diol 1250. On the other hand, while the length of chain soft segment increased (in the case of PU5-2000 and PUU5-2000), free N–H band shifted to higher frequencies (to 3440 and 3420 cm^{-1} , respectively) as result of the long chain of the soft segment. In the case of branched sample (PU5-900T), peak I is observed at 3414 cm^{-1} . Differences in frequencies showed that bond environment was changed and affected free N–H stretching absorbance frequency.

In PUs synthesized from PCL diol with molecular weight 1250, the H-bonded N–H stretching in HS (peak II) shifted systematically to lower frequencies (from 3389 to 3343 cm^{-1}) as a consequence of increase in HS content. Shifts to lower frequencies revealed that the average H-bond distance decreases resulting from

allophanate formation which gets the chains closer, so that the average strength of H-bonds increases with increasing HDI content in the system. Conversely, PU5-2000 having longer soft segment leads to be observed peak II centered at 3387 cm^{-1} . It was observed that PUU5-2000 was strongly hydrogen bonded due to having the lowest frequency value (3324 cm^{-1}) in peak II. This could be due to having strong bidentate hydrogen bonding via urea bonds. PU5-900T has peak II centered at 3378 cm^{-1} , arising from that regular branching of soft segment did not allow forming strong H-bonds in the polymer structure.

As HS content increases for PU1.5-1250, PU2.5-1250 and PU5-1250 samples, stronger H bonds were formed between HS and SS. As seen in Table 3-3 peak III shifted from 3336 to 3311 cm^{-1} for these samples. Strongest hydrogen bonds appears to be established in HS and SS for PUU5-2000, which has the lowest peak III position centered at 3294 cm^{-1} . On the other hand, PU5-2000 has peak III centered at 3317 cm^{-1} . Peak III is observed for PU5-900T at 3334 cm^{-1} .

As a conclusion, it can be seen that the H-bonded N–H groups in hard segments (peak II) for PUU5-2000 appears at the lowest frequency whereas that for PU1.5-1250 is at the highest frequency, suggesting the H-bond strength of N–H in PU1.5-1250 is the weakest and H-bond strength of N–H in PUU5-2000 is the highest. It can also be said that PU5-1250 has the strongest H-bond between HS-SS due to having lowest frequency in the corresponding band.

In addition to knowledge of frequency shifts, band areas also give extra information about phase separation by comparing area percentages of free N–H, N–H with H-bonds in HS-HS, and N–H with H-bonds in SS-HS. All N–H band areas were estimated on the basis of total N–H stretching band area and listed in Table 3-4.

The area of the free N–H band is directly related to the number or concentration of free N–H groups. In PUs synthesized from PCL diol with molecular weight 1250, band area of free N–H stretching are approximately proportional to increase in hard segment ratio. Free N–H groups increased with hard segment concentration in these polymeric materials from 4.6% to 33.6%. In contrast, H-bonded N–H groups in HS-HS decreased substantially with increase in hard segment content from 46.5% to 15.7% for the same materials. This shows that as crosslinking increases which is a result of increase in HDI content, microphase segregation decreased for PUs synthesized from PCL diol with molecular weight 1250. The deconvolution of N–H stretching area results of these samples showed that most of the N–H vibrations do not participate in hydrogen bonding as HDI concentration increased by reason of allophanate formation for PUs consisting of PCL diol 1250.

Table 3-4 : Deconvolution results of the N–H region with peak area for all PUs.

Sample	Peak Area (%)					
	I	II	III	IV	V	VI
	(Free) Urethane	(HS-HS) Urethane	(HS-SS) Urethane or urea	Fermi resonance	(Free) Urea	(HS-HS) Urea
PU1.5-1250	4.6	46.5	36.9	12.1	-	-
PU2.5-1250	24.7	23.4	48.7	3.2	-	-
PU5-1250	33.6	15.7	43.2	7.5	-	-
PU5-2000	8.7	43.1	38.5	9.7	-	-
PUU5-2000	7.8	49.1	5.4	5.2	25.2	7.3
PU5-900T	14.5	29.8	30.4	25.3	-	-

As the length of soft segment increases as in PU5-2000, HS-HS interaction via H-bond reached to 43.1% of the total area. The amount of free N–H groups contains 8.7% of total area.

PUU5-2000 has two types of HS-HS interactions contributing from urethane (peak II) and urea (peak VI) groups. The total area of these bands constitutes

56.4% of the total area, which has the highest HS-HS interaction over remaining samples.

PU5-900T contains 14.5% as free N–H groups, while 29.8% is observed as HS-HS interaction in urethane groups. The data in Table 3-4 suggest that the peak contribution for the hydrogen bonded N–H from urea as well as urethane region was highest for the sample PUU5-2000 and lowest for PU5-1250. The areas assigned to H-bonding between HS-SS (peak III) have similar areas in almost all polymers. PU5-2000 possesses just 38.5% of the total area and PUU5-2000 has marked decrease in the band area (to 5.4%) for phase mixing. Both PU5-2000 and PUU5-2000 prefer H bonds in the hard segment domains. This can arise from the longer soft segment is more suitable for the formation of H-bonds in hard segments during synthesis without solvents.

Comparing peak II and peak III, PU1.5-1250 indicated phase segregation since deconvoluted area in HS-HS overcame that in HS-SS (46.5% versus 36.9%). In a similar way, PU2.5-1250 and PU5-1250 showed phase mixing. A detailed analysis of deconvoluted N–H peaks for polymers synthesized from PCL diol with molecular weight 1250 permits to conclude that the phase separation exhibits following order:

$$\text{PU1.5-1250} > \text{PU2.5-1250} > \text{PU5-1250}$$

It was observed that PU5-1250 was weakly hydrogen bonded but PUU5-2000 was strongly hydrogen bonded. This could be due to having strong bidentate hydrogen bonding via urea bonds. As seen in the Table 3-4, PU5-2000 has higher phase separation (43.1%) and less phase mixing (38.5%) compared to PU5-1250 arising from that PU having longer soft segments in PU5-2000 allow to form readily hydrogen bonds in hard-hard segments. PUU5-2000 has the highest concentration of hydrogen bonding in the hard segment (56.4%, the total of associated urethane and urea) and the highest shift in this corresponding bond frequency

(from 3389 to 3324 cm^{-1}) compared to others, resulting from partial replacement of urethane groups with urea groups. In contrast, the amount of phase mixing is higher PU5-900T was higher compared to the amount of phase separation even though it has the highest hard segment content. The branched structure of polyol in this sample leads to approximately equal phase mixing (30.4%) and phase separation (29.8%). Moreover, it has the highest second frequency for peak II (3378 cm^{-1}) showing the second weakest H-bond in hard segments. This lower frequency defines the strength of hydrogen bond in hard segment domains is inconsiderable when compared with difunctional polyol compositions with different ratios, as well as the types of the polyol as exist in PU2.5-1250, PU5-1250, PU5-2000 and PUU5-2000. It was concluded from that suggestion, the phase separation follows the order given below:

$$\text{PUU5-2000} > \text{PU5-2000} > \text{PU5-1250} > \text{PU5-900T}$$

The results showed that PU copolymers with different hard segment ratio as well as different soft segment structures and molecular weights exhibit different interactions in the molecular chains.

3.1.1.2 The C=O Stretching Region

The C=O stretching vibration is used to evaluate complementary results to the N-H stretching region [130]. The existence of hydrogen bonding prolongs the carbonyl bond and results in the reduction of the stretching vibration frequency. Hence, the hydrogen bonded $\nu(\text{C=O})$ band comes out at a lower frequency compared to that of the free $\nu(\text{C=O})$ band [191].

The deconvolution study on amide I mode in the range (1800–1600 cm^{-1}) has been widely studied to evaluate the structure-property relationship in PUs. The frequency-structure correlation is a result of interaction depending on the distance

and orientation between the many amide I vibrations of each of the urethane/urea groups [130,174].

Before deconvolution of the amide I band, a flat baseline was chosen in between 1800 and 1600 cm^{-1} and the spectra was corrected by subtracting the baseline. The deconvoluted spectrum of PUs clearly comprises a number of bands as shown in Figure 3-7 for different samples with various hard segment concentration ranging from 17 to 48% in PUs. Although, the chemical structures of the urethane groups are identical in different compounds, there is a remarkable difference in the C=O region of their IR spectra. Polyester-based polyurethanes involve five characteristic absorption peaks in this region, while the sample consisting of urea groups have two additional peaks due to existence of urea groups. Table 3-3 provides information about the assignation of bands. These bands centered at I, II, III, IV, V and VI can be assignable to free C=O in ester groups of soft segments (1741-1727 cm^{-1}), H-bonded C=O in ester groups of soft segments (1729-1709 cm^{-1}), free C=O in urethane linkages (1713-1691 cm^{-1}), H-bonded C=O groups in urethane linkages (1696-1665 cm^{-1}), C=O in allophanate and/or biuret linkages (1656-1620 cm^{-1}), free C=O in urea linkages (1696 cm^{-1}), and H-bonded C=O in urea linkages (1636 cm^{-1}), respectively.

Table 3-5 : Infrared stretching band assignments of the C=O group in the PUs as seen from the deconvoluted IR spectra.

Band	Wavenumber (cm^{-1})	Assignment
I	1741-1728	free C=O (ester)
II	1729-1709	H-bonding in HS-SS (ester)
III	1713-1691	free C=O (urethane)
IV	1696-1665	H-bonding in HS-HS (urethane)
V	1656-1620	allophanate and/or biuret
VI	1696	free C=O (urea)
VII	1636	H-bonding in HS-HS (urea)

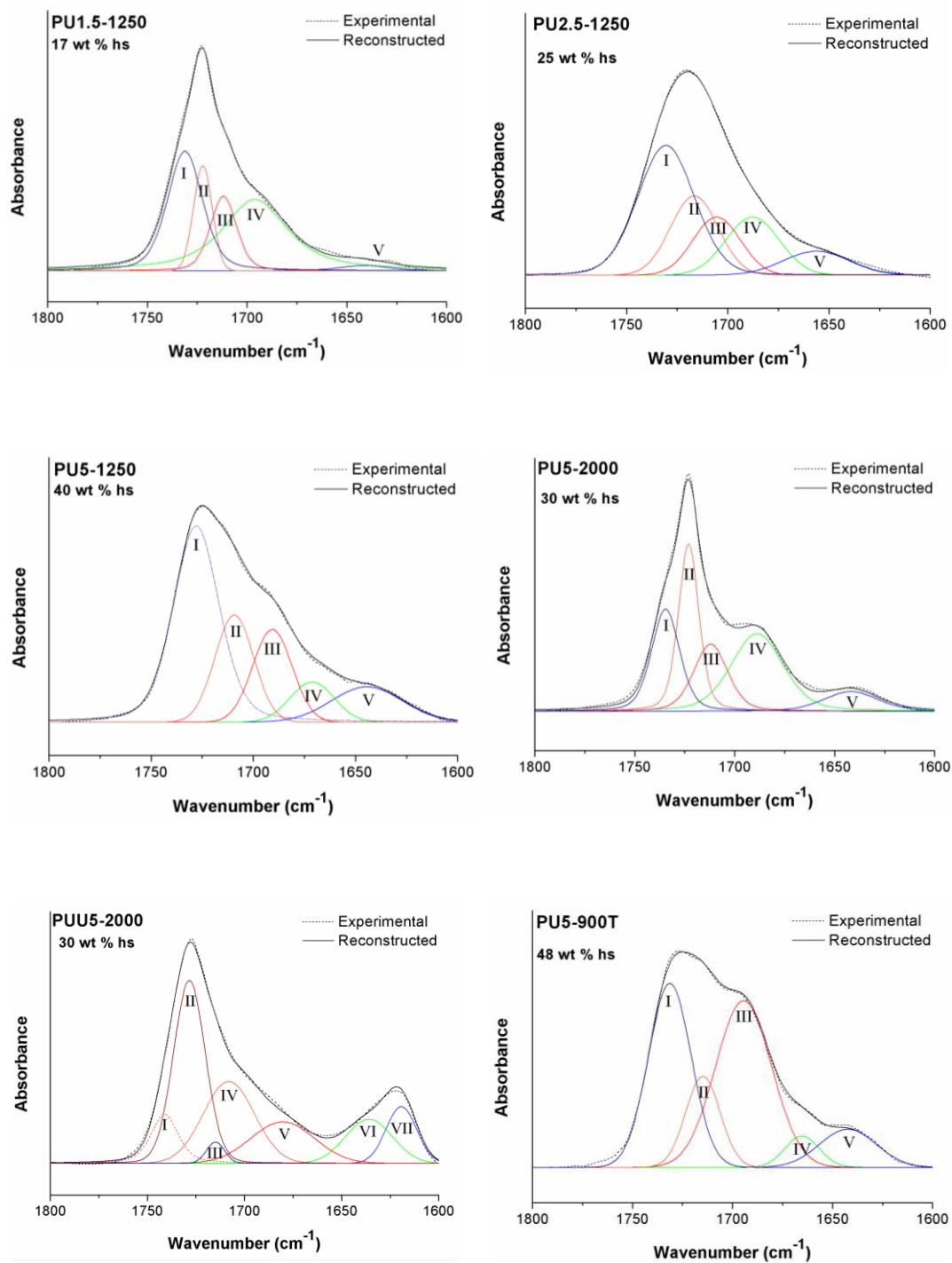


Figure 3-7 : The deconvoluted C=O region of IR spectra for all PUs.

The deconvolution peak positions and areas of amide I region for all polymers are listed in Table 3-6 and Table 3-7, respectively.

Table 3-6 : Deconvolution results of the C=O region with peak position for all PUs.

Sample	Peak Position (cm ⁻¹)						
	I	II	III	IV	V	VI	VII
	(Free) Ester	(HS-SS) Ester	(Free) Urethane	(HS-HS) Urethane	Allophanate (and/or biuret)	(Free) Urea	(HS-HS) Urea
PU1.5-1250	1731	1722	1712	1696	1641	-	-
PU2.5-1250	1730	1717	1706	1688	1656	-	-
PU5-1250	1728	1709	1691	1671	1643	-	-
PU5-2000	1735	1723	1712	1689	1642	-	-
PUU5-2000	1741	1729	1713	1680	1620	1696	1636
PU5-900T	1731	1715	1694	1665	1642	-	-

As seen in Table 3-6, absorbance of free carbonyl in ester groups of soft segments (peak I) in PUs composed of PCL diol 1250 shifted slightly to lower frequencies (from 1731 to 1728 cm⁻¹). Polymers with longer polyols in their structure, namely PU5-2000 and PUU5-2000, possessed higher wavenumber of free carbonyl in ester groups of soft segments centered at 1735 and 1741 cm⁻¹, respectively. The observed closer absorbance of free carbonyl in ester groups of soft segments in PU5-900T was observed at centered around 1731 cm⁻¹.

Hydrogen bonded carbonyl in ester groups of soft segments (peak II) contributed to phase mixing. For PUs consisting of PCL diol 1250, this peak shifted to lower frequencies from 1722 to 1709 cm⁻¹ as hard segment content increased by result of increase in the strenght of H-bond. The strenght of H-bond between HS-SS lead to higher frequency shifts in PU5-2000 (1723 cm⁻¹) and PUU5-2000 (1729 cm⁻¹). It revealed that PU5-2000 formed stronger H-bonds in HS-SS. PU5-900T showed peak II maximum at 1715 cm⁻¹, much lower than that of PU5-2000 and PUU5-2000.

A comparison of hydrogen bonding strength in HS-HS with increasing hard segment content suggests that enhancement in the strength of hydrogen bonding takes place with increasing hard segment content resulting in shift from 1696 to 1671 cm^{-1} for polymeric materials containing PCL diol 1250. PU5-2000 possess hydrogen bonding in urethane groups at centered at 1689 cm^{-1} . PUU5-2000 has its carbonyl peak in HS-HS maximum at 1680 cm^{-1} , whereas the urea compound which can form very strong, bidentate hydrogen bonding shows a peak maximum at 1636 cm^{-1} , much lower than that of carbonyl in ester groups in soft segment or in urethane linkages.

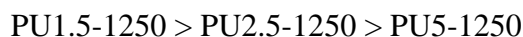
A comparison of the amount of free C=O and hydrogen-bonded C=O as shown in Figure 3-7 support our previous observation of hydrogen bonding strength from the deconvolution study of N-H region.

Table 3-7 : Deconvolution results of the C=O region with peak area for all PUs.

Sample	Peak Area (%)						
	I	II	III	IV	V	VI	VII
	(Free) Ester	(HS-SS) Ester	(Free) Urethane	(HS-HS) Urethane	Allophanate (and/or biuret)	(Free) Urea	(HS-HS) Urea
PU1.5-1250	31.6	13.2	14.7	38.5	2.0	-	-
PU2.5-1250	40.4	20.0	14.6	16.6	8.4	-	-
PU5-1250	45.0	18.9	16.6	8.1	11.4	-	-
PU5-2000	21.1	25.3	16.7	29.2	7.7	-	-
PUU5-2000	8.7	29.6	2.1	23.6	14.1	10.8	11.1
PU5-900T	33.3	13.3	39.6	4.6	9.2	-	-

Within PUs synthesized from PCL diol with molecular weight 1250, PU5-1250 has the highest band area of free carbonyl in ester groups in soft segments (45.0%) and lowest band area of H-bonded urethane carbonyl (8.1%). However, PU1.5-1250 has highest amount of hydrogen bonded groups (38.5%) in HS-HS (peak IV). Comparing the area of H-bonds in HS-HS (peak IV) and H-bonds in

HS-SS (peak II) and free carbonyl groups, thus, microphase segregation can be as in the following order:



An increase in the hard segment content results in some dispersion of soft segment in the hard domains for PUs containing same polyol in their backbone. This gives complementary structural information to the N–H stretching vibration.

PU5-2000 has 25.3% H-bonded carbonyl in ester groups in soft segments and 29.2% associated urethane carbonyl. Having more hydrogen bonded urethane carbonyls showed that better phase separation in PU5-2000 over PU5-1250 (18.9%, H-bonded carbonyl in ester groups in soft segments and 8.1%, H-bonded carbonyl in urethane linkages).

The broadness of the $\nu_{\text{C=O}}$ band in PUU5-2000 indicates that C=O may have very different H-bonded states due to either the different distances among the same type of H-bond or the different H-bonds between C=O and other proton donors. Therefore, PUU5-2000 has two additional peaks due to exposure to atmospheric humidity. Although urea units are more polar in nature when compared to urethane units, high crosslinking via secondary reactions of urethane and urea groups does not entirely allow interchain association in PUU5-2000. PUU5-2000 compound which can form very strong, bidentate hydrogen bonding exhibits a peak maximum at 1636 cm^{-1} , much lower than that of the ester or urethane. The other interesting observation from the deconvolution of C=O region was to verify whether the area of the free urea carbonyl groups is higher than that of the bonded urea carbonyl group for PUU5-2000. The presence of urea bonds interferes with the ordering of the hard segment and allows polyester carbonyls to compete with the urea carbonyls for the urea N–H groups, resulting in a mixed state of conventional and three-dimensional urea H-bonds as illustrated in Figure 3-8. Table 3-7 revealed that the amount of hydrogen bonded carbonyls in associated

urea (11.1%) is higher than free carbonyls in urea groups (10.8%). It can be seen from Table 3-7, PUU5-2000 has the highest fraction in the amount of bonded hydrogen in HS-HS (23.6%, H-bonded carbonyl in urethane bonds and 11.1%, H-bonded carbonyl in urea bonds) to that of free carbonyls (8.7%, in ester groups of soft segments and 2.1% in urethane linkages and also 10.8%, in urea linkages) compared to other samples. Therefore, PUU5-2000 possessed the highest microphase separation.

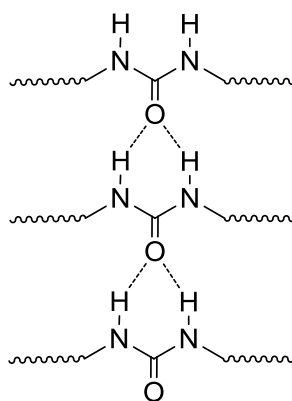


Figure 3-8 : The hard segments in PUU5-2000 constitute hydrogen bonding between the chains via urea bonds.

The experimental results revealed that incorporation of a triol soft segment into polyurethane structure accomplished maximum reduction in H-bond formation in HS-HS. PU5-900T (4.6%) creates a least favourable hydrogen bonding interaction in hard segment when compared to the all remaining materials.

Similarly, the analysis of hydrogen bonding interaction in relation to the free carbonyl in urethane linkages with the structural variation for comparison between PU1.5-1250, PU2.5-1250, PU5-1250, PU5-2000 and PU5-900T shows that the free carbonyl content in urethane bonds was least in PU1.5-1250 (31.6%, free carbonyl in ester groups of soft segments; and 14.7%, free carbonyl in

urethane linkages) and highest in PU5-900T (33.3%, free carbonyl in ester groups of soft segments; and 39.6%, free carbonyl in urethane linkages). Consequently, microphase segregation within the same mol ratio (NCO/OH) samples shows the following order:

$$\text{PUU5-2000} > \text{PU5-2000} > \text{PU5-1250} > \text{PU5-900T}$$

On the basis of all IR analysis, it may be concluded that the amount of excess HDI for PU synthesis without solvent and the nature of polyol type (linearity and molecular weight) have great influence on phase segregation, which consequently result a new morphology with an altered hydrogen-bonding. Increase in chemical crosslinks between the polymer chains decreased the extent of H-bonds markedly in HS-HS in the case of PU1.5-1250, PU2.5-1250 and PU5-1250. Branched structure of the polyol having three OH functional groups in PU5-900T resulted in regular crosslinking and reduction in phase separation. The existence of longer soft segment in polymers increased concentration of H-bonds in HS-HS. It is obvious that urea groups makes stronger H-bonds between HS-HS, resulting in better phase segregation in PUU5-2000. Furthermore, the relative amount of H-bonds in HS-HS or HS-SS and subsequently affect overall properties of polyurethanes. It indicated that the average H-bond distance decreases as wavenumber shifts to lower frequencies. This is due to allophanate and/or biuret formation which gets the chains closer, so that the average strength of H-bonds increases with increasing HDI content in the system.

3.1.2 Differential Scanning Calorimetry

Differential scanning calorimetry (DSC) was utilized as complementary technique with FTIR-ATR to examine microphase structure and properties by characterizing thermal transitions of the polyurethanes and to determine interaction between functional groups.

In the development of polymers for any certain applications, it is important to know their thermal properties to determine the resulting physical properties of the materials under different environmental conditions. For example, if the value of the glass transition temperature (T_g) of the polymer is above that of the application area, the polymer is rigid. In contrast, if the T_g values are below that, this indicates the elastomeric nature of the materials.

An attempt has been made to correlate the thermal behavior and the morphology change introduced upon changing the HDI concentration and type of polyol soft segment. The DSC results obtained by scanning from -100 to 200°C and the related thermal property data are summarized in Table 3-8. Representative DSC curves are shown in Figure 3-9, Figure 3-10 and Figure 3-11 for PCL diol 1250 based polyurethanes, PCL diol 2000 based polyurethanes and PCL triol based polyurethanes, respectively. Furthermore, DSC thermograms were recorded for pure soft segments with corresponding polyurethanes. The arrows in DSC thermograms indicate the position of the soft segment T_g . DSC thermal behavior is apparent in two temperature ranges, which are T_g and T_m of soft segment (melting temperature). Polyurethane films were all rubbery form because of the relatively low glass transition temperatures of the PCL-based polyols used in their formation.

Figure 3-9 shows the DSC thermograms of the PCL diol 1250 and the three types of PU samples. For PU samples prepared with PCL diol with molecular weight of $1250 \text{ g}\cdot\text{mol}^{-1}$, the soft segment glass transition temperatures (a second order transition), appear in -54.4°C , -53.1°C and -52.7°C for PU1.5-1250, PU2.5-1250 and PU5-1250, respectively. On the other hand, T_g of -69.4°C for pure PCL diol 1250 was observed. This indicates that interactions between the macrochains increased with increasing HDI content. It is also corroborated by the report that T_g increases with increasing hard segment concentration for polyurethanes [192]. T_g values can be employed as an designation of the relative purity of the soft segment regions. The more the soft domains are contaminated with dissolved hard

segments, the higher shift towards higher temperatures will be observed in T_g. The soft segment T_g is also affected by the restriction imposed at the hard segment-soft segment junction and at phase boundaries [193]. The melting temperature corresponds to the melting of soft segments. DSC revealed the melting peaks for PCL diol 1250 at 52.9°C for PU1.5-1250 at 29.4°C, for PU2.5-1250 at 24.2°C and for PU5-1250 at 21.4°C during the second heating cycle. Even though crosslinking restricted the movement of polymer chains, there were still PCL parts sufficiently long to crystallize.

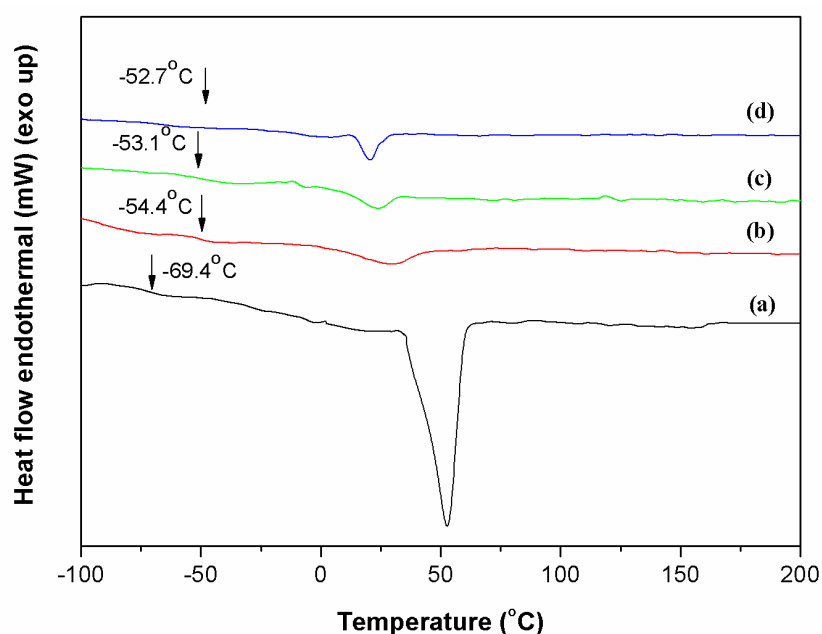


Figure 3-9 : DSC thermograms of PU's: (a) PCL diol 1250, (b) PU1.5-1250, (c) PU2.5-1250, (d) PU5-1250 (arrow designates the position of the soft segment T_g).

In literature, transitions at higher temperatures correspond to the melting of hard segments crystallites. The transition at around 55-80°C arises from the break-up of short-range order of the hard segments [108]. The transition at around 100-180°C corresponds to the break-up of the long range order of hard segments. The transition at around 190-220°C represents the melting of the microcrystalline

hard segments. However, the melting of hard segment domains was not observed for all PUs.

In a similar way, the DSC thermograms of PCL diol 2000 based polymers as shown in Figure 3-10 revealed that there are increases in Tg's of soft segment. On making the polymer with 30% hard segment content, the Tg of soft segment in PU5-2000 showed an increase from -64.1°C to -56.9°C. The slightly higher Tg of PUU5-2000 (-58.3°C) than that of PU5-2000 (-56.9°C) indicates that PUU5-2000 had less interaction between hard and soft segments than that of PU5-2000 even though their soft segments are identical. The thermal behavior differences between PU5-2000 and PUU5-2000 may have been caused by some of the extra hydrogen on nitrogen groups in urea linkages. These extra active hydrogen groups are able to form hydrogen bonds with the carbonyl groups in urethane or urea linkages and therefore increase the phase separation. The decrease in Tg of PU5-2000 is consistent with the assumption that some hard segments are dissolved in the soft segment matrix phase.

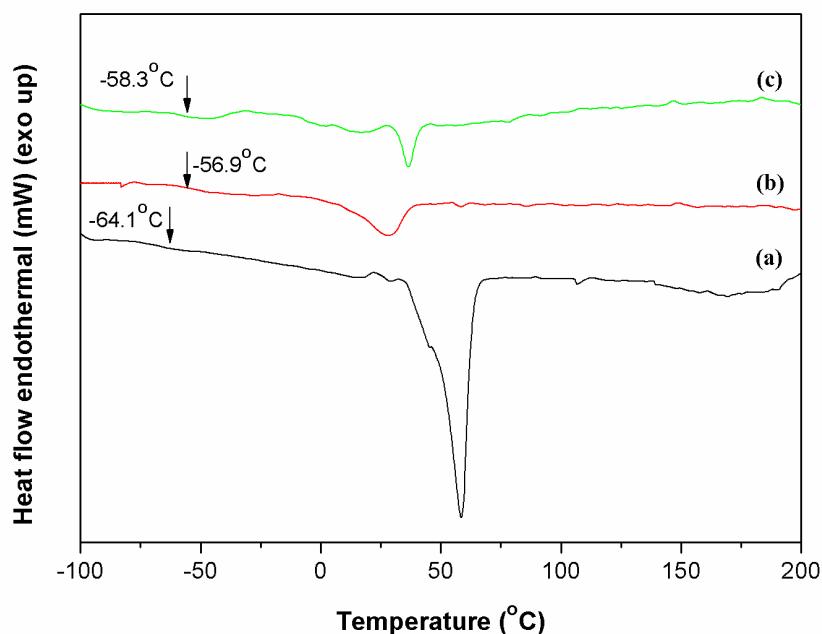


Figure 3-10 : DSC thermograms of PU's: (a) PCL diol 2000, (b) PU5-2000, (c) PUU5-2000 (arrow designates the position of the soft segment Tg).

Table 3-8 : Results of the DSC analysis of PU (\pm SD, n=3).

Polymer code	Tg(°C)	Tm (°C)	ΔHm (J/g)
PCL diol 1250	-69.4 \pm 1.6	52.9 \pm 1.4	111.4 \pm 4.5
PU1.5-1250	-54.4 \pm 1.6	29.4 \pm 1.7	29.3 \pm 4.3
PU2.5-1250	-53.1 \pm 3.1	24.2 \pm 1.3	23.5 \pm 2.4
PU5-1250	-52.7 \pm 2.5	21.4 \pm 2.6	19.9 \pm 1.3
PCL diol 2000	-64.1 \pm 1.8	58.5 \pm 2.5	107.8 \pm 3.4
PU5-2000	-56.9 \pm 1.9	29.6 \pm 1.5	37.8 \pm 1.6
PUU5-2000	-58.3 \pm 2.1	36.7 \pm 2.1	12.6 \pm 4.3
PCL triol 900	-68.7 \pm 1.2	15.2 \pm 2.3	37.9 \pm 3.7
PU5-900T	-24.8 \pm 3.1	-1.1 \pm 1.8	1.4 \pm 0.5

In general increase in the melting temperatures can be described in terms of the improved molecular weight and the strong interaction between molecular chains arising from the regular orientation of chain molecules.

The Tg exhibited by PU5-2000 (-56.9°C) is less than that of PU5-1250 (-52.7°C) as the longer segments of the former are less compatible. Furthermore, the Tg's for PU5-1250 (-52.7°C), PU5-2000 (-56.9°C) and PUU5-2000 (-58.3°C) are significantly lower than that for PU5-900T (-24.8°C). This is due to better phase separation in PU5-1250, PU5-2000 and PUU5-2000 compared to PU5-900T as evidenced by IR analysis. A secondary factor may arise from the branching structure of soft segment for PU5-900T leading to readily phase mixing. In addition, shorter soft segment chains are not acceptable to form well ordered soft segment domains.

As seen in Figure 3-11, the thermal behavior of PU5-900T demonstrates Tg at -24.8°C. On the other hand, PCL triol 900 shows the thermal behavior with Tg at -68.7°C and Tm at 15.2°C. The Tg value of PU5-900T (-24.3°C) was substantially higher than that of pure PCL triol (-68.7°C). The most significant increase in Tg and the small melting endotherm peak at -1.1°C may have been caused by shorter chain length and the increase in the number of crosslink sites

disrupting the crystalline formation in PU5-900T. Another reason can be that PU5-900T has highest phase mixing resulting in the production of amorphous regions even though it has the highest hard segment content.

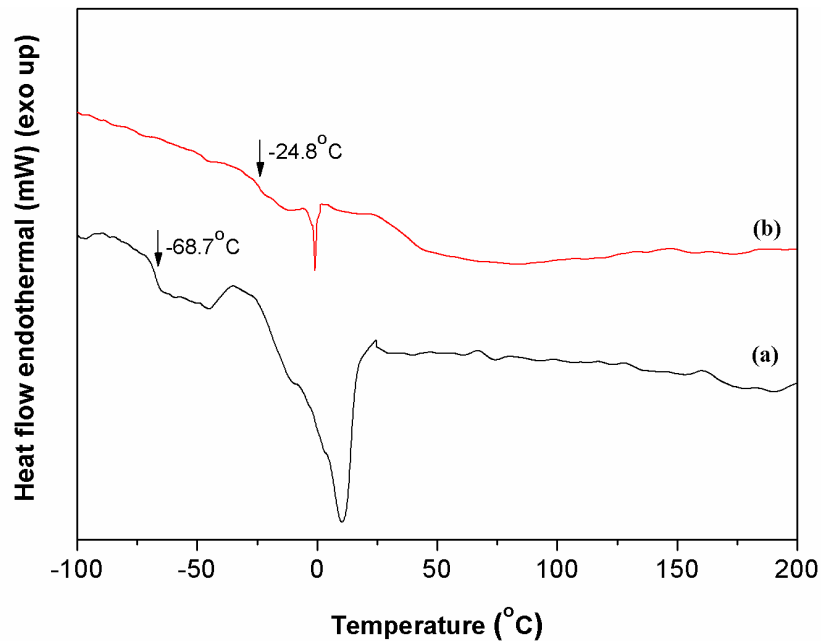


Figure 3-11 : DSC thermograms of PU's: (a) PCL triol 900, (b) PU5-900T (arrow designates the position of the soft segment Tg).

As a conclusion, the molecular weight of the macroglycol is the dominant factor for the melting temperature of soft segments. It can also be concluded that as phase mixing increases glass transition temperature of the material shifted to higher temperatures due to disentanglement of polyol chains by H-bond fixation in soft segments, which disrupts well-ordered orientation in SS. Based on the thermal behaviors of these PU materials, all materials possess elastomer characteristics at ambient conditions as well as at body temperature.

3.1.3 Dynamical Mechanical Analysis Measurements

Dynamic mechanical analysis is an effective technique in the characterization studies of viscoelastic materials where an oscillating force is applied to the material and resulting strain or deformation is measured. The viscoelastic behavior of the crosslinked films were evaluated at 1, 2, 4, 10 and 20 Hz in terms of storage modulus (E'), loss modulus (E'') and phase angle ($\tan \delta$) as a function of temperature. Storage modulus measures the stored energy, representing the ability to recover from deformation (elasticity) and the loss modulus measures the energy dissipated as heat, representing viscous portion of the material. On the other hand, $\tan \delta$ is the ratio E'' to E' [194]. Temperature was ramped from -100°C to a temperature at which the sample became too soft, as evidenced by an increasing gap between sample fixtures. Figure 3-12 (a-f) compares dynamic mechanical behaviors of the samples as a function of temperature at 1Hz. Results obtained for 2, 4, 10 and 20 Hz are given in APPENDIX B-E. Multiple segmental relaxations in DMA confirms the presence of heterophase morphology in polyurethanes. Since segmental relaxations are associated with a maximum in energy dissipation, in this work, a peak in loss modulus is used as an indicator of the α relaxation, which is equivalent to the glass transition process in a quiescent system. Table 3-11 listed transitions obtained from storage modulus.

Figure 3-12 (a) displays dynamic mechanical temperature sweep data for PU1.5-1250. The presence of three mechanical relaxation processes (peaks in E') indicates microphase separated nature of the sample as observed in FTIR analysis. Since DMA can recognize small transition regions that are beyond the resolution of DSC, the same results were not obtained by DSC. At temperatures below T_g , PU film exhibits glassy behavior and at that glassy plateau region, E' was found to be 855 MPa. The rapid decrease (transition region) in E' between two plateaus (glassy and rubbery plateau regions) corresponds to the temperature region in which the soft segments are in rubbery state and are attached at either ends to glassy hard domains which serve as crosslink points. The relaxation at lower

temperature of about -53°C can be assigned to the α relaxation or the glass transition of PCL diol 1250 soft segment, while the second relaxation at about 24°C can be assigned to the α relaxation or the glass transition of hard-soft segment interactions. Transition at about 62°C corresponds to relaxation of hard segments. This is immediately followed by sample flow from about 93°C . The behavior of E' and $\tan \delta$ was consistent with that of E'' for the soft segment relaxation, although a difference of few degrees was noted between the peak E'' and peak $\tan \delta$ values.

Dynamic mechanical temperature sweep data of PU2.5-1250 is provided in Figure 3-12 (b). The figure also displays two prominent segmental relaxations in E'' at about -45°C , corresponding to the soft segment T_g . On the other hand, the width next to it indicates a phase mixing at 20°C corresponding to T_g of the mixed segments. A reduction in E' as the sample passes these two transitions is also seen in the figure. This is immediately followed by sample flow from about 62°C .

Dynamic mechanical temperature sweep data of PU5-1250 is provided in Figure 3-12 (c). The figure displays a prominent segmental relaxations in E'' at about -50°C .

It can be concluded that the microstructure of PCL diol 1250 based PUs consist of slightly segregated hard and soft segment phases possibly driven by the formation of hydrogen bonding between the urethane functional groups of the hard segments. Having the strong interaction between hard segments PU1.5-1250 showed higher phase separation than PU2.5-1250 and PU5-1250. PU5-1250 exhibited generally phase mixing behavior. DMA results showed the same phase separation order which can be supported by deconvolution results. The hardness (E') of PCL which has flexible chains decreased by the addition of HDI at 25°C and 37°C .

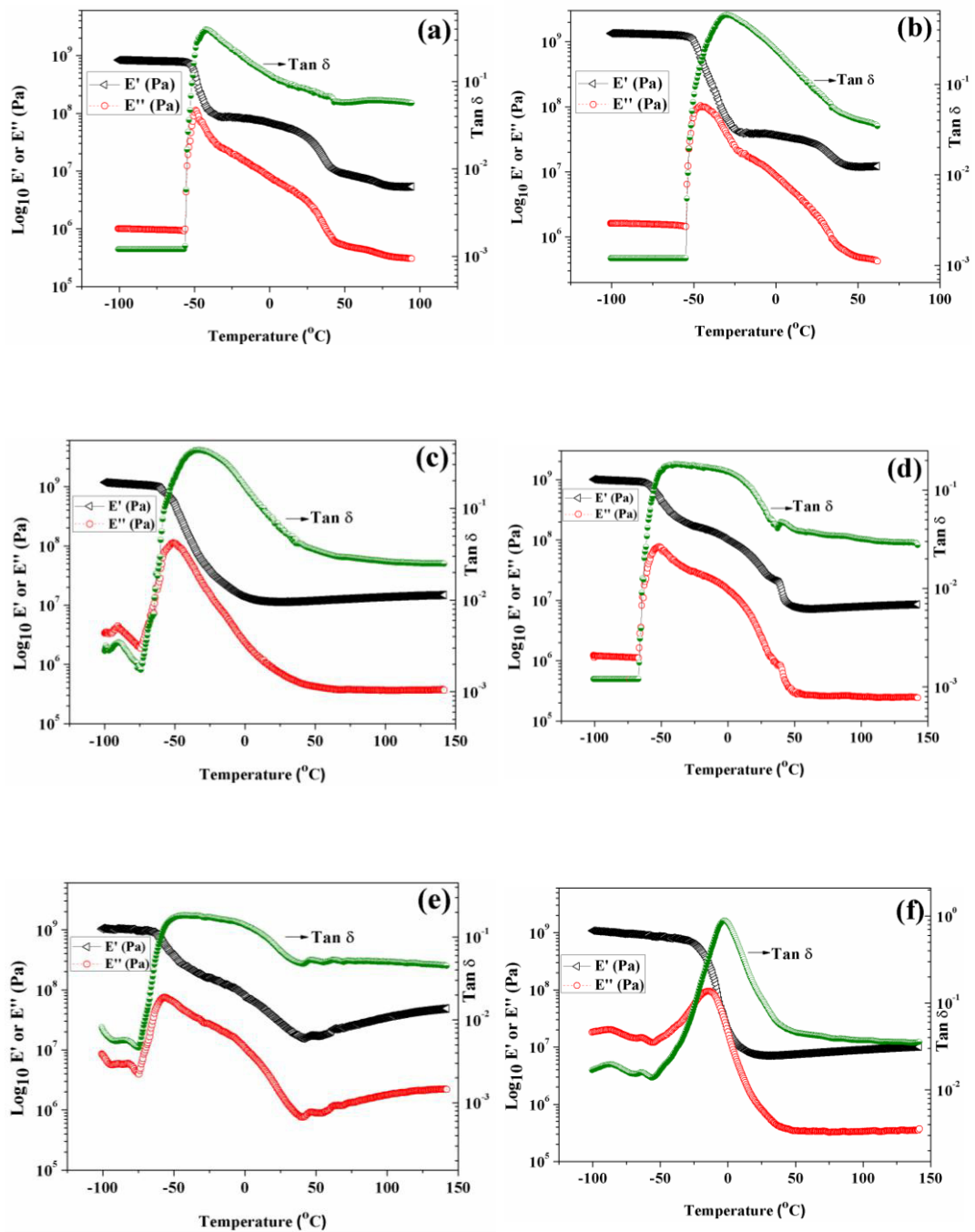


Figure 3-12 : DMA curves of all PUs : (a) PU1.5-1250; (b) PU2.5-1250; (c) PU5-1250; (d) PU5-2000; (e) PUU5-2000; (f) PU5-900T (conditions: $5^{\circ}\text{C}/\text{min}$, 1 Hz, film in tensile mode).

DMA behavior of PU5-2000 is plotted in Figure 3-12 (d). From storage modulus results the existence of three phase morphology in the sample is evident. The lower α relaxation in E'' (-52°C) corresponds to the glass transition of PCL diol 2000 segment, the presence of a second relaxation due to hard segment glass transition, at about 39°C is subtle but still observable. There is another phase at 1°C showing transition for mixed phase. Furthermore, the DMA response of PUU5-2000 (Figure 3-12 (e)) shows the lower α relaxation in E'' at -59°C and the second relaxation at 46°C and 59°C assigned to hard segment relaxations. For this sample two relaxations in hard segments were observed due to two different crystalline formation between hard segment domains. Additionally, PUU5-2000 exhibited one more transition at -10°C corresponding to glass transition of mixed phase.

Similarly, the DMA plot of PU5-900T in terms of E' , E'' and $\tan \delta$ is shown in Figure 3-15 (f). The E' , E'' , and $\tan \delta$ responses exhibited the presence of a broad single relaxation at -26°C corresponding to the PCL triol 900 glass transition. The presence of a second transition corresponding to hard segments is subtle and barely discernible. The disappearance of this second relaxation is seen by incorporation of branched polyol into the polymer backbone.

PU5-2000 and PUU5-2000 polymers have a marked decrease in soft segment glass transition was noticed. This observed decrease in soft segment relaxation temperature is again consistent with previously presented DSC data and suggest increased phase segregation in hard segments. Also when compared with the all PU samples, the soft segment glass transition of PU5-900T was seen to increase with the use of branched polyol in the synthesis. A plausible explanation for these observations is that the branching discourages hard segment packing and thereby promotes mixing with the soft segments. The IR data presented earlier clearly supports the hypothesis for disordered hard segment phase.

Polyurethanes are commonly used in the production of medical devices ranging from catheters to total artificial hearts. This utilizes the importance of dynamical mechanical behavior at room temperature and body temperature. Therefore, the storage modulus values of the prepared PU films were calculated at both 25°C and 37°C, and are given in Table 3-11. PU5-2000 exhibits the highest value for E' at 25°C in the rubbery plateau region of the curve. PU5-2000 has the highest storage value at body temperature. At room and body temperature, the storage modulus was 12-14 times as high as the loss modulus. This meant that the energy change required for displacement was mainly reversible.

Table 3-9 : Transitions Obtained from Storage Modulus at 1 Hz.

Sample code	Transitions		
	T _{g1} (°C)	T _{g2} (°C)	T _{gM} (°C)
PU1.5-1250	-53	62	24
PU2.5-1250	-45	-	20
PU5-1250	-50	-	-
PU5-2000	-52	39	1
PUU5-2000	-59	46 and 59	-10
PU5-900T	-26	-	-

T_{g1}: Soft segment glass transition temperature, T_{g2}: hard segment glass transition temperature, T_{gM}: mixed phase glass transition temperature.

Table 3-10 : Storage Modulus and Loss Modulus of PUs at 1 Hz at 25°C and 37°C.

Sample code	$E' \times 10^6$ at	$E' \times 10^6$ at	$E'' \times 10^6$ at	$E'' \times 10^6$ at
	25°C (Pa)	37°C (Pa)	25°C (Pa)	37°C (Pa)
PU1.5-1250	37.1	15.3	3.1	1.1
PU2.5-1250	25.2	14.5	2.1	0.7
PU5-1250	11.3	11.5	0.7	0.5
PU5-2000	33.8	20.4	2.4	0.8
PUU5-2000	27.4	16.5	1.8	0.8
PU5-900T	7.2	7.2	0.8	0.4

The simultaneous gradual weakening of the hard segment relaxation might be due to two plausible effects operating simultaneously: 1) excess isocyanate forbid hard segment packing, arising from the formation of allophanate leading to a large proportion of hard segments to mix with the soft segments, and 2) pendant chains plasticize hard segments so much that PU5-900T fail to exhibit a discernable hard segment glass transition. The evidence for the first mentioned effect was seen from IR data presented earlier. DMA results showed following order of phase separation:

$$\text{PUU5-2000} > \text{PU5-2000} > \text{PU5-1250} > \text{PU5-900T}$$

This observation is determined by their phase separation morphology according to the existence of a multitude of transitions and then their relative glass transition values.

3.1.4 X-Ray Diffraction Measurements

X-Ray diffraction techniques examine the long-range order produced as a consequence of very short-range interactions. In order to get an idea of the morphological state of the synthesized polyurethane, X-Ray diffraction analysis was carried out. Crystalline structures of all polyurethanes were compared in Figure 3-13 at a range of 5–80°. Figure 3-14 is helpful to examine in more detailed analysis between 2θ values of 5–40°.

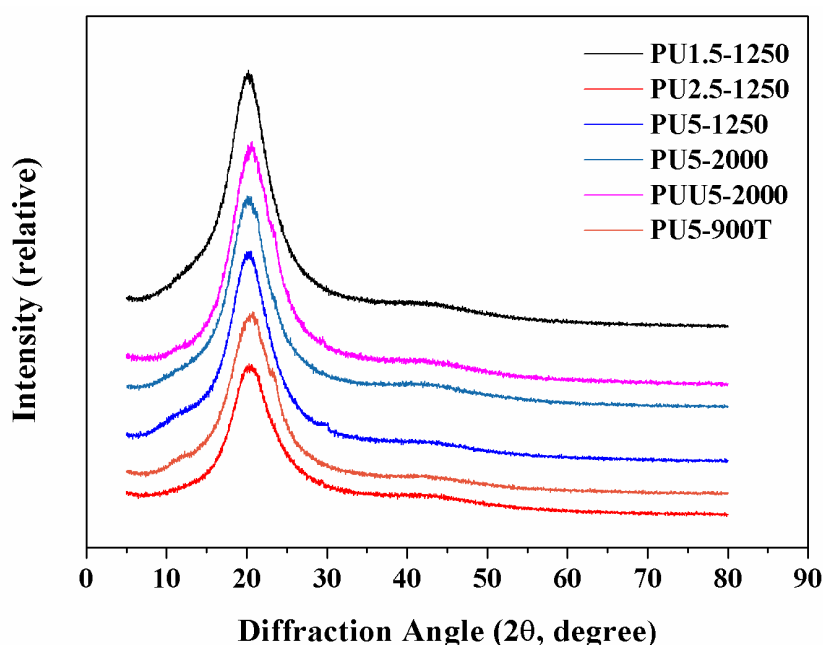


Figure 3-13 : The XRD curves of different PU films in the range between 5 and 80°.

In literature, the characteristic peaks of PCL (semi-crystalline) are at $2\theta = 21^\circ$ and $2\theta = 23.5^\circ$ [195]. For polyurethane samples, a broad diffraction peak can be obviously observed in the range between $2\theta \sim 20.28^\circ$ - 20.88° indicating PCL crystalline phase, not identical with those of pure PCL. It can be concluded that the orderly arrangement of crystalline phase is preserved in the PU samples after crosslinking. On the other hand, the crystallinity of the branched polymers are

lower than for their linear analogues due to shorter chain length and the increase in the number of crosslink sites disrupting the crystalline structure. In all PUs, the positions of the PCL crystals remain almost constant though the intensity of the peaks indicating crystallinity content increased according to following order:

PU1.5-1250 > PUU5-2000 > PU5-2000 > PU5-1250 > PU5-900T > PU2.5-1250

In literature, the peak located at around $11^\circ 2\theta$ is assigned to the crystallinity of hard segments. In this study, no sharp peak due to crosslinking is found in any diffractogram, but the peak correspond to the hard segment crystallinity appears as a shoulder at around $11^\circ 2\theta$ because of band overlapping.

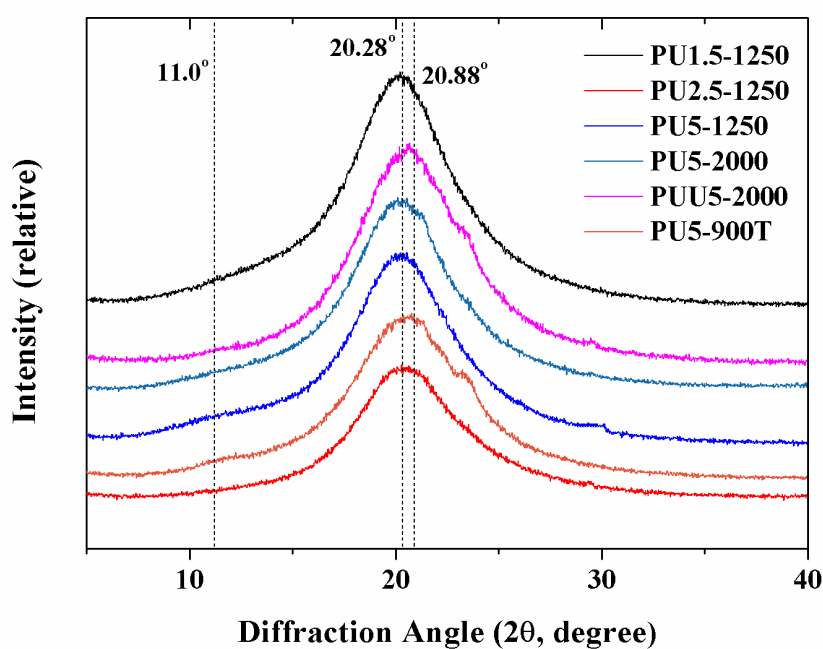


Figure 3-14 : The XRD curves of different PU films in the range between 5 and 40° .

3.2 Tensile Test Results

The mechanical film properties such as ultimate tensile strength (UTS), modulus of elasticity (E), and elongation at break (ϵ) values were measured and related to chemical composition. Results of the tensile tests are illustrated in Figure 3-15 and summarized in Table 3-11. The elastomeric properties of the PU vary with number of variables, including soft segment molecular weight and hard segment concentrations, as a consequence of the alteration in hydrogen-bonding characteristics. PU films were flexible with tensile strengths ranging from 1.9 MPa to 14.3 MPa, modulus 2.9 MPa to 56.5 MPa and breaking strains from 63.7% to 1170.0%. As the HS content was gradually changed from 17% to 48%, the elastic modulus generally showed increase. Because the mechanical behavior of urea based polyurethanes mainly depend on micro domain characteristics, the observed mechanical properties can be clarified from that point of view.

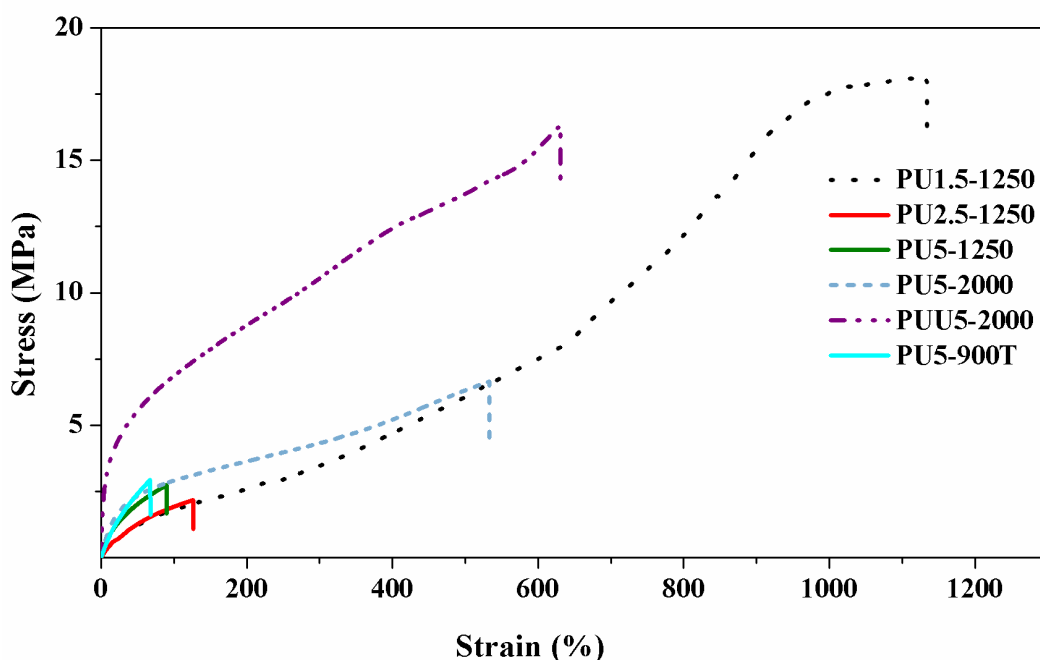


Figure 3-15 : Stress-strain graphs of PUs.

Table 3-11 : Tensile properties of PU films (\pm SD, n=5).

Polymer code	Mechanical properties			HS content (wt.%)
	UTS (MPa)	<i>E</i> (MPa)	ϵ (%)	
PU1.5-1250	14.3 \pm 4.1	2.9 \pm 0.5	1171.0 \pm 114.9	17
PU2.5-1250	1.9 \pm 0.3	4.5 \pm 0.4	106.1 \pm 34.9	25
PU5-1250	2.7 \pm 0.4	9.9 \pm 1.5	85.9 \pm 21.4	40
PU5-2000	5.6 \pm 1.7	7.9 \pm 1.8	432.3 \pm 145.8	30
PUU5-2000	16.3 \pm 4.3	56.5 \pm 6.8	653.8 \pm 116.7	30
PU5-900T	2.7 \pm 0.2	8.1 \pm 1.2	63.7 \pm 12.9	48

For PUs synthesized from the same polyol, PU1.5-1250, PU2.5-1250 and PU5-1250 series, PU2.5-1250 has the lowest tensile strength (1.9 MPa) when compared to PU1.5-1250 (14.3 MPa) and PU5-1250 (2.7 MPa). The higher content of hard segments in PU5-1250 leads to an increase of Young's modulus and a decrease in ultimate tensile strength and elongation at break even though it has lowest phase separation supported by IR analysis due to more covalent crosslinks between chains. Therefore, the mechanical properties of polyurethanes with the same molecular weights were dependent on the hard-segment content. As discussed previously, the characteristic of the crosslinked polymers are governed by the nature of the constituent monomers and their relative concentration, but also by the resultant distance between the crosslinking points. If the distance between crosslink points is tight, the chain length between the crosslinks is short and the higher modulus is observed for this type of polymers. Thus, crosslinking contributed to enhancing elastomeric properties of the polymers by recover after deformation since crosslink resist creep effectively. PU1.5-1250 has improved mechanical properties because of the larger volume fraction and strong cohesiveness of hard segments, which is a general trend reported from phase-separated PUs [133,196,197]. The relative changes in concentration of free carbonyl group can also alter the morphology of the PU and consequently affect the final mechanical properties of polymers. PU2.5-1250 has the highest free carbonyl content as estimated by deconvolution in section 3.1.1.2 in Table 3-6.

Thus, increase in free carbonyl content results in decrease in ultimate tensile strength. The addition of excess isocyanate into the polymer matrix leads to the formation of a crack-free film which in turn enhances the mechanical and corrosion resistance properties. PU1.5-1250 exhibits remarkable elongation (1171.0%) at break. However, PU2.5-1250 exhibits lower (106.1%) and PU5-2000 has even more lower elongation (85.9%).

The primary consequences of increasing the molecular weight of the soft block for a given overall molar ratio of hard block to polyol block, as in the case of PU5-1250 and PU5-2000, results in a decrease in modulus from 9.9 MPa to 7.9 MPa and an increase in elongation from 85.9% to 432.3%, as illustrated in Table 3-11.

Among polyurethanes, urea based polyurethane suggests better mechanical properties over remaining materials as given in Table 3-11, which reflect the regularity of its chain structure and its ability to crystallize upon extension with the addition of urea bonds in PUU5-2000. This polymers have the highest values for tensile strength, modulus and elongation. A polyol having a more symmetrical structure will enhance the formation of organized structures in hard segment domains, and thus, more complete phase segregation. Since PU5-900T possesses highly branched structure and large number of reactive end groups composed of three armed soft segment prevents formation of ordered structures, resulting in decrease in tensile strength (2.7 MPa) and elongation (63.7 MPa).

PU films were flexible with tensile strengths ranging from 1.9 to 14.3 MPa, and breaking strains from 63.7% to 1170.0%. With decreasing hard segment content (HS = 25%) in PU2.5-1250, Young modulus of 2.5-1250 decreased, but the elongation at break about 1.2 times greater and work to break were about 2.2 times greater than PU5-1250.

Since PU5-900T possesses highly branched structure, large number of reactive end groups, excellent flow and processing characteristics due to low amount of inter or intramolecular entanglements. It can be easily visualized that the allophanate linkages are potential crosslink points and hence can cause significant effect on the ultimate mechanical properties. The addition of more isocyanate to polyurethane promotes the interfacial adhesion between the domains and the matrix, without domain reductions because in these specific systems the disperse phase is a copolymer and thermosetting material, respectively. These compounds replace linear polymers to reduce viscosity, increase reaction rate, and improve toughness because of their highly branched molecular structures.

Therefore, by appropriate variations in chemical structure, molecular weight and composition it is possible to obtain polymers with different strength, Young's modulus and elasticity for a wide range of mechanical properties. In general, increase in hard segment ratio contributed to better mechanical properties. An exception to this trend was the PU1.5-1250 material, which, regardless of the low hard-segment content (17%), showed a relatively high value of tensile strength. This may be due to better phase separation. The tensile force acting on the material might have led to better orientation and/or crystallization within the hard segment domains.

3.3 Hydrophilicity Results

The effect of composition on surface properties were also evaluated in a semi-quantitative manner through the use of contact angle measurements. The polyurethane with different hard segment ratios analysed and water contact angle values are summarized in Table 3-12. Contact angle is dependent on polymer surface hydrophilicity which is one important parameter in biomedical applications affected by phase separation. The contact angles vary from 72.7° to 82.4°.

Table 3-12 : Static water contact angle measurement of PUs with different hard segments (\pm SD, n=5).

Polymer code	Water contact angle ($^{\circ}$)	HS content (wt.%)
PU1.5-1250	74.3 \pm 1.5	17
PU2.5-1250	79.8 \pm 3.1	25
PU5-1250	79.3 \pm 3.5	40
PU5-2000	72.7 \pm 1.6	30
PUU5-2000	82.4 \pm 2.4	30
PU5-900T	78.1 \pm 1.2	48

An increase in contact angle was observed in PU1.5-1250 and PU5-2000. The largest contact angle obtained for the PUU5-2000 indicating the presence of a largest hydrophobic surface. It was expected that the longer PCL incorporated in the soft segment of the polyurethanes define a more hydrophobic behavior, owing to the existence of more hydrocarbons sequence. However, the insertion of excess isocyanate compounds altered the surface wetting characteristic of the polymeric matrix with reducing the extent of polar groups on the surface by introducing allophanate and/or biuret linkages.

3.4 Effect of Heparin Blending on Mechanical and Hydrophilicity Properties

Table 3-13 shows the mechanical properties and hydrophilicity results for PUU5-2000 and PUU5-2000-HP. After the addition of aqueous solution of heparin to the polymer, and after curing the samples it was observed that tensile strength decreased from 16.3 MPa to 11.3 MPa and modulus increased from 56.5 MPa to 74.6 MPa due to formation of urea groups within the polymer structure. Elongation was resulted in a decrease from 653.8% to 295.1 %. This can be explained by disruption of polymer crystallization in soft segments due to heparin addition.

Table 3-13 : Mechanical properties and static water contact angle results of PUU5-2000 and PUU5-2000-HP.

Polymer code	Mechanical properties			Water contact angle (°)
	UTS (MPa)	E (MPa)	ϵ (%)	
PUU5-2000	16.3±4.3	56.5±6.8	653.8±116.7	82.4±2.4
PUU5-2000-HP	11.3±2.9	74.6±5.4	295.1±47.2	60.9±3.1

CHAPTER 4

CONCLUSION

Despite the apparent simplicity of polyurethane synthesis, any alterations in the polyol and prepolymer ratio (NCO/OH) cause substantial morphological changes in the polymer chains, leading to modifications in overall properties of the material.

This study aimed to examine chemical, mechanical, thermal and wettability properties of polyurethanes synthesized with varying NCO/OH ratio and polyol type without adding any other ingredients. Polyurethanes with potential applications in medical implants were obtained from aliphatic diisocyanates and PCL diol or triol. The research reported on the investigation of six different types of polyurethanes, which were prepared by the direct reaction of the two components ($-NCO/-OH$) with hard segment content of 17%, 25%, 30%, 40% and 48%. Excess HDI was utilized in order to introduce crosslinking into the polymer structures via formation of allophanate and/or biuret linkages. The effect of excess isocyanate on the properties of final polyurethanes was examined using FTIR-ATR, DSC, DMA and XRD. In addition, mechanical properties and surface wettability were studied. An aqueous solution of heparin, that is a natural polymer, was blended with PUU5-2000 sample which was previously shown to have good tensile and elongation properties. The idea with using aqueous heparin is to obtain a polymer with better wetting properties.

Phase separation and phase mixing were investigated in order to examine their effects on ultimate properties of PUs. IR analysis by deconvolution method in N-H and C=O regions revealed that increase in chemical crosslinks between the polymer chains decreased the extent of H-bonds markedly in HS-HS in the case

of PU1.5-1250, PU2.5-1250 and PU5-1250. Branched structure of the polyol having three OH functional groups in PU5-900T resulted in regular crosslinking and reduction in phase separation. The existence of longer soft segment in polymers increased concentration of H-bonds in HS-HS. It is obvious that urea groups make stronger H-bonds between HS-HS, resulting in better phase segregation in PUU5-2000.

DSC analysis exhibited two transitions, that is T_g and T_m of soft segments in the thermograms for all PUs. Phase mixing was supported by decrease in T_g values of soft segments resulting as a consequence of increase in HDI content. This may be due to allophanate and/or biuret formation bringing the chains closer would prefer H-bonds in HS-SS rather than H-bonds in HS-HS. The second reason can be decrease in urethane content when the excess isocyanates form crosslinks. The melting temperatures for the PUs composed of PCL diol 1250 decreased to lower temperatures because of disruption of crystalline structures in soft segments as HDI content increased. Urea containing compound, namely PUU5-2000 exhibited higher melting temperature as a result of stronger bidentate H-bonds in hard segment domains. The nature (molecular weight and type) of the polyol and HDI concentration have significant influence on the melting temperature of soft segments for this type of synthesis.

DMA results indicated that two glass transitions are obviously seen for samples claimed as phase segregated. One of them shows T_g of soft segment at around -50°C and the other exhibits T_g of hard segment as a small peak at around 50°C.

Evaluation of mechanical properties revealed that highest elongation value was obtained with PU1.5-1250 having least HDI content and the second highest elongation value was observed with PUU5-2000. Crosslink density is another factor which influences the elongation. Thus, elongation values decreased as HDI amount increasing in polymer samples prepared with the same polyol due to the higher crosslink the shorter chain length between the crosslinks.

When comparing all PUs except PU1.5-1250 with respect to their wettability, no significant difference was obtained. PU1.5-1250 films showed better hydrophilicity due to absence of crosslinking which enables the tending of polar groups towards to film surface by conformational rotation of the polymer chains. Incorporation of heparin into the polymer matrix produced more hydrophilic films (water contact angle reduced from 80° to 60°) compared to films without additive.

This study explains composition-property relations of polyurethanes prepared in different compositions of polyol and HDI. Further studies are planned to examine composition-property-cell affinity relations for the similar structures in order to optimize the preparation conditions to get the desired physical and mechanical properties.

REFERENCES

- [1] R. Arshady, *Desk reference of functional polymers: Synthesis and applications*, Washington, DC: American Chemical Society, 1997.
- [2] J. C. M. V. Hest, "Biosynthetic-synthetic polymer conjugates," *Journal of Macromolecular Science, Part C: Polymer Reviews*, vol. 47, 2007, pp. 63-92.
- [3] D. Cunliffe, S. Pennadam, and C. Alexander, "Synthetic and biological polymers-merging the interface," *European Polymer Journal*, vol. 40, 2004, pp. 5-25.
- [4] A. Burke and N. Hasirci, "Polyurethanes in biomedical applications," *Advances in Experimental Medicine and Biology*, vol. 553, 2004, pp. 83-101.
- [5] S. Kutay, T. Tincer, and N. Hasirci, "Polyurethanes as biomedical materials," *British Polymer Journal*, vol. 23, 1990, pp. 267-272.
- [6] P. Vermette, H. J. Griesser, G. Laroche, and R. Guidoin, *Biomedical applications of polyurethanes*, Texas, USA: Eureka.com, 2001.
- [7] H. Yeganeh, M. Lakouraj, and S. Jamshidi, "Synthesis and properties of biodegradable elastomeric epoxy modified polyurethanes based on poly(ϵ -caprolactone) and poly(ethylene glycol)," *European Polymer Journal*, vol. 41, 2005, pp. 2370-2379.
- [8] A. Christenson, E. M. Anderson, and J. M. Hiltner, "Biodegradation mechanisms of polyurethane elastomers," *Corrosion Engineering, Science and Technology*, vol. 42, 2007, pp. 312-323.
- [9] O. Bayer, "Das di-isocyanat-polyadditionsverfahren (Polyurethane)," *Angewandte Chemie*, vol. 59, 1947, pp. 257-272.
- [10] M. Brunette, S. L. Hsu, and J. Macknight, "Structural and mechanical properties of polybutadiene-containing polyurethanes," *Polymer Engineering and Science*, vol. 21, 1981, pp. 163-171.

- [11] T. G. Grasel and S. L. Cooper, “*Surface properties and blood compatibility of polyurethaneureas,*” *Biomaterials*, vol. 7, 1986, pp. 315-328.
- [12] W. J. Pangman, “*Compound prosthesis,*” U.S. Patent 3559214, 1965.
- [13] W. J. Pangman, “*Compound prosthesis device,*” U.S. Patent 2842775, 1958.
- [14] M. P. Mandorino and J. E. Salvatore, “*Polyurethane polymer (ostamer): Its use in fractured and diseased bones; experimental results,*” *Surgical Forum*, vol. 9, 1958, pp. 762-765.
- [15] M. P. Mandorino and J. E. Salvatore, “*Polyurethane polymer; its use in fractured and diseased bones,*” *American Journal of Surgery*, vol. 97, 1959, pp. 442-446.
- [16] M. P. Mandorino and J. E. Salvatore, “*A polyurethane polymer (ostamer): Its use in fractured and diseased bones. Report of thirty-five cases,*” *Archives of Surgery*, vol. 80, 1960, pp. 623-627.
- [17] B. Dreyer, T. Akutsu, and W. J. Kolff, “*Testing of artificial heart valves,*” *Journal of Applied Physiology*, vol. 14, 1959, pp. 475-478.
- [18] B. Dreyer, T. Akutsu, and W. J. Kolff, “*Aortic grafts of polyurethane in dogs,*” *Journal of Applied Physiology*, vol. 15, 1960, pp. 18-22.
- [19] L. Pinchuk, “*A review of the biostability and carcinogenicity of polyurethanes in medicine and the new generation of ‘biostable’ polyurethanes,*” *Journal of Biomaterials Science, Polymer Edition*, vol. 6, 1995, pp. 225-267.
- [20] J. W. Boretos, D. E. Detmer, and J. H. Donachy, “*Segmented polyurethane: A polyether polymer, II. Two years experience,*” *Journal of Biomedical Materials Research*, vol. 5, 1971, pp. 373-387.
- [21] J. W. Boretos and W. S. Pierce, “*Segmented polyurethane: A polyether polymer. An initial evaluation for biomedical applications,*” *Journal of Biomedical Materials Research*, vol. 2, 1968, pp. 121-130.
- [22] E. Bezon, J. A. Barra, A. Karaterki, J. Braesco, J. C. Pillet, and P. Mondine, “*Mechanical system of left ventricle cannulation: Control of tightness by experimental left ventricular assistance,*” *Chirurgie*, vol. 121, 1996, pp. 447-452.

- [23] S. A. Guelcher, "Biodegradable polyurethanes: Synthesis and applications in regenerative medicine," *Tissue Engineering. Part B*, vol. 14, 2008, pp. 3-17.
- [24] E. Nyilas, R. C. Leinbach, J. B. Caulfield, M. J. Buckley, and W. G. Austen, "Development of blood-compatible elastomers. 3. Hematologic effects of Avcothane intra-aortic balloon pumps in cardiac patients," *Journal of Biomedical Materials Research*, vol. 6, 1972, pp. 129-154.
- [25] E. Nyilas and R. S. Ward, "Development of blood-compatible elastomers. V. Surface structure and blood compatibility of avcothane elastomers," *Journal of Biomedical Materials Research*, vol. 11, 1977, pp. 69-84.
- [26] E. Nyilas, "Development of blood compatible elastomers. II. Performance of Avcothane blood contact surfaces in experimental animal implantations," *Journal of Biomedical Materials Research*, vol. 6, 1972, pp. 97-127.
- [27] M. D. Lelah, L. K. Lambrecht, B. R. Young, and S. L. Cooper, "Physicochemical characterization and in vivo blood tolerability of cast and extruded biomer," *Journal of Biomedical Materials Research*, vol. 17, 1983, pp. 1-22.
- [28] C. S. Sung, C. B. Hu, E. W. Merrill, and E. W. Salzman, "Surface chemical analysis of Avcothane and Biomer by Fourier transform IR internal reflection spectroscopy," *Journal of Biomedical Materials Research*, vol. 12, 1978, pp. 791-804.
- [29] S. Young, G. Pincus, and N. H. Hwang, "Dynamic evaluation of the viscoelastic properties of a biomedical polymer (biomer)," *Biomaterials, Medical Devices and Artificial Organs*, vol. 5, 1977, pp. 233-254.
- [30] S. W. Graham and D. M. Hercules, "Surface spectroscopic studies of Avcothane," *Journal of Biomedical Materials Research*, vol. 15, 1981, pp. 349-361.
- [31] N. Hasirci and A. Burke, "Polyurethanes in biomedical applications," *Advances in Experimental Medicine and Biology*, vol. 553, 2004, pp. 83-101.
- [32] R. J. Zdrahala, "Biomedical applications of polyurethanes: A review of past promises, present realities, and a vibrant future," *Journal of Biomaterials Applications*, vol. 14, 1999, pp. 67-90.

- [33] R. E. Phillips, M. C. Smith, and R. J. Thoma, “*Biomedical applications of polyurethanes: Implications of failure mechanisms,*” *Journal of Biomaterials Applications*, vol. 3, 1988, pp. 207-227.
- [34] A. Atala and R. P. Lanza, “*Methods of tissue engineering,*” Gulf Professional Publishing, 2002.
- [35] S. Gogolewski and K. Gorna, “*In vitro degradation of novel medical biodegradable aliphatic polyurethanes based on ϵ -caprolactone and Pluronic® with various hydrophilicities,*” *Polymer Degradation and Stability*, vol. 75, 2002, pp. 113-122.
- [36] M. Siepe, M. N. Giraud, E. Liljensten, U. Nydegger, P. Menasche, T. Carrel, and H. T. Tevaearai, “*Construction of skeletal myoblast-based polyurethane scaffolds for myocardial repair,*” *Artificial Organs*, vol. 31, 2007, pp. 425-433.
- [37] A. E. Hafeman, B. Li, T. Yoshii, K. Zienkiewicz, J. M. Davidson, and S. A. Guelcher, “*Injectable biodegradable polyurethane scaffolds with release of platelet-derived growth factor for tissue repair and regeneration,*” *Pharmaceutical Research*, vol. 25, 2008, pp. 2387-2399.
- [38] Y. Zhu, C. Gao, J. Guan, and J. Shen, “*Engineering porous polyurethane scaffolds by photografting polymerization of methacrylic acid for improved endothelial cell compatibility,*” *Journal of Biomedical Materials Research Part A*, vol. 67, 2003, pp. 1367-1373.
- [39] K. Gorna and S. Gogolewski, “*Biodegradable porous polyurethane scaffolds for tissue repair and regeneration,*” *Journal of Biomedical Materials Research Part A*, vol. 79, 2006, pp. 128-138.
- [40] C. R. Lee, S. Grad, K. Gorna, S. Gogolewski, A. Goessl, and M. Alini, “*Fibrin–polyurethane composites for articular cartilage tissue engineering: A preliminary analysis,*” *Tissue Engineering*, vol. 11, 2005, pp. 1562-1573.
- [41] C. M. Hill, Y. H. An, Q. K. Kang, L. A. Hartsock, S. Gogolewski, and K. Gorna, “*Osteogenesis of osteoblast seeded polyurethane-hydroxyapatite scaffolds in nude mice,*” *Macromolecular Symposia*, vol. 253, 2007, pp. 94-97.

- [42] C. Schlickewei, S. Verrier, S. Lippross, S. Pearce, M. Alini, and S. Gogolewski, "*Interaction of sheep bone marrow stromal cells with biodegradable polyurethane bone substitutes,*" *Macromolecular Symposia*, vol. 253, 2007, pp. 162-171.
- [43] K. Walinska, A. Iwan, K. Gorna, and S. Gogolewski, "*The use of long-chain plant polyprenols as a means to modify the biological properties of new biodegradable polyurethane scaffolds for tissue engineering. A pilot study,*" *Journal of Materials Science, Materials in Medicine*, vol. 19, 2008, pp. 129-135.
- [44] S. Gogolewski and K. Gorna, "*Biodegradable polyurethane cancellous bone graft substitutes in the treatment of iliac crest defects,*" *Journal of Biomedical Materials Research. Part A*, vol. 80, 2007, pp. 94-101.
- [45] J. Guan, K. L. Fujimoto, M. S. Sacks, and W. R. Wagner, "*Preparation and characterization of highly porous, biodegradable polyurethane scaffolds for soft tissue applications,*" *Biomaterials*, vol. 26, 2005, pp. 3961-3971.
- [46] M. Borkenhagen, R. C. Stoll, P. Neuenschwander, U. W. Suter, and P. Aebischer, "*In vivo performance of a new biodegradable polyester urethane system used as a nerve guidance channel,*" *Biomaterials*, vol. 19, 1998, pp. 2155-2165.
- [47] T. C. McDevitt and K. A. Woodhouse, S. D. Hauschka, C. E. Murry, and P. S. Stayton, "*Spatially organized layers of cardiomyocytes on biodegradable polyurethane films for myocardial repair,*" *Journal of Biomedical Materials Research. Part A*, vol. 66, 2003, pp. 586-595.
- [48] J. D. Fromstein and K. A. Woodhouse, "*Elastomeric biodegradable polyurethane blends for soft tissue applications,*" *Journal of Biomaterials Science, Polymer Edition*, vol. 13, 2002, pp. 391-406.
- [49] C. M. Agrawal, J. E. Parr, and S. T. Lin, "*Synthetic bioabsorbable polymers for implants,*" *Astm International*, 2000.
- [50] S. Sharifpoor, C. A. Simmons, R. S. Labow, and J. P. Santerre, "*Functional characterization of human coronary artery smooth muscle cells under cyclic mechanical strain in a degradable polyurethane scaffold,*" *Biomaterials*, vol. 32, 2011, pp. 4816-4829.

- [51] C. Alperin, P. W. Zandstra, and K. A. Woodhouse, “*Polyurethane films seeded with embryonic stem cell-derived cardiomyocytes for use in cardiac tissue engineering applications,*” *Biomaterials*, vol. 26, 2005, pp. 7377-7386.
- [52] S. Sharifpoor, R. S. Labow, and J. P. Santerre, “*Synthesis and characterization of degradable polar hydrophobic ionic polyurethane scaffolds for vascular tissue engineering applications,*” *Biomacromolecules*, vol. 10, 2009, pp. 2729-2739.
- [53] S. Grad, L. Kupcsik, K. Gorna, S. Gogolewski, and M. Alini, “*The use of biodegradable polyurethane scaffolds for cartilage tissue engineering: potential and limitations,*” *Biomaterials*, vol. 24, 2003, pp. 5163-5171.
- [54] S. L. Chia, K. Gorna, S. Gogolewski, and M. Alini, “*Biodegradable elastomeric polyurethane membranes as chondrocyte carriers for cartilage repair,*” *Tissue Engineering*, vol. 12, 2006, pp. 1945-1953.
- [55] S. Gogolewski, K. Gorna, and A. S. Turner, “*Regeneration of bicortical defects in the iliac crest of estrogen-deficient sheep, using new biodegradable polyurethane bone graft substitutes,*” *Journal of Biomedical Materials Research. Part A*, vol. 77, 2006, pp. 802-810.
- [56] K. Gorna and S. Gogolewski, “*Preparation, degradation, and calcification of biodegradable polyurethane foams for bone graft substitutes,*” *Journal of Biomedical Materials Research. Part A*, vol. 67, 2003, pp. 813-827.
- [57] K. Gorna, S. Polowinski, and S. Gogolewski, “*Synthesis and characterization of biodegradable poly(ϵ -caprolactone urethane)s. I. Effect of the polyol molecular weight, catalyst, and chain extender on the molecular and physical characteristics,*” *Journal of Polymer Science Part A: Polymer Chemistry*, vol. 40, 2002, pp. 156-170.
- [58] J. P. Santerre, K. Woodhouse, G. Laroche, and R. S. Labow, “*Understanding the biodegradation of polyurethanes: From classical implants to tissue engineering materials,*” *Biomaterials*, vol. 26, 2005, pp. 7457-7470.
- [59] K. Ulubayram and N. Hasirci, “*Polyurethanes: effect of chemical composition on mechanical properties and oxygen permeability,*” *Polymer*, vol. 33, 1992, pp. 2084-2088.
- [60] M. D. Lelah, *Polyurethanes in medicine*, Florida: CRC Press, 1986.

- [61] K. C. Saunders and J. H.; Frisch, *Polyurethane: Chemistry and technology*, New York: Wiley-Interscience, 1964.
- [62] P. Wright, *Solid polyurethane elastomers*, New York: Gordon & Breach Sci Pub, 1969.
- [63] M. Szycher, *Szycher's handbook of polyurethanes*, Boca Raton, FL, USA: CRC Press, 1999.
- [64] R. Hock and K. Herrington, *Flexible polyurethane foams*, MI: Midland, 1991.
- [65] D. C. Allport, D. S. Gilbert, and S. M. Outterside, *MDI and TDI: Safety, health & environment, a source book and practical guide*, Chichester, UK: Wiley Publishers, 1998.
- [66] P. F. Bruins, *Polyurethane technology*, New York: Interscience Pub., 1969.
- [67] J. M. Buist and H. Gudgeon, *Advances in polyurethane technology*, London: MacLaren and Sons Ltd., 1968.
- [68] C. Hepburn, *Polyurethane elastomers*, Elsevier Applied Science, 1992.
- [69] I. Goodman, *Telechelic polymers: Synthesis and applications*, Florida, USA: CRC Press Inc., 1989
- [70] S. Petersen, "Niedermolekulare umsetzungsprodukte aliphatischer diisocyanate 5. Mitteilung über polyurethane," *Justus Liebigs Annalen der Chemie*, vol. 562, 1949, pp. 205-228.
- [71] C. W. van Hoogstraten, "Para-nitrophenyl iso-cyanate as a reagent for alcohols and amino-compounds," *Recueil des Travaux Chimiques des Pays-Bas*, vol. 51, 1932, pp. 414-433.
- [72] K. Dusek, M. Spirikova, and I. Havlicek, "Network formation of polyurethanes due to side reactions," *Macromolecules*, vol. 23, 1990, pp. 1774-1781.
- [73] K. A. Pigott, *Urethane polymers*, Kirk-Othmer Encyclopedia of Chemical Technology, vol. 21, pp. 100-106.
- [74] H. Kleimann, "Die basenkatalysierte isocyanat-amin-reaktion," *Angewandte Makromolekulare Chemie*, vol. 98, 1981, pp. 185-194.

- [75] K. Dusek, M. Spirkova, and I. Havlicek, "Network formation of polyurethanes due to side reactions," *Macromolecules*, vol. 23, 1990, pp. 1774-1781.
- [76] A. W. Hofmann, "Umwandlung des phenylcyanats in phenylcyanurat," *Berichte der deutschen chemischen Gesellschaft*, vol. 18, 1885, pp. 764-766.
- [77] L. C. Raiford and H. B. Freyermuth, "Formation and properties of some uretediones," *The Journal of Organic Chemistry*, vol. 08, 1943, pp. 230-238.
- [78] A. W. Hofmann, "Umwandlung des Phenylcyanats in Phenylcyanurat," *Berichte der Deutschen Chemischen Gesellschaft*, vol. 18, 1885, pp. 764-766.
- [79] G. Woods, *The ICI polyurethane book*, John Wiley & Sons, 1990.
- [80] A. T. Thi, A. T. Camberlin and Y. Lam, "Synthèse et propriétés de polyuréthannes réticulés par des cycles isocyanurates," *Die Angewandte Makromolekulare Chemie*, vol. 111, 1983, pp. 29-51.
- [81] M. A. Semsarzadeh and A. H. Navarchian, "Effects of NCO / OH ratio and catalyst concentration on structure , thermal stability , and crosslink density of Poly (urethane-isocyanurate)," *Polymer*, vol. 90, 2003, pp. 963-972.
- [82] C. Smeltz, "Index volume xxvii - 1962-1963," *The Educational Forum*, vol. 27, 1963, pp. 504-510.
- [83] E. Dyer and R. E. Read "New catalysts for the conversion of isocyanates to carbodiimides," *The Journal of Organic Chemistry*, vol. 612, 1961, pp. 4677-4678.
- [84] H. Ulrich, "Polar addition of isocyanates to carbon-nitrogen bonds," *Accounts of Chemical Research*, vol. 2, 1969, pp. 186-192.
- [85] H. G. Khorana, "The chemistry of carbodiimides," *Chemical Reviews*, vol. 53, 1953, pp. 145-166.
- [86] W. Neumann and P. Fischer, "Carbodiimide aus isocyanaten," *Angewandte Chemie*, vol. 74, 1962, pp. 801-806.

- [87] J. Monagle, W. Campbell, F. Mcsiiane, and F. Mcshane, "*Carbodiimides. II. Mechanism of the catalytic formation from isocyanates,*" vol. 84, 1962, pp. 4288-4295.
- [88] T. W. Campbell and J. J. Monagle, "A new synthesis of mono- and polycarbodiimides," *Journal of American Chemical Society*, vol. 8, 1962, p. 1493.
- [89] T. W. Cambell, "*Carbodiimides. I. Conversion of isocyanates to carbodiimides with phospholine oxide catalyst,*" *Organic and Biological Chemistry*, vol. 84, 1962, pp. 3673-3677.
- [90] H. Holtschmidt and G. Oertel, "*Isocyanates of esters of some acids of phosphorus and silicion,*" *Angewandte Chemie International Edition in English*, vol. 1, 1962, pp. 617-621.
- [91] J.J. Monagle, "*Carbodiimides. III. Conversion of Isocyanates to Carbodiimides. Catalyst Studies,*" *Journal of Organic Chemistry*, vol. 27, 1962, pp. 3851–3855.
- [92] Y. K. Jhon, I. W. Cheong, and J. H. Kim, "*Chain extension study of aqueous polyurethane dispersions,*" *Colloids and Surfaces A: Physicochemical and Engineering Aspects*, vol. 179, 2001, pp. 71-78.
- [93] M. L. Berins, *SPI plastics engineering handbook*, New York: Van Nostrand Reinhold, 1976.
- [94] M. L. Berins, *SPI plastics engineering handbook*, New York: Van Nostrand Reinhold, 1960.
- [95] M. L. Berins, *Plastics engineering handbook of the Society of the Plastic Industry Inc.*, New York: Van Nostrand Reinhold, 1991.
- [96] S. L. Axelrood, C. W. Hamilton, and K. C. Frisch, "*A one-shot method for urethane and urethane-urea elastomers,*" *Industrial & Engineering Chemistry*, vol. 53, 1961, pp. 889-894.
- [97] N. M. K. Lamba, *Polyurethanes in biomedical applications*, Boca Raton, Florida: CRC Press, 1998.
- [98] H. R. D. Braun, H. Cherdron, and M. Rehahn, *Polymer synthesis: Theory and practice : Fundamentals, methods, experiments*, Berlin Heidelberg: Springer, 2005.

- [99] N. Hasirci, “*Polyurethanes*,” High Performance Biomaterials, S. Michael, ed., Lancaster, Pennsylvania, U.S.A, 1991, pp. 71-91.
- [100] R. J. Young and P. A. Lovell, *Introduction to polymers*, London: Chapman & Hall, 1991.
- [101] B. D. Rattier, *Biomaterials science: An introduction to materials in medicine*, San Diego: Academic Press, 1996.
- [102] J. W. C. Van Bogart, P. E. Gibson, and S. L. Cooper, “*Structure-property relationships in polycaprolactone-polyurethanes*,” Journal of Polymer Science: Polymer Physics Edition, vol. 21, 1983, pp. 65-95.
- [103] G. Oertel, ed., *Polyurethane handbook chemistry, raw materials, processing, application, properties*, New York: Hanser, 1993.
- [104] S. L. Cooper and A. V. Tobolsky, “*Properties of linear elastomeric polyurethanes*,” Journal of Applied Polymer Science, vol. 10, 1966, pp. 1837-1844.
- [105] Y. Ikeda, M. Tabuchi, Y. Sekiguchi, Y. Miyake, and S. Kohjiya, “*Effect of solvent evaporation rate on microphase-separated structure of segmented poly (urethane-urea) prepared by solution casting*,” Macromolecular Chemistry and Physics, vol. 195, 1994, pp. 3615-3628.
- [106] F. Li, J. Hou, W. Zhu, X. Zhang, M. Xu, X. Luo, D. Ma, and B. K. Kim, “*Crystallinity and morphology of segmented polyurethanes with different soft-segment length*,” Journal of Applied Polymer Science, vol. 62, 1996, pp. 631-638.
- [107] K. Nakamae, T. Nishino, and S. Asaoka, “*Microphase separation and surface properties of segmented polyurethane-effect of hard segment content*,” International Journal of Adhesion and Adhesives, vol. 16, 1996, pp. 233-239.
- [108] R. W. Seymour and S. L. Cooper, “*Thermal analysis of polyurethane block polymers*,” Macromolecules, vol. 6, 1973, pp. 48-53.
- [109] J. T. Koberstein and T. P. Russell, “*Simultaneous SAXS-DSC study of multiple endothermic behavior in polyether-based polyurethane block copolymers*,” Macromolecules, vol. 19, 1986, pp. 714-720.

- [110] J. T. Koberstein and A. F. Galambos, “*Multiple melting in segmented polyurethane block copolymers,*” *Macromolecules*, vol. 25, 1992, pp. 5618-5624.
- [111] J. T. Koberstein and L. M. Leung, “*Compression-molded polyurethane block copolymers. 2. Evaluation of microphase compositions,*” *Macromolecules*, vol. 25, 1992, pp. 6205-6213.
- [112] J. T. Koberstein, I. Gancarz, I. B. M. Alnuuien, H. Road, and S. Jose, “*The effects of morphological transitions on hydrogen bonding in polyurethanes: Preliminary results of simultaneous DSC-FTIR experiments,*” *Polymer*, vol. 24, 1986, pp. 2487-2498.
- [113] R. J. Goddard and S. L. Cooper, “*Polyurethane cationomers with pendant trialkylammonium groups : Effects of ion content , alkyl group , and neutralizing anion,*” *Journal of Polymer Science Part B: Polymer Physics*, vol. 32, 1994, pp. 1557-1571.
- [114] J. Foks, H. Janik, and R. Russo, “*Morphology, thermal and mechanical properties of solution-cast polyurethane films,*” *European Polymer Journal*, vol. 26, 1990, pp. 309-314.
- [115] J. P. Santerre and R. S. Labow, “*The effect of hard segment size on the hydrolytic stability of polyether-urea-urethanes when exposed to cholesterol esterase,*” *Journal of Biomedical Materials Research*, vol. 36, 1997, pp. 223-232.
- [116] Z. Zhang, M. King, R. Guidoin, M. Therrien, C. Doillon, W. L. Diehl-Jones, and E. Huebner, “*In vitro exposure of a novel polyesterurethane graft to enzymes: A study of the biostability of the vascugraft arterial prosthesis,*” *Biomaterials*, vol. 15, 1994, pp. 1129-1144.
- [117] Y. Doi, Y. Kumagai, N. Tanahashi, and K. Mukai “*Structural effects on biodegradation of microbial and synthetic poly (hydroxyalkanoates),*” *Biodegradable Polymers and Plastics*, E.A. M. Vert, ed., Royal Society of Chemistry, 1992, pp. 139- 146.
- [118] Y. Tsai, T. Yu, and Y. Tseng, “*Physical properties of crosslinked,*” *Polymer International*, vol. 47, 1998, pp. 445-450.
- [119] C. K. Frisch and A. J. Dieter, “*Overview of urethane elastomers,*” *Polymer-Plastics Technology and Engineering*, vol. 4, 1975, pp. 1-21.

- [120] Y. U. Xue-ha, M. R. Nagarajan, T. G. Grasel, and P.E. Gibson, "Polydimethylsiloxane-polyurethane elastomers : Synthesis and properties of segmented copolymers and related zwitterionomers," *Physics*, vol. 23, 1985, pp. 2319-2338.
- [121] B. F. d'Arlas, L. Rueda, K. de la Caba, I. Mondragon, and A. Eceiza, "Microdomain composition and properties differences of biodegradable polyurethanes based on MDI and HDI," *Polymer Engineering & Science*, vol. 48, 2008, pp. 519-529.
- [122] R. Bonart, L. Morbitzer, and G. Hentze, "X-ray investigations concerning the physical structure of cross-linking in urethane elastomers. II. Butanediol as chain extender," *Journal of Macromolecular Science, Part B: Physics*, vol. 3, 1969, pp. 337-356.
- [123] L. M. Leung and J. T. Koberstein, "Small-angle scattering analysis of hard-microdomain structure and microphase mixing in polyurethane elastomers," *Journal of Polymer Science: Polymer Physics Edition*, vol. 23, 1985, pp. 1883-1913.
- [124] S. G. Musselman, T. M. Santosusso, J. D. Barnes, and L. H. Sperling, "Domain structure and interphase dimensions in poly (urethaneurea) elastomers using DSC and SAXS," *Journal of Polymer Science Part B: Polymer Physics*, vol. 37, 1999, pp. 2586-2600.
- [125] S. L. Cooper and C. B. Wang, "Morphology and properties of segmented polyether polyurethaneureas," *Macromolecule*, vol. 16, 1983, pp. 775-786.
- [126] C. D. Eisenbach, M. Baurgartner, and C. Gihter "Polyurethane elastomers with monodisperse segments and their model precursors: Synthesis and properties," *Advances in Elastomers and Rubber Elasticity*, J.L. and J.E. Mark, ed., New York: Plenum Press, 1986, pp. 51-87.
- [127] T. O. Ahn, S. U. Jung, H. M. Jeong, and S. W. Lee, "The properties of polyurethanes with mixed chain extenders and mixed soft segments," *Journal of Applied Polymer Science*, vol. 51, 1994, pp. 43-49.
- [128] S. Das, D. F. Cox, G. L. Wilkes, D. B. Klinedinst, I. Yilgor, E. Yilgor, and F. L. Beyer, "Effect of symmetry and h-bond strength of hard segments on the structure-property relationships of segmented, nonchain extended polyurethanes and polyureas," *Journal of Macromolecular Science, Part B*, vol. 46, 2007, pp. 853-875.

- [129] C. Spaans, “*Biomedical polyurethanes based on 1,4-butanediisocyanate: An exploratory study*,” University of Groningen, 2000.
- [130] A. Mishra, D. Chattopadhyay, B. Sreedhar, and K. Raju, “*FT-IR and XPS studies of polyurethane-urea-imide coatings*,” *Progress in Organic Coatings*, vol. 55, 2006, pp. 231-243.
- [131] A. Takahara, A. J. Coury, R. W. Hergenrother, and S. L. Cooper “*Effect of soft segment chemistry on the biostability of segmented polyurethanes. I. In vitro oxidation*,” *Journal of Biomedical Materials Research*, vol. 25, 1991, pp. 341-356.
- [132] Y. Xiu, D. Wanc, C. Hu, S. Yinc, and J. Li, “*Morphology-property relationship of segmented polyurethaneurea : Influences of soft-segment structure and molecular weight*,” *Polymer*, vol. 48, 1993, pp. 867-869.
- [133] J. H. Silver, C. W. Myers, F. Lim, and S. L. Cooper, “*Effect of polyol molecular weight on the physical properties and haemocompatibility of polyurethanes containing polyethylene oxide macroglycols*,” *Biomaterials*, vol. 15, 1994, pp. 695-704.
- [134] K. Gisselält, B. Edberg, and P. Flodin, “*Synthesis and properties of degradable poly (urethane urea)s to be used for ligament reconstructions*,” *Biomacromolecules*, vol. 3, 2002, pp. 951-958.
- [135] J. D. Fromstein and K. A. Woodhouse, “*Elastomeric biodegradable polyurethane blends for soft tissue applications*,” *Journal of Biomaterials Science: Polymer Edition*, vol. 13, 2002, pp. 391-406.
- [136] G. A. Abraham, A. Marcos-Fernández, and J. S. Román, “*Bioresorbable poly (ester-ether urethane)s from L-lysine diisocyanate and triblock copolymers with different hydrophilic character*,” *Journal of Biomedical Materials Research: Part A*, vol. 76, 2006, pp. 729-736.
- [137] P. Ping, W. Wang, X. Chen, and X. Jing, “*Poly (ϵ -caprolactone) polyurethane and its shape-memory*,” *Synthesis*, vol. 6, 2005, pp. 587-592.
- [138] J. H. Saunders and K. C. Frisch, *Polyurethanes chemistry and technology, Part II*, Florida: Robert E. Krieger Publishing Company, 1983.
- [139] R. W. Seymour, A. E. Allegrezza, and S. L. Cooper, “*Segmental orientation studies of block polymers. I. Hydrogen-bonded polyurethanes*,” *Macromolecules*, vol. 6, 1973, pp. 896-902.

- [140] C. S. Paik Sung, C. B. Hu, and C. S. Wu, “*Properties of segmented polyether poly (urethaneureas) based on 2,4-toluene diisocyanate. I. Thermal transitions, X-ray studies, and comparison with segmented polyurethanes,*” *Macromolecules*, vol. 13, 1980, pp. 111-116.
- [141] Y. W. Tang, R. S. Labow, and J. P. Santerre, “*Enzyme-induced biodegradation of polycarbonate-polyurethanes: dependence on hard-segment chemistry,*” *Journal of Biomedical Materials Research*, vol. 57, 2001, pp. 597-611.
- [142] Q. Zhao, N. Topham, J. M. Anderson, A. Hiltner, G. Lodoen, and C. R. Payet, “*Foreign-body giant cells and polyurethane biostability: in vivo correlation of cell adhesion and surface cracking,*” *Journal of Biomedical Materials Research*, vol. 25, 1991, pp. 177-183.
- [143] D. S. Katti, S. Lakshmi, R. Langer, and C. T. Laurencin, “*Toxicity, biodegradation and elimination of polyanhydrides,*” *Advanced Drug Delivery Reviews*, vol. 54, 2002, pp. 933-961.
- [144] T. M. Chapman, “*Models for polyurethane hydrolysis under moderately acidic conditions: A comparative study of hydrolysis rates of urethanes, ureas, and amides,*” *Journal of Polymer Science Part A: Polymer Chemistry*, vol. 27, 1989, pp. 1993-2005.
- [145] V. Gajewski, “*Chemical degradation of polyurethane,*” *Rubber World*, vol. 202, 1990, pp. 15-18.
- [146] K. Stokes, R. Mcvenes, and J. M. Anderson, “*Polyurethane elastomer biostability,*” *Journal of Biomaterials Applications*, vol. 9, 1995, pp. 321-354.
- [147] D. W. Brown, R. E. Lowry, and L. E. Smith, “*Crystallinity in hydrolytically aged polyester polyurethane elastomers,*” *Durability of Macromolecular Materials*, 1979, pp. 145-153.
- [148] R. Smith, D. F. Williams, and C. Oliver, “*The biodegradation of poly (ether urethanes),*” *Journal of Biomedical Materials Research*, vol. 21, 1987, pp. 1149-1166.
- [149] G. A. Skarja and K. A. Woodhouse, “*Synthesis and characterization of degradable polyurethane elastomers containing an amino acid-based chain extender,*” *Journal of Biomaterials Science, Polymer Edition*, vol. 9, 1998, pp. 271-295.

- [150] G. A. Skarja and K. A. Woodhouse, "Structure-property relationships of degradable polyurethane elastomers containing an amino acid-based chain extender," *Journal of Applied Polymer Science*, vol. 75, 2000, pp. 1522-1534.
- [151] V. Kumar, R. S. Cotran, and S. L. Robbins, *Basic pathology*, Philadelphia: Saunders, 2003.
- [152] H. Ischiropoulos, L. Zhu, and J. S. Beckman, "Peroxynitrite formation from macrophage-derived nitric oxide," *Archives of Biochemistry and Biophysics*, vol. 298, 1992, pp. 446-451.
- [153] W. H. Koppenol, J. J. Moreno, W. A. Pryor, H. Ischiropoulos, and J. S. Beckman, "Peroxynitrite, a cloaked oxidant formed by nitric oxide and superoxide," *Chemical Research on Toxicology*, vol. 5, 1992, pp. 834-842.
- [154] E. M. Christenson, J. M. Anderson, and A. Hiltner, "Oxidative mechanisms of poly (carbonate urethane) and poly (ether urethane) biodegradation: In vivo and in vitro correlations," *Journal of Biomedical Materials Research, Part A*, vol. 70, 2004, pp. 245-55.
- [155] K. Sutherland, J. R. Mahoney, A. J. Coury, and J. W. Eatonil, "Degradation of biomaterials by phagocyte-derived oxidants," *Journal of Clinical Investigation*, vol. 92, 1993, pp. 2360-2367.
- [156] G. F. Meijs, S. J. Mccarthy, E. Rizzardo, Y. Chen, R. C. Chatelier, A. Brandwood, and K. Schindhelm, "Degradation of medical-grade polyurethane elastomers : The effect of hydrogen peroxide in vitru," *Biomedical Materials*, vol. 27, 1993, pp. 345-356.
- [157] H. Bergstrand, "The generation of reactive oxygen-derived species by phagocytes," *Inflammatory Indices in Chronic Bronchitis*, C.G.A. Persson, ed., Boston: Birkhauser Verlag Base, 1990, pp. 199-211.
- [158] C. D. Capone, "Biostability of a non-ether polyurethane," *Journal of Biomaterials Applications*, vol. 7, 1992, pp. 108-129.
- [159] Q. Zhao, M. P. Agger, M. Fitzpatrick, J. M. Anderson, A. Hiltner, K. Stokes, and P. Urbanski, "Cellular interactions with biomaterials: in vivo cracking of pre-stressed Pellethane 2363-80A," *Journal of Biomedical Materials Research*, vol. 24, 1990, pp. 621-637.

- [160] T. Nie, A. Baldwin, N. Yanaguchi, and K. L. Kiick, "Production of heparin-functionalized hydrogels for the development of responsive and controlled growth factor delivery systems," *Journal of Controlled Release*, vol. 122, 2007, pp. 287-296.
- [161] D. S. W. Benoit and K. S. Anseth, "Heparin functionalized PEG gels that modulate protein adsorption for hMSC adhesion and differentiation," *Acta Biomaterialia*, vol. 1, 2005, pp. 461-470.
- [162] D. S. W. Benoit, S. D. Collins, and K. S. Anseth, "Multifunctional hydrogels that promote osteogenic hMSC differentiation through stimulation and sequestering of BMP2," *Advanced Functional Materials*, vol. 17, 2007, pp. 2085-2093.
- [163] O. Jeon, S. J. Song, H. S. Yang, S. H. Bhang, S. W. Kang, M. A. Sung, and J. H. Lee, "Long-term delivery enhances in vivo osteogenic efficacy of bone morphogenetic protein-2 compared to short-term delivery," *Biochemical and Biophysical Research Communications*, vol. 369, 2008, pp. 774-780.
- [164] T. Takada, T. Katagiri, M. Ifuku, N. Morimura, M. Kobayashi, K. Hasegawa, A. Ogamo, and R. Kamijo, "Sulfated polysaccharides enhance the biological activities of bone morphogenetic proteins," *Journal of Biological Chemistry*, vol. 278, 2003, pp. 43229 -43235.
- [165] B. Zhao, T. Katagiri, H. Toyoda, T. Takada, T. Yanai, T. Fukuda, U.-il Chung, T. Koike, K. Takaoka, and R. Kamijo, "Heparin potentiates the in vivo ectopic bone formation induced by bone morphogenetic protein-2," *Journal of Biological Chemistry*, vol. 281, 2006, pp. 23246 -23253.
- [166] T. Spivak-Kroizman, M. A. Lemmon, I. Dikic, J. E. Ladbury, D. Pinchasi, J. Huang, M. Jaye, G. Crumley, J. Schlessinger, and I. Lax, "Heparin-induced oligomerization of FGF molecules is responsible for FGF receptor dimerization, activation, and cell proliferation," *Cell*, vol. 79, 1994, pp. 1015-1024.
- [167] M. Gümüsderelioglu and S. Aday, "Heparin-functionalized chitosan scaffolds for bone tissue engineering," *Carbohydrate Research*, vol. 346, 2011, pp. 606-613.

- [168] X. Yu, A. Bichtelen, X. Wang, Y. Yan, and F. Lin, “*Compatible polymers complex with improved biocompatibility for hepatic tissue engineering,*” *Journal Of Bioactive And Compatible Polymers*, vol. 20, 2005, pp. 15-28.
- [169] A. Eceiza, K. de la Caba, G. Kortaberria, N. Gabilondo, C. Marieta, M. A. Corcuera, and I. Mondragon, “*Influence of molecular weight and chemical structure of soft segment in reaction kinetics of polycarbonate diols with 4,4'-diphenylmethane diisocyanate,*” *European Polymer Journal*, vol. 41, 2005, pp. 3051-3059.
- [170] D.P. Queiroz, M. N. de Pinho, and C. Dias, “*ATR–FTIR studies of poly (propylene oxide)/polybutadiene bi-soft segment urethane/urea membranes,*” *Macromolecules*, vol. 36, 2003, pp. 4195-4200.
- [171] N. B. Colthup, L. H. Daly, and S. E. Wiberley, *Introduction to infrared and raman spectroscopy*, London: Academic press Ltd., 1990.
- [172] S. J. McCarthy, G. F. Meijs, N. Mitchell, P. A. Gunatillake, G. Heath, A. Brandwood, and K. Schindhelm, “*In-vivo degradation of polyurethanes: transmission-FTIR microscopic characterization of polyurethanes sectioned by cryomicrotomy,*” *Biomaterials*, vol. 18, 1997, pp. 1387-409.
- [173] P. Yu, J. J. McKinnon, C. R. Christensen, and D. a Christensen, “*Using synchrotron transmission FTIR microspectroscopy as a rapid, direct, and nondestructive analytical technique to reveal molecular microstructural-chemical features within tissue in grain barley,*” *Journal of Agricultural and Food Chemistry*, vol. 52, 2004, pp. 1484-94.
- [174] D. K. Chattopadhyay, A. K. Mishra, B. Sreedhar, and K. V. S. N. Raju, “*Thermal and viscoelastic properties of polyurethane-imide/clay hybrid coatings,*” *Polymer Degradation and Stability*, vol. 91, 2006, pp. 1837-1849.
- [175] R. W. Seymour, G. M. Estes, and S. L. Cooper, “*Infrared studies of segmented polyurethane elastomers. I. Hydrogen bonding,*” *Macromolecules*, vol. 3, 1970, pp. 579-583.
- [176] B. Yang, W. M. Huang, C. Li, and L. Li, “*Effects of moisture on the thermomechanical properties of a polyurethane shape memory polymer,*” *Polymer*, vol. 47, 2006, pp. 1348-1356.

- [177] V. P. Ubale, A. D. Sagar, N. N. Maldar, and M. V. Birajdar “*Synthesis and characterization of aromatic–aliphatic polyamides,*” *Journal of Applied Polymer Science*, vol. 79, 2001, pp. 566-571.
- [178] B. D. Kaushiva, S. R. McCartney, G. R. Rossmly, and G. L. Wilkes, “*Surfactant level influences on structure and properties of flexible slabstock polyurethane foams,*” *Polymer*, vol. 41, 2000, pp. 285-310.
- [179] M. van der Schuur, B. Noordover, and R. J. Gaymans, “*Polyurethane elastomers with amide chain extenders of uniform length,*” *Polymer*, vol. 47, 2006, pp. 1091-1100.
- [180] I. Yilgor, E. Yilgor, I. G. Guler, T. C. Ward, and G. L. Wilkes, “*FTIR investigation of the influence of diisocyanate symmetry on the morphology development in model segmented polyurethanes,*” *Polymer*, vol. 47, 2006, pp. 4105-4114.
- [181] H. Tan, J. Li, M. Guo, R. Du, X. Xie, Y. Zhong, and Q. Fu, “*Phase behavior and hydrogen bonding in biomembrane mimicing polyurethanes with long side chain fluorinated alkyl phosphatidylcholine polar head groups attached to hard block,*” *Polymer*, vol. 46, 2005, pp. 7230-7239.
- [182] M. M. Coleman, K. H. Lee, D. J. Skrovanek, and P. C. Painter, “*Hydrogen bonding in polymers. 4. Infrared temperature studies of a simple polyurethane,*” *Macromolecules*, vol. 19, 1986, pp. 2149-2157.
- [183] T.-Chin Wen and M.-sieng Wu, “*Spectroscopic investigations of poly (oxypropylene) glycol-based waterborne polyurethane doped with lithium perchlorate,*” *Macromolecules*, 1999, pp. 2712-2720.
- [184] Y. S. Hu, Y. Tao, and C. P. Hu, “*Polyurethaneurea/vinyl polymer hybrid aqueous dispersions based on renewable material,*” *Biomacromolecules*, vol. 2, 2001, pp. 80-84.
- [185] M. A. Harthcock, M. D. Meadows, and R. E. Guerra, “*Model MDI/butanediol polyurethanes : Molecular structure, morphology, physical and mechanical properties,*” *Polymer*, vol. 24, 1986, pp. 1401-1439.
- [186] L. Xiaolie, L. Jin and M. A. Dezhru, “*Exploration of the difference of reaction rates for polyester and polyether urethane prepolymers with 3,3'-Dichloro-4,4'-Diaminodiphenylmethane,*” *Journal of Applied Polymer Science*, vol. 57, 1995, pp. 467-472.

- [187] V. Romanova, V. Begishev, V. Karmanov, A. Kondyurin, and M. F. Maitz, “*Fourier transform Raman and Fourier transform infrared spectra of cross-linked polyurethaneurea films synthesized from solutions*,” *Journal of Raman Spectroscopy*, vol. 33, 2002, pp. 769-777.
- [188] D. P. Queiroz, M. N. De Pinho, and C. Dias, “*ATR-FTIR studies of poly (propylene oxide)/polybutadiene bi-soft segment urethane/urea membranes*,” *Macromolecules*, vol. 36, 2003, pp. 4195-4200.
- [189] L. J. Bellamy, *The infra-red spectra of complex molecules*, New York: Wiley Inter-science Publication, 1958.
- [190] J. Liu and D. Ma, “*Study on synthesis and thermal properties of polyurethane-imide copolymers with multiple hard segments*,” *Journal of Applied Polymer Science*, vol. 84, 2002, pp. 2206-2215.
- [191] D.F. Varnell, J.P. Runt, and M.M. Coleman, “*Fourier transform infrared studies of polymer blends. 6. Further observations on the poly (bisphenol A carbonate)-poly (ϵ -caprolactone) system*,” *Macromolecules*, vol. 14, 1981, pp. 1350-1356.
- [192] K. Ulubayram and N. Hasirci, “*Properties of plasma-modified polyurethane surfaces*,” *Colloids and Surfaces B: Biointerfaces*, vol. 1, 1993, pp. 261-269.
- [193] T.R. Hesketh, J. W. C. Van Bogart, and S. L. Cooper, “*Differential scanning calorimetry analysis of morphological changes in segmented elastomers*,” *Polymer Engineering and Science*, vol. 20, 1980, pp. 190-197.
- [194] S. Krause, “*Microphase separation and block size*,” *Block and Graft Copolymers*, W.V. Burke John J., ed., New York: Syracuse University Press, 1973, p.143.
- [195] A. R. Sarasam, R. K. Krishnaswamy, and S. V. Madihally, “*Blending chitosan with polycaprolactone : Effects on physicochemical and antibacterial properties*,” *Society*, vol. 7, 2006, pp. 1131-1138.
- [196] C. Li, X. Yu, T. a Speckhard, and S. L. Cooper, “*Synthesis and properties of polycyanoethylmethylsiloxane polyurea urethane elastomers: A study of segmental compatibility*,” *Journal of Polymer Science Part B: Polymer Physics*, vol. 26, 1988, pp. 315-337.

- [197] C. Z. Yanc, “*Synthesis and characterization of polydimethylsiloxane polyurea-urethanes and related zwitterionomers,*” *Journal of Polymer Science: Part B: Polymer Physics*, vol. 29, 1991, pp. 75-86.

APPENDIX A

POLYMER SYNTHESIS SETUP

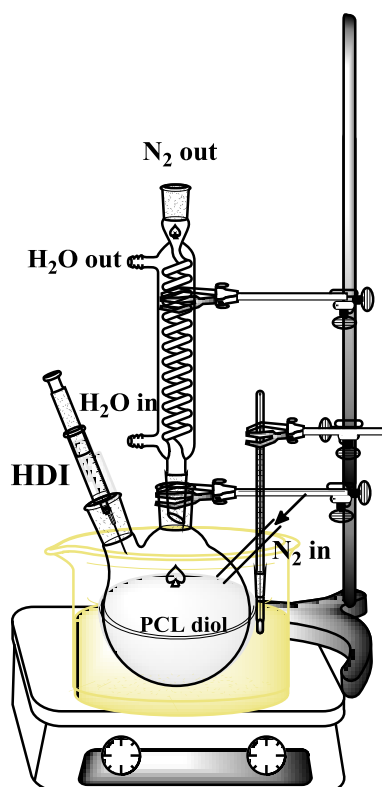


Figure A-1 : Polymer Synthesis Setup.

In polymer synthesis, three-necked round-bottomed flask is equipped with a magnetic stirrer, a thermometer and a reflux condenser. One of the necks and the top of the condenser are equipped with glass stopper during vacuum process. The glass stopper in the neck of the flask and the top of the condenser is replaced with rubber septum when the system is under nitrogen atmosphere.

APPENDIX B

IMAGES OF THE PREPARED FILMS

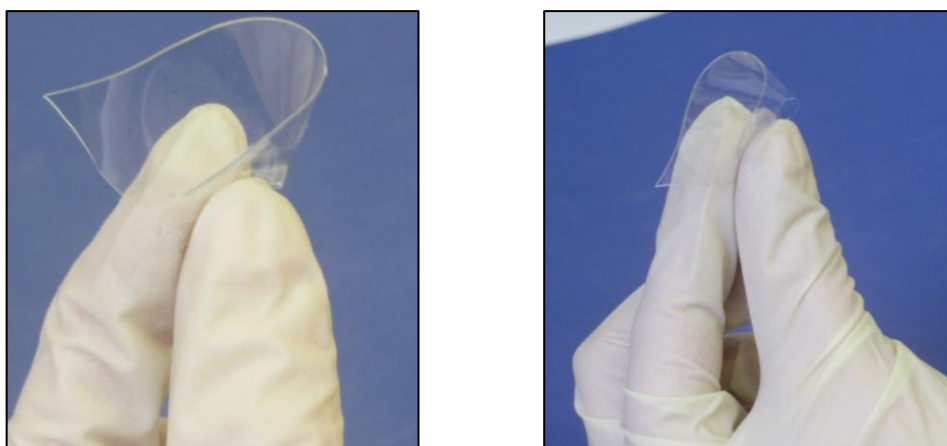


Figure B-1 : Images of PU5-900T Films.

APPENDIX C

DMA RESULTS AT 2 Hz

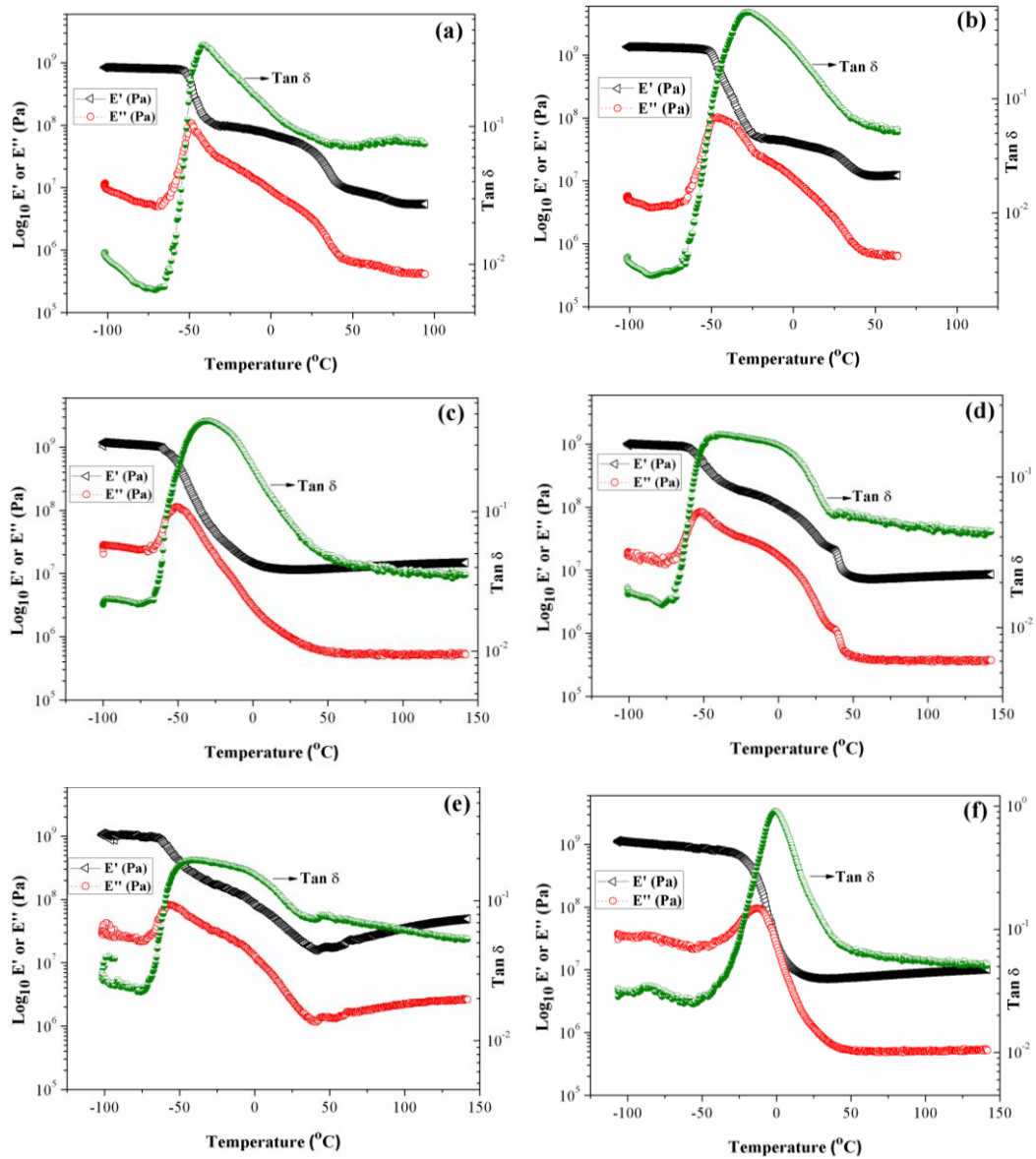


Figure C-1 : DMA Results; (a) PU1.5-1250; (b) PU2.5-1250; (c) PU5-1250; (d) PU5-2000; (e) PU5-2000; (f) PU5-900T (conditions: 5° C/min, 2 Hz, film in tensile mode).

APPENDIX D

DMA RESULTS AT 4 Hz

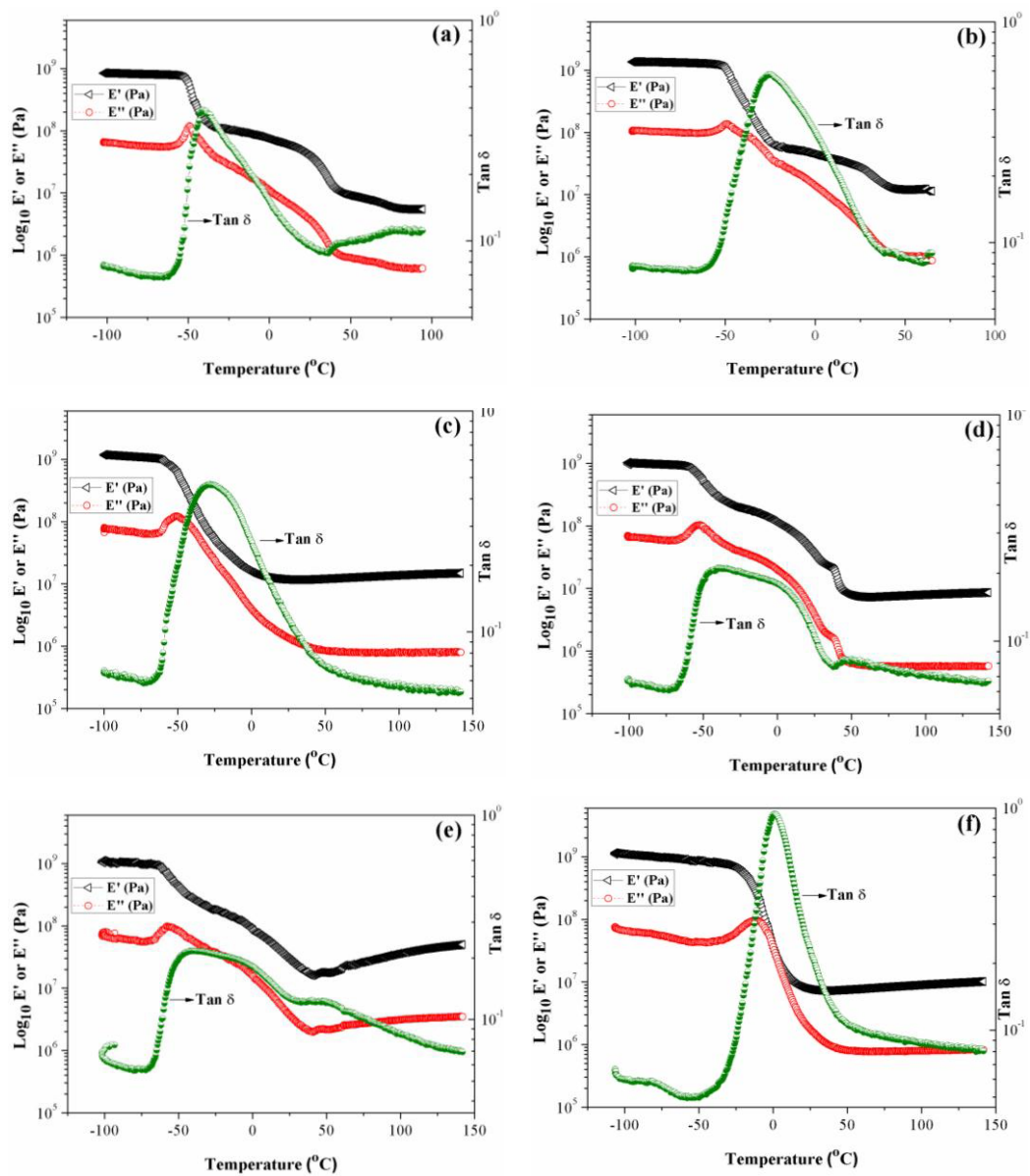


Figure D-1 : DMA Results; (a) PU1.5-1250; (b) PU2.5-1250; (c) PU5-1250; (d) PU5-2000; (e) PU5-2000; (f) PU5-900T (conditions: 5°C/min, 4 Hz, film in tensile mode).

APPENDIX E

DMA RESULTS AT 10 Hz

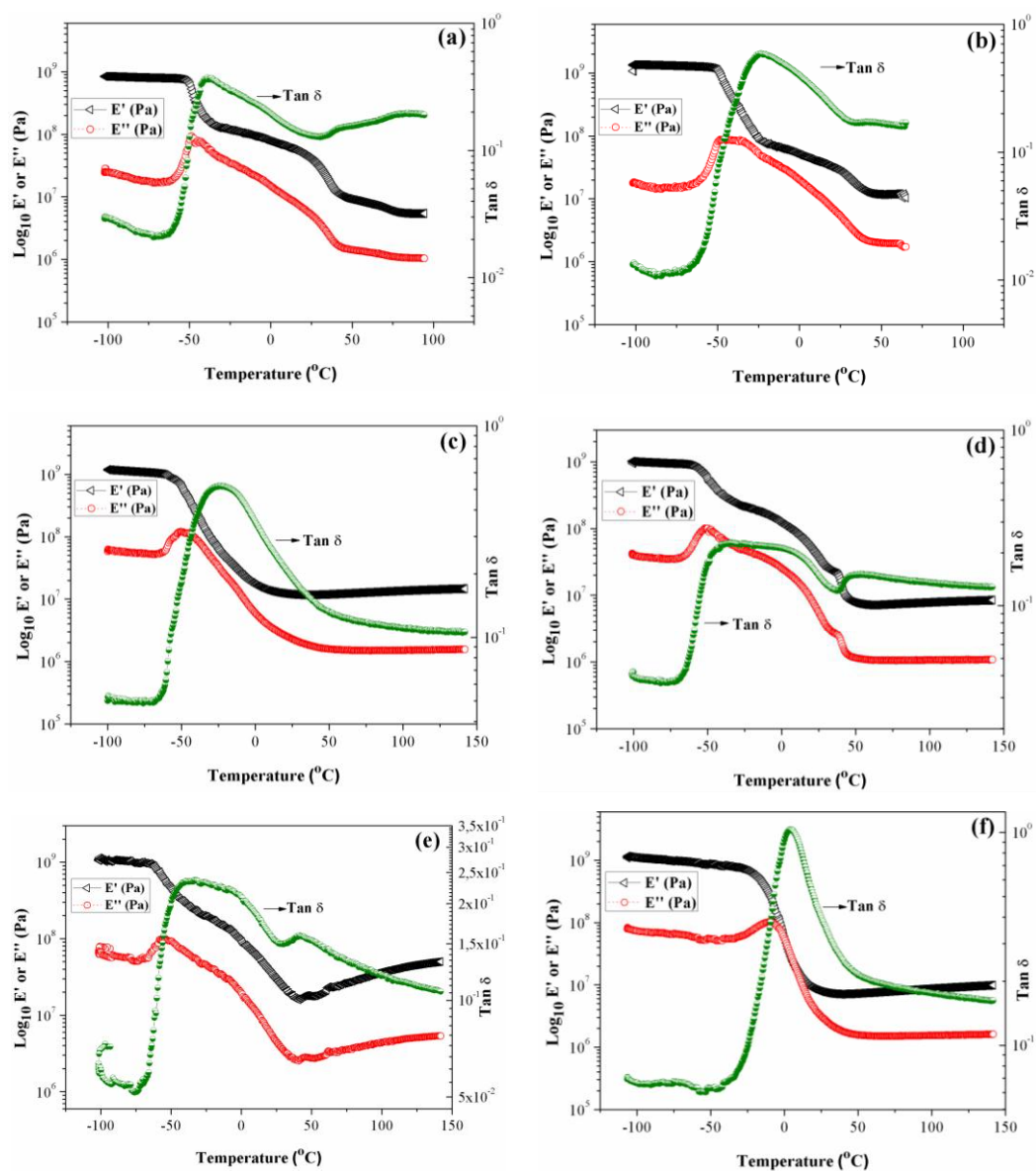


Figure E-1 : (a) PU1.5-1250; (b) PU2.5-1250; (c) PU5-1250; (d) PU5-2000; (e) PUU5-2000; (f) PU5-900T (conditions: 5°C/min, 10 Hz, film in tensile mode).

APPENDIX F

DMA RESULTS AT 20 Hz

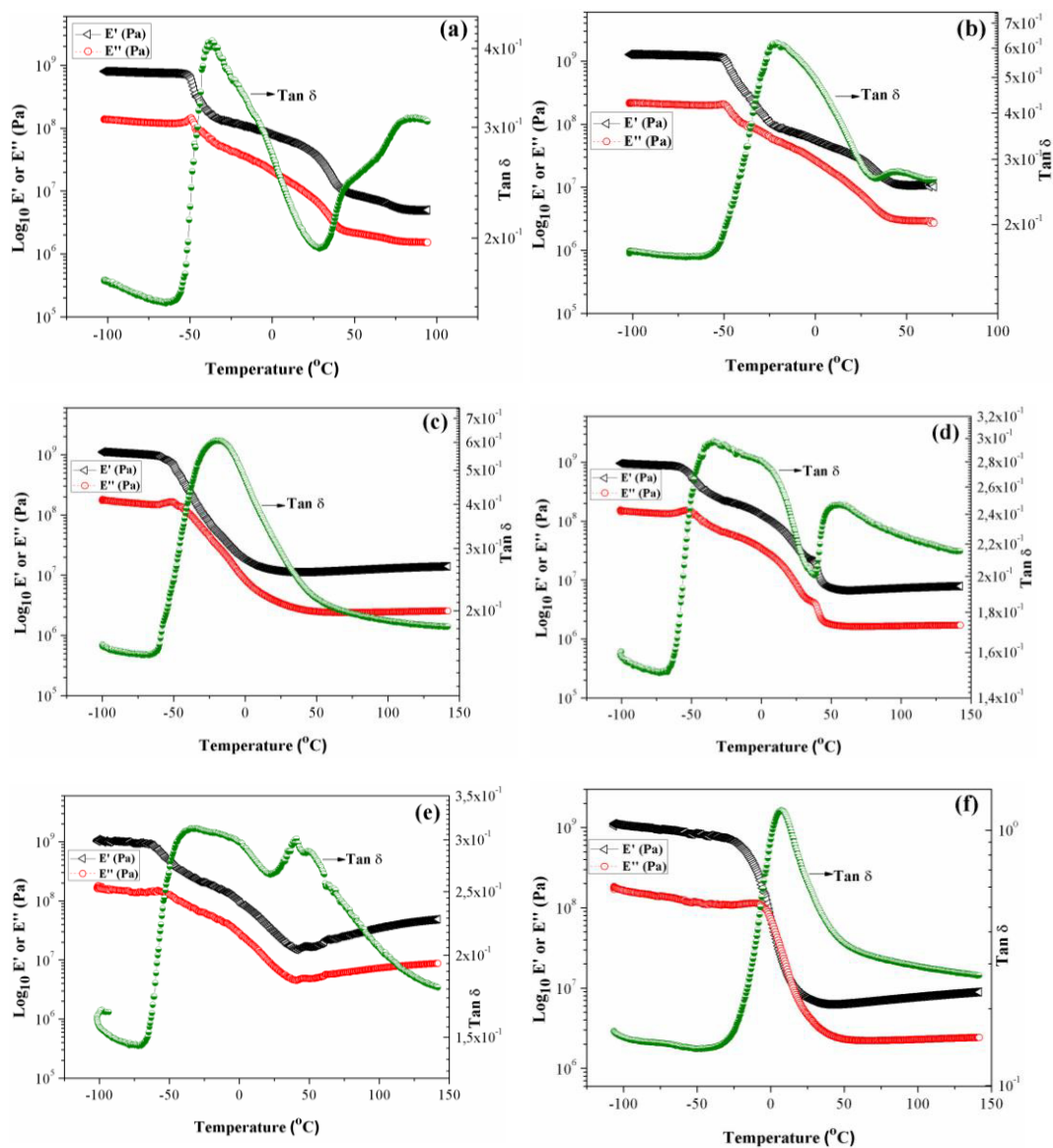


Figure F-1 : (a) PU1.5-1250; (b) PU2.5-1250; (c) PU5-1250; (d) PU5-2000; (e) PUU5-2000; (f) PU5-900T (conditions: 5°C/min, 20 Hz, film in tensile mode).

APPENDIX G

DMA RESULTS: TAN δ VALUES AT DIFFERENT FREQUENCIES

The phase angle ($\tan \delta$) associated with glass transition of PCL increased with frequency as evident from shifting towards higher temperatures. The sharper $\tan \delta$ transition were observed for PU1.5-1250, PU2.5-1250, PU5-1250 and PU5-900T, suggests more uniform crosslinks compared to PU5-2000 and PUU5-2000. PU5-2000 and PUU5-2000 displayed two broadest $\tan \delta$ transitions, demonstrating the greatest degree of heterogeneity of crosslinks. Broad $\tan \delta$ transitions showed non-uniformity of crosslinks in these polymers. Tg values showed differences according to applied frequencies. For PU5-1250, Tg values are observed at -33°C, -30°C, -27°C, -23°C and -18°C at 1, 2, 4, 10 and 20 Hz, respectively. Glass transition temperatures increased with applied frequency due to well-orientation in terms of applied oscillating force.

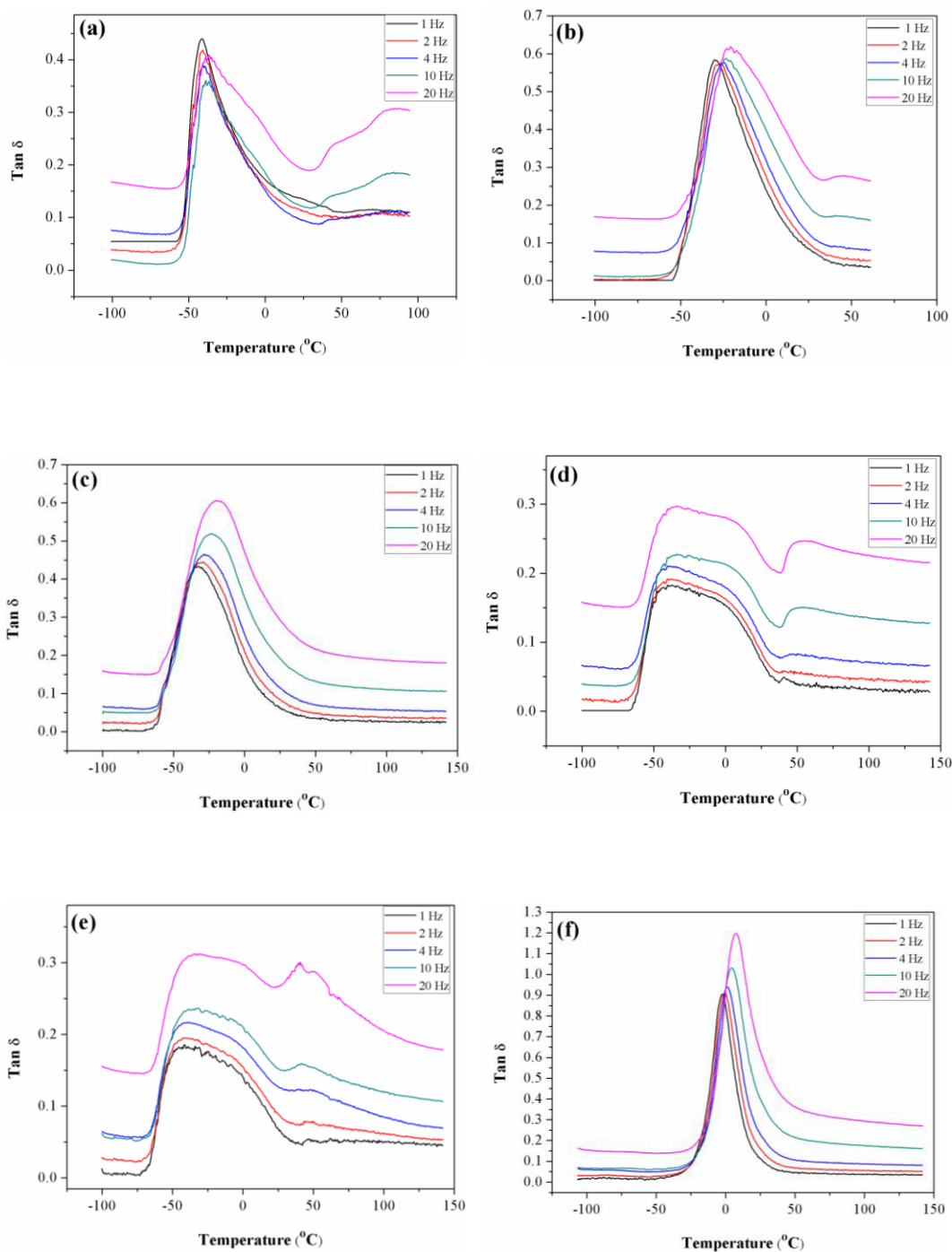


Figure G-1 : $\tan \delta$ Values; (a) PU1.5-1250; (b) PU2.5-1250; (c) PU5-1250; (d) PU5-2000; (e) PU5-2000; (f) PU5-900T (conditions: $5^{\circ}\text{C}/\text{min}$, 1 Hz, 2 Hz, 4 Hz, 10 Hz and 20 Hz, film in tensile mode).

APPENDIX H

FORMATION AND CHARACTERIZATION OF POLYURETHANE BLENDS

The incorporation of additives in the polymer matrix is one of the smarter ways to improve mechanical properties and hydrophilicity. The inclusion not only helps in strengthening the mechanical properties but it also helps in increasing the hydrophilicity. Therefore, different polysaccharides and proteins were added into PU samples and their effect on mechanical and hydrophilicity properties were examined. It was intended to design the present study rather different way to assess the importance of the blend formation on material property.

H.1 Materials and Characterizations

Properties of the materials used in preparation of PU blends were given as given in Table H-1 and H-2.

Table H-1 : Properties of the polysaccharides for preparation of blends.

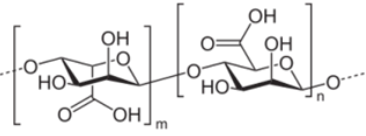
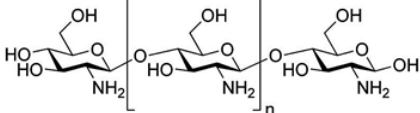
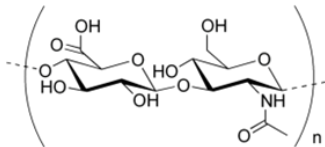
Polysaccharide (Code)	Chemical structure	Properties
Alginic acid (Sigma-A2033)		<ul style="list-style-type: none"> • $M_w=80.000-120.000 \text{ g.mol}^{-1}$,
Chitosan (Fluka Biochemica-50494)		<ul style="list-style-type: none"> • % 78 dd, • $M_w=120.000 \text{ g.mol}^{-1}$
Hyaluronic acid (Sigma-53747)		<ul style="list-style-type: none"> • anionic, non-sulfated glycosaminoglycan, • distributed widely throughout connective, epithelial, and neural tissues

Table H-2 : Properties of the proteins for preparation of blends.

Protein (Code)	Chemical structure	Properties
Gelatin (Scharlau-51393)	Alanine 9%, aspartic acid 6%, arginine 8%, glycine 27%, proline and hydroxyproline 25%, glutamic acid 10% other amino acids 15%	<ul style="list-style-type: none"> • denaturation $T \sim 55^\circ\text{C}$
Bovine serum albumin (BSA) (Boehringer Mannheim-100030)	a low content of tryptophan and methionine and a high content of cystine and the charged amino acids, aspartic and glutamic acids, lysine, and arginine	<ul style="list-style-type: none"> • $M_w=68.000$, • denaturation $T \sim 62^\circ\text{C}$

Water contact angles of the films were measured by using a goniometer (CAM 200, Finland). A typical drop volume, 5 μL deionized water drops were introduced to the polymer surface using a micro-syringe and at least five measurements were achieved for each sample. Tensile strength, elongation, and modulus of films were determined by a mechanical testing machine (Lloyd Instrument, Ltd., Fareham, UK), equipped with a 100 N load cell. For tensile test; film samples were cut as rectangular strips (10 mm x 50 mm). In tensile tests; the gauge length was 10 ± 2 mm. The thickness of each film specimen was determined by a micrometer having measurements from different parts and the average values were used in the calculations. At least 5 specimens were tested for each type of films and the average values were obtained. As a result, ultimate elongation, ultimate stress, and Young's modulus values were obtained through a cross-head speed of $10 \text{ mm}\cdot\text{min}^{-1}$.

H.2 Preparation of PU blends

Three different polysaccharides and two different proteins, as listed in Table H-1 and Table H-2, were dissolved in deionized water in various compositions. Subsequently as mentioned in Table H-3, maximum amount of polysaccharides and proteins are dissolved in deionized water via applying temperature to increase solubility to a critical value (55°C). In a similar approach, previously prepared PU5-2000 was mixed with prepared solutions to generate urea bonds in high yield, which is assigned as PUU5-2000. Then they were added to 1 g PrePU5-2000 and it was stirred by a spatula for 5 minutes. After casting the solution in glass petri dishes, they have been cured in a vacuum oven at 55°C against the danger of denaturation. After addition of the solutions to prepolymer; porosity, phase separation, transparency or opacity were observed for the samples. Details of this experiment are noted in Table H-3.

Table H-3 : Preparation of solutions added to PU5-2000.

Solute	Concentration (w/v)	Amount of added solution into 1 g PU5-2000 (μL)	Observations after addition
Alginate	0.04	100 μ L	Porosity
Chitosan	0.02	300 μ L	Highest porosity
HA	0.60	100 μ L	Little phase separation, little porosity
Gelatin	0.15	100 μ L	Form opacity, porosity
BSA	0.15	400 μ L	Phase separation
Alginate + gelatin	0.04 alginate + 0.02 gelatin	200 μ L	Form opacity, little porosity

H.3 Experimental Results

In order to investigate the effects of different compounds used in the production of PU blends on mechanical and hydrophilicity behavior were examined. The results of mechanical properties depends on molecular weight of used compounds. The different functional groups in the compounds lead to variations in wettability of polymers. The mechanical and hydrophilicity results of different polymer blends were listed in Table H-4 and H-5, respectively.

Table H-4 : Summary of mechanical properties of PU blend films (\pm SD, n=5).

Sample Code	UTS (MPa)	E (MPa)	ϵ (%)
PUU5-2000	16.3 \pm 4.3	56.5 \pm 6.8	653.8 \pm 116.7
PUU5-2000-Alginate	6.7 \pm 1.4	76.3 \pm 12.3	94.3 \pm 38.6
PUU5-2000-Chitosan	6.8 \pm 1.7	39.0 \pm 5.4	156.7 \pm 165
PUU5-2000-HA	13.0 \pm 3.8	59.7 \pm 15.0	457.6 \pm 227
PUU5-2000-Gelatin	9.9 \pm 3.8	60.1 \pm 3.8	242.5 \pm 3.8
PUU5-2000-BSA	12.4 \pm 2.4	70.4 \pm 10.1	282.8 \pm 96.8
PUU5-2000-Alginate-gelatin	9.0 \pm 1.5	68.5 \pm 25.2	183.7 \pm 32.5

Table H-5 : Static water contact angle measurement of PU blend films (\pm SD, n=5).

Sample Code	Water Contact Angle ($^{\circ}$)
PUU5-2000	82.4 \pm 2.4
PUU5-2000-Alginate	76.2 \pm 2.7
PUU5-2000-Chitosan	80.0 \pm 4.6
PUU5-2000-HA	71.8 \pm 5.5
PUU5-2000-Gelatin	81.9 \pm 2.4
PUU5-2000-BSA	78.5 \pm 1.3
PUU5-2000-Alginate-gelatin	81.6 \pm 2.3